

<http://researchcommons.waikato.ac.nz/>

Research Commons at the University of Waikato

Copyright Statement:

The digital copy of this thesis is protected by the Copyright Act 1994 (New Zealand).

The thesis may be consulted by you, provided you comply with the provisions of the Act and the following conditions of use:

- Any use you make of these documents or images must be for research or private study purposes only, and you may not make them available to any other person.
- Authors control the copyright of their thesis. You will recognise the author's right to be identified as the author of the thesis, and due acknowledgement will be made to the author where appropriate.
- You will obtain the author's permission before publishing any material from the thesis.

**MAPPING VEGETATION WITH REMOTE SENSING AND GIS DATA
USING OBJECT-BASED ANALYSIS AND MACHINE LEARNING
ALGORITHMS**

A thesis
submitted in fulfilment
of the requirements for the degree
of
Doctor of Philosophy in Geography and Environmental Planning
at
The University of Waikato
by
PHAM THI HONG LIEN



THE UNIVERSITY OF
WAIKATO
Te Whare Wānanga o Waikato

2018

To my paternal grandparents, Pham Vu & Kieu Thi Bay, who love, care, and
educate me

To my parents, Pham Van Thanh & Tran Thi Hop, who I owe my life

To my younger sister as my best friend, Hong Hoa

To my nephew as my inspiration, Nhat Minh

I dedicate you this thesis,

me te aroha!

ABSTRACT

Remote sensing technology is an efficient tool for various practical applications of environmental resources management. Advances in this technology include the diverse range of high quality data sources and image analysis techniques. Object-based image analysis (OBIA) and machine learning algorithms are recent advances, which this thesis evaluates.

OBIA and machine learning algorithms are first tested using a combination of multiple datasets for identifying individual tree species. These datasets include Quickbird, LiDAR, and GIS derived terrain data. Improvements in tree species classification were obtained and the best data combination was terrain context (based on slope, elevation, and wetness), tree height, canopy shape, and branch density (based on LiDAR return intensity).

The availability of a range of classifiers and different data pre-processing techniques adds to the complexity of image analysis. The combinations of these techniques result in a large number of potential outcomes and these need to be evaluated. Therefore, the second part of this research investigated and compared tree species classification performance for different methods (Naïve Bayes - NB , Logistic Regression - LR, Random Forest - RF, and Support Vector Machine - SVM), combined with various dimensionality reduction (DR) methods (Correlation-based feature selection filter, Information Gain, Wrapper methods, and Principal Component Analysis). When DR was used prior to classification, only the NB classifier had a significant improvement in accuracy. SVM and RF had the best classification accuracy, and this was achieved without DR.

The final part of this thesis demonstrates a new method using OBIA for mapping the biomass change of mangrove forests in Vietnam between 2000 and 2011 from SPOT images. First, three different mangrove associations were identified using two levels of image segmentation followed by a SVM classifier and a range of spectral, texture and GIS information for classification. The RF regression model that integrated spectral, vegetation association type, texture, and vegetation indices obtained the highest accuracy.

ACKNOWLEDGMENTS

I am deeply grateful to Buddhism for providing me mental strength and a positive attitude to overcome difficulties during my PhD journey.

I am thankful to my Chief supervisor, Dr Lars Brabyn, for his guidance and supervision during my PhD. I specially thank you for supporting me on the field trips in New Zealand and giving me an independent space to develop my academic knowledge and research skills. I thank you for providing me the opportunity to do GIS tutoring for your graduate students. My research and work experience with you will be important to my future professional career.

My special thanks to my co-supervisor, Dr. Anne-Marie d’Hauteserre, who always listened, supported, and encouraged me when I faced difficult times during my research. Without your great and on-time support, I could not start field trips in New Zealand and complete my thesis.

I am thankful to the great team of NZ Aid Scholarship officers: Rachael, Deonne, and Thomas. Thank you so much for your tremendous support during my studying at the University of Waikato.

I also thank Salman Ashraf, Henry Gouk, Jeffery Garae, Mathew Allan, Glen Stichbury, Hamid Dimyati, Greg Bennett, Shailesh Shrestha, and Dang Duc Thanh who provided technical advice and mental support for my PhD journey. I am also grateful for the support on the field trips that I received from Paul Andrews, Dr. Vo Quoc Tuan, Le Van Sinh, Huynh Duc Hoan, Phan Van Trung, Le Thanh Sang, Bui Nguyen The Kiet, Le Thi Thuy Hoa, and other members at the Cangio Mangrove Protection Forest Management Board.

A special thank to Ms. Andrea Haines from the Student Learning Centre for improving my academic writing skills. I would like to thank Heather Morrell for her great and fast support during the thesis and publication writing and submission.

I also thank Nguyen Nguyen, Chi Nguyen, Ha Ta, Tu Dang for providing accommodation and treating me well during my trip in Wellington, where I cooperated with Salman Ashraf for my first paper.

I would like to thank all lecturers and staff of the Geography and Environmental Planning Programme who made my PhD environment comfortable and friendly.

Special thanks to friends at the Geography and Environmental Planning Programme who shared all my difficulties and happiness during my PhD. To Rini, as a friend and a great flatmate, who accompanied me and shared happy moments during tough years. To Anoosh, Sunita, Sandi, Dinesha, and Dung for interesting conversation and yummy food. To Ilaham, Chaminda, and John who provided me good advice to keep going with my PhD.

To my Vietnamese friends, Hao Truong, Nhung Nguyen, Nam Pham, Hien Nguyen, Tinh Doan and Nuong Nguyen for encouraging me to continue my PhD after a very difficult first year of my PhD.

To Dung Nguyen family, Toan Phuoc family, Danh Le, and Ly Ho, who provided me nice accommodation during my PhD oral examination period. To my landowners, Leona and Chris, who provided me with nice and comfortable home environment to relax after stressful studying hours.

I would like to thank technical help from forums such as IEEE Image Analysis and Data Fusion, the eCognition Community, and Stack Overflow.

A special thank given to my paternal grandmother Kieu Thi Bay and late grandfather Pham Vu who took care of and encouraged me to study hard during my childhood. Without their love and care, I cannot start my PhD.

Thanks to my Mom Tran Thi Hop, late father Pham Van Thanh, and younger sister Pham Thi Hong Hoa who always support me and share my difficulties in life.

TABLE OF CONTENTS

ABSTRACT	v
ACKNOWLEDGMENTS	vii
TABLE OF CONTENTS.....	ix
LIST OF FIGURES	xiii
LIST OF TABLES	xv
LIST OF ACRONYMS & ABBREVIATIONS.....	xvii
CHAPTER 1 INTRODUCTION AND THE RESEARCH CONTEXT	1
1.1 Remote sensing research	1
1.2 Remote sensing of coastal vegetation	3
1.3 Aim of this research	5
1.3.1 Specific research questions	5
1.4 Scope of this research.....	6
1.5 Thesis structure and chapter outlines	8
REFERENCES.....	11
CHAPTER 2 A LITERATURE REVIEW OF ADVANCED IMAGE ANALYSIS TECHNIQUES FOR MAPPING VEGETATION	13
2.1 Introduction	13
2.2 Pixel-based versus object-based approach	13
2.3 Object-based image segmentation.....	15
2.4 Combining GIS data with remotely sensed data	16
2.5 Classification algorithms.....	17
2.5.1 Support Vector Machine	19
2.5.2 Random Forest	22
2.6 Accuracy assessment.....	23
2.7 Conclusion	24
REFERENCES.....	25
CHAPTER 3 COMBINING QUICKBIRD, LIDAR, AND GIS TOPOGRAPHY INDICES TO IDENTIFY A SINGLE NATIVE TREE SPECIES IN A COMPLEX LANDSCAPE USING AN OBJECT-BASED CLASSIFICATION APPROACH.....	31
3.1 Introduction	32
3.2 Materials.....	34

3.2.1	Study area	34
3.2.2	Field data collection.....	34
3.2.3	Image data.....	35
3.3	Methods	35
3.3.1	Step 1 - Image and data pre-processing.....	36
3.3.2	Step 2 - Distinguishing trees from buildings	38
3.3.3	Step 3 - Delineating individual tree crowns	39
3.3.4	Step 4 - Feature extraction and selection.....	41
3.3.5	Step 5- Classification and accuracy assessment	48
3.4	Results and Discussions	49
3.4.1	The contribution of different features.....	52
3.5	Conclusion.....	54
REFERENCES		56
CHAPTER 4 AN EVALUATION OF DIMENSIONALITY REDUCTION		
AND CLASSIFICATION TECHNIQUES FOR IDENTIFYING TREE		
SPECIES USING INTEGRATED QUICKBIRD IMAGERY AND LIDAR		
DATA.....		61
4.1	Introduction	61
4.2	Materials	62
4.2.1	Study area and data sets.....	62
4.3	Methods	63
4.3.1	Dimensionality reduction methods.....	66
4.3.2	Classification techniques	68
4.3.3	Validation and comparison method.....	71
4.4	Results and Discussions	71
4.4.1	Comparison of dimensionality reduction and non-dimensionality reduction for the different classifiers.....	72
4.4.2	Comparing the performance of different classifiers using different training sample sizes and no DR	75
4.4.3	Comparing the performance of the best combinations of classifier and DR (or no DR).....	76
4.5	Conclusion.....	79
REFERENCES		81

CHAPTER 5 MONITORING MANGROVE BIOMASS CHANGE IN VIETNAM USING SPOT IMAGES AND AN OBJECT-BASED APPROACH COMBINED WITH MACHINE LEARNING ALGORITHMS.....	85
5.1 Introduction	86
5.2 Materials.....	88
5.2.1 Study area.....	88
5.2.2 Field data collection	89
5.2.3 Image data	91
5.3 Methods.....	91
5.3.1 Image data pre-processing.....	92
5.3.2 Classifying different mangrove associations	93
5.3.3 Estimating biomass	95
5.3.4 Accuracy assessment.....	101
5.4 Results and Discussion.....	101
5.4.1 Classification results	101
5.4.2 Variable importance	104
5.4.3 Variable selection for the final three RF models	105
5.4.4 Biomass distribution and change between 2000 -2011.....	108
5.4.5 The role of different feature variables for predicting biomass.....	110
5.5 Conclusion	111
REFERENCES.....	113
CHAPTER 6 DISCUSSION AND CONCLUSION.....	119
6.1 Key questions addressed by this research	119
6.2 Limitations	121
6.3 Implications for mapping vegetation and future research.....	122
6.4 Overall conclusion	123
REFERENCES.....	125
REFERENCES.....	127
APPENDICES	141
APPENDIX 1 Co-authorship form.....	142
APPENDIX 2 Co-authorship form.....	143
APPENDIX 3 Co-authorship form.....	144

LIST OF FIGURES

Figure 1.1. The sequence of image analysis techniques and the choices available	2
Figure 2.1. The (a) panel shows the linear SVM separable case while the (b) panel shows the linearly non-separable case. Source: adapted from Hastie et al. (2009).	20
Figure 3.1. QuickBird image of the Coromandel study area. The coordinate is in NZTM2000 projection system.	34
Figure 3.2. Workflow of tree species classification	36
Figure 3.3. The LiDAR derived height above bare ground model	37
Figure 3.4. Decision steps for distinguishing trees and buildings	39
Figure 3.5. The relationship between tree crown size and height	40
Figure 3.6. a) A subset image showing crown overlap. b) Segmentation of the image - red polygons represent the ground reference crowns and the blue polygons representing automatic segmentation	41
Figure 3.7. The effect of different <i>ntree</i> and <i>mtry</i> values on the performance of RF measured by OOB estimate of error rate using only QuickBird data	45
Figure 3.8. The effect of different <i>ntree</i> and <i>mtry</i> values on the performance of RF measured by OOB estimate of error rate using both QuickBird and LiDAR data.	46
Figure 3.9. The importance of different features measured by mean decrease accuracy (a) using spectral data (b) using both spectral and LiDAR data.	47
Figure 3.10. Box-and-whisker plot showing the statistics of reflectance of different tree species across 4 multi-spectral bands.	53
Figure 3.11. Box-and-whisker plot showing the statistics of the standard deviation of intensity of all returns of different tree species.	53
Figure 3.12. Box-and-whisker plot showing the statistics of the maximum height of all returns of different tree species	54
Figure 4.1. Work flow of mapping tree species using dimensionality reduction and classification techniques.	64
Figure 4.2. Individual tree crowns are represented by polygons.	64
Figure 4.3. Classification accuracy (OA) of NB, LR, RF, and SVM with different DR and no DR using a range of training samples per class	74
Figure 4.4. Classification accuracy (OA) of NB, LR, RF, and SVM with different training sizes per class with no DR	75

Figure 4.5. The classification accuracy of the best combination of classifier and DR (or no DR) for different training sample size per class. Note: the DR (or no DR) changes with the sample size.....	79
Figure 5.1. SPOT4 image of the Cangio study area. The coordinate is in WGS 1984 UTM zone 48N projection system.	89
Figure 5.2. A workflow of estimating ABG in the Cangio mangrove forest from SPOT data and ground inventory data.....	92
Figure 5.3. The RMSE _{OOB} is stable after $n_{tree} = 1000$ for all three cases: spectral + texture + vegetation association type + vegetation indices (123 variables); spectral + texture + vegetation indices (122 variables); and spectral + vegetation indices (10 variables) used respectively.....	100
Figure 5.4. Mangrove classification map of the Cangio in: (a) 26 th March 2000 and (b) 24 th February 2011	102
Figure 5.5. The importance of different features measured by %InMSE (the percentage increase in the mean squared error) determined from 100 runs of the RF for: (a) all 123 variables used (spectral + texture + VI + vegetation association type); (b) 122 variables used (spectral + texture + VI); (c) 10 variables (spectral + VI).	105
Figure 5.6. The number of variables used and the average RMSE of models based on 100 times of 10-fold cross validation: (a) all 123 variables; (b) 122 variables; (c) 10 variables.....	106
Figure 5.7. Plots of the observed and predicted biomass values using RF with a) Model 1; b) Model 2; c) Model 3	108
Figure 5.8. Biomass map of the Cangio mangrove forest: (a) 2000 derived from SPOT4 and (b) 2011 derived from SPOT5	109

LIST OF TABLES

Table 3.1. Ground-truthed data	35
Table 3.2. Image object features used for classifications.....	43
Table 3.3. Confusion matrix of classification accuracies obtained through RF feature selection and SVM classifier.....	50
Table 3.4. Confusion matrix of classification accuracies obtained through SVM classifier without feature selection.....	51
Table 4.1. Image object features were used for classifications.....	65
Table 4.2. Comparison between four different classifiers combined with four different DR methods and no DR. Paired t-test (corrected) between the use of DR and no DR at 0.05 significance level from 10-fold CV repeated 5 times. Note: (b) and (w) denote that the result was statistically better or worse respectively than the no DR, while (-) denotes that there was no significant difference.....	73
Table 4.3. Comparing NB, LR, RF, and SVM using all features and different training set sizes with 10-fold CV repeated 5 times and paired t-tester (corrected) at 0.05 significance level. Note: Bolded OA and Kappa scores indicate the highest performance, b and w denote the result is statistically better or worse than the classifier compared; while - denotes there is no significant difference between classifiers.....	76
Table 4.4. Comparing the best classification accuracy of NB, LR, RF, and SVM and different training set sizes with 10-fold CV repeated 5 times and paired t-tester (corrected) at 0.05 significance level. Note: Bolded OA and Kappa scores indicate the highest performance, b and w denote that the result is statistically significantly better or worse respectively than the classifier compared; while - denotes there is no significant difference between classifiers.	78
Table 5.1. Species-specific biomass allometric equations for the Cangio mangrove forest.....	90
Table 5.2. Descriptive statistics of biomass plots	90
Table 5.3. Variables for calculating biomass (spectral and texture variables were also used for classification).....	96
Table 5.4. Confusion matrix of classification accuracies obtained through SVM classifier in 2000 and 2011	103
Table 5.5. Summary of settings for Random Forest Models	107

Table 5.6. Calibration and validation results	107
Table 5.7. General descriptive statistics of AGB in the Cangio mangrove forest in the years 2000 and 2011	109

LIST OF ACRONYMS & ABBREVIATIONS

AD	Allocation Disagreement
AGB	Above-Ground Biomass
ANN	Artificial Neural Network
ATCOR	Atmospheric Correction Algorithm
CFS	Correlation-Based Feature Selection
CHM	Canopy Height Model
CMM	Canopy Maxima Model
DBH	Diameter at Breast Height
DEM	Digital Elevation Model
DR	Dimensionality Reduction
DT	Decision Tree
EVI	Enhanced Vegetation Index
FLAASH	Fast Line-of-sight Atmospheric Analysis of Hypercubes
GLCM	Grey-Level Co-occurrence
GLDV	Gray-Level Difference Vector
GPS	Global Positioning System
INFOGAIN	Information Gain
K	Kappa coefficient of agreement
LiDAR	Light Detection And Raging
LR	Logistic Regression
MIR	Mid-Infrared
ML	Maximum Likelihood
MSAVI	Modified Soil-Adjusted Vegetation Index
NB	Naïve Bayes
NDVI	Normalized Difference Vegetation Index
NDWI	Normalized Difference Water Index
NIR	Near InfraRed
OA	Overall Accuracy
OBIA	Object-based Image Analysis
OOB	Out-Of-Bag
OSAVI	Optimized Soil-Adjusted Vegetation Index
PA	Producer's Accuracy

PCA	Principal Component Analysis
QD	Quantity Disagreement
RBF	Radial Basis Function
RF	Random Forest
SAVI	Soil-Adjusted Vegetation Index
SPOT	Satellite Pour l'Observation de la Terre
SS	Sequential Selection
SVM	Support Vector Machine
TD	Total Disagreement
TWI	Topographical Wetness Index
UA	User's Accuracy

CHAPTER 1

INTRODUCTION AND THE RESEARCH CONTEXT

The motivation for this research was to develop techniques for monitoring change to coastal vegetation using remote sensing. Natural and anthropogenic disturbances of coastal vegetation are a major issue. Monitoring the spatial extent of coastal vegetation is an important step in understanding these disturbances, and remote sensing technology is a useful tool for providing such information. This thesis researches the use of advanced remote sensing techniques, including object-based image analysis and machine learning algorithms for coastal vegetation.

The first sections of this introduction chapter provide an overview of previous remote sensing research and what this thesis will do to address the gaps in the literature. Next sections provide the aim and scope of this research. The final section provides information about thesis structure and chapter outlines.

1.1 Remote sensing research

Remote sensing has been demonstrated to be cost efficient and effective for many practical applications such as biodiversity monitoring, agriculture planning, and forest fire control and management. Remote sensing is a rapidly changing technology due to new data sources becoming available as well as advancing image analysis techniques.

Image analysis is a combination of different data sets, pre-processing, and image classification techniques. Figure 1.1 shows the sequence of these techniques and the choices available, which are represented on the left of this Figure as data sources, image analysis, dimensionality reduction, and classifiers. These techniques interact and can impact on the accuracy of the final classification. For example, using the object-based image analysis for high resolution multispectral data can extract more input variables for classification such as contextual variables than the pixel-based approach. The large number of input data requires pre-processing steps using dimensionality reduction methods to obtain higher classification accuracy. The preferred combination of analysis techniques therefore requires research.

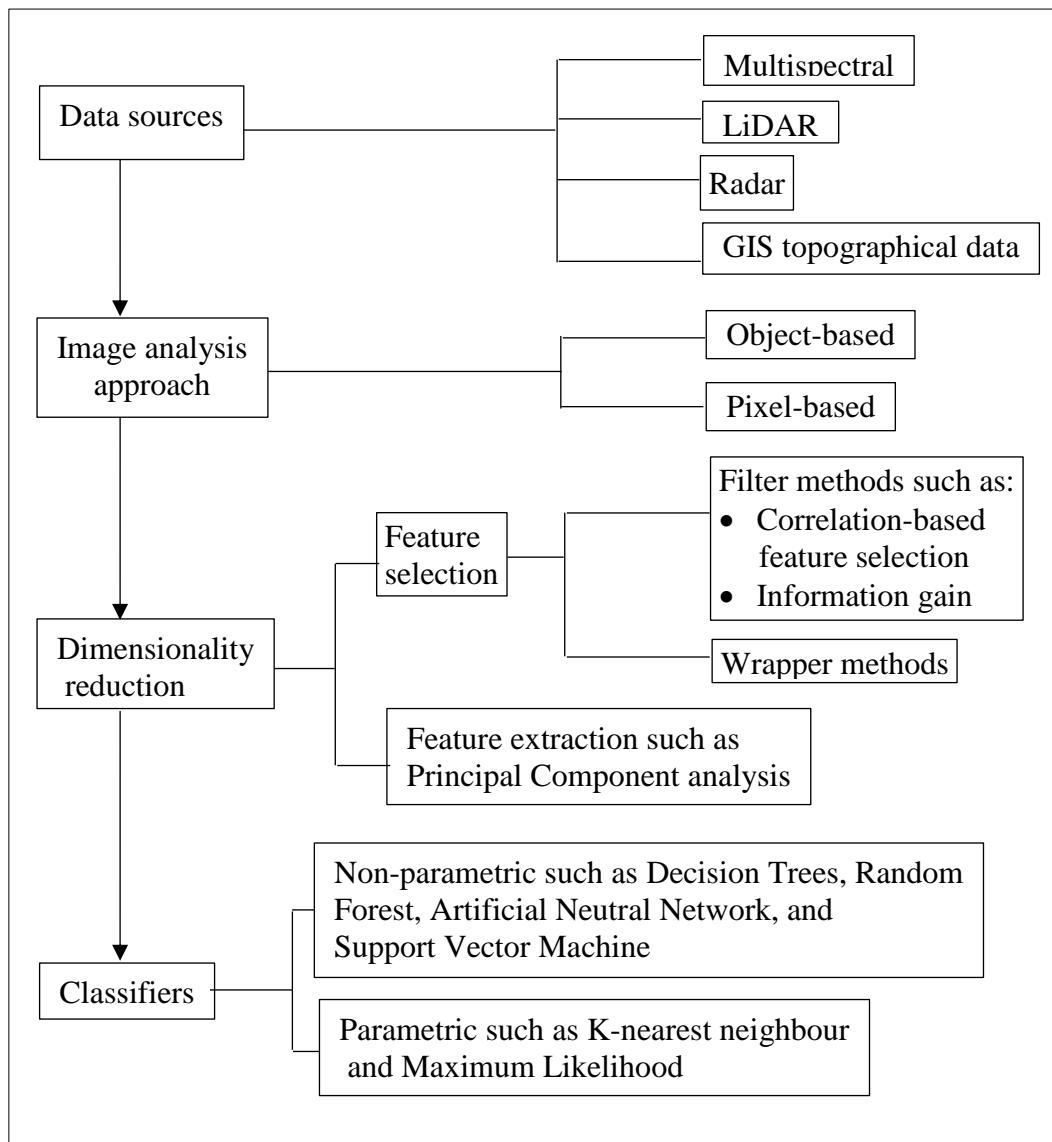


Figure 1.1. The sequence of image analysis techniques and the choices available

Traditionally remotely sensed data has mainly focused on multispectral images, but now there is a wide range of data sets that can be used in remote sensing, which includes hyperspectral images, LiDAR, and RADAR data, as well as GIS topographical data that provides environmental context. Spectral data can now be combined with tree height and shape, as well as landform and wetness indices. Using simultaneously multiple data sets introduces new challenges in image analysis and this research investigates whether such data sets improve image classification accuracy.

As well as advances in the number and quality of available data sets, techniques for image analysis have also improved. Traditionally images have been classified at the

pixel level but a more sophisticated technique is the use of object-based image analysis (OBIA; see chapter 2 for details). The OBIA first joins pixels into objects (this process is known as segmentation), and then classification is performed on these objects using the diversity of spectral, textural, and contextual information. In contrast to the pixel-based approach, the OBIA exploits various information simultaneously such as spectral, spatial, shape, textural, and contextual information. The effectiveness of using OBIA combined with multiple data sets depends on the classification targets and the types of data sources available. However, there is no general framework about how to integrate OBIA and multiple data sets for mapping vegetation; therefore research is required. In addition, the level of segmentation used depends on the data and the objects being identified. This level needs to be investigated to produce the most optimal results.

Combining multiple datasets can result in high computational demand as well as feature redundancy that compromise classification performance. Therefore, pre-processing the data using dimensionality reduction methods is often done to not only reduce processing time but also improve the classification accuracy. There are many dimensionality reduction techniques to choose from such as Correlation-based feature selection filter, Information gain, and Wrapper methods. Choosing the best dimensionality reduction methods is important for improving classification accuracy and will be explored in this research.

In addition to the above techniques, several image classification algorithms have been developed. These include parametric classifiers such as Maximum Likelihood, and K-nearest neighbour, as well as non-parametric methods such as Decision Trees, Artificial Neural Network, Random Forest, and Support Vector Machine (see details in Chapter 2). The choice of classification algorithms depends on the data properties and this is investigated to determine which is best for classification accuracy.

1.2 Remote sensing of coastal vegetation

Another aspect of remote sensing research is developing new applications of remote sensing such as single tree mapping and biomass estimation. The performance of different remote sensing techniques, such as described previously, will vary with

different vegetation types. It is therefore necessary to choose a particular context for the research as it is not practical to research their accuracy with all the different vegetation types. This thesis focuses on using remote sensing techniques for mapping coastal vegetation and testing their accuracies. The reason for choosing coastal vegetation is twofold. Firstly the research was supported by an international collaboration between the University of Waikato in NZ and the University of Bremen in Germany, called INTERCOAST. This collaboration focuses on coastal research.

The second reason was because of the importance of coastal vegetation. Coastal ecosystems such as dunes, mangrove forests, salt marshes, and coral reefs provide several important services such as purifying the water from human wastes and pollutants, preventing coastal erosion, and minimizing the impact of natural disasters such as flood, tsunamis and hurricane (Tanaka et al., 2007; Wang and Wang, 2010). In addition, coastal ecosystems provide scenic beauty and recreation (Álvarez-Molina et al., 2012). However, those ecosystems are facing increased natural and anthropogenic disturbances such as climate change, sea level rise, storms, land use change and encroachment by urban development (Álvarez-Molina et al., 2012; Wang and Wang, 2010). Providing accurate up-to-date information about the characteristics of the coastal vegetation such as the presence of individual species, distribution, and biomass is necessary to help managers and policy makers decide on appropriate conservation and restoration strategies within a restricted time span.

Coastal vegetation can be mapped using a range of methods. Traditional vegetation mapping methods such as field surveys or aerial photography interpretation are time-consuming, costly and provide inconsistent results (Castillejo-González et al., 2009; Xie et al., 2008). Compared to traditional field surveys, the use of satellite remotely sensed data has many advantages such as significantly lower costs; it is also quicker and more suitable for use over extensive areas (Castillejo-González et al., 2009; Xie et al., 2008). Given these strengths, remote sensing data have been commonly used for identifying coastal vegetation and measuring its physical characteristics.

Many studies using remote sensing have mapped vegetation at a coarse spatial resolution data which is defined by Xie et al. (2008) as pixels with ground sampling distance of 30 m or greater and identified vegetation types that often include several different species. Given the desire to provide the most detailed and accurate results, vegetation maps should use high quality remotely sensed data and advanced image analysis techniques. This research thus focuses on mapping single trees in New Zealand, where high quality data is available.

Although this study uses high quality data, such as LIDAR and QuickBird images, for New Zealand, it is important to be mindful that many developing countries do not have access to such data because of the expense. Developing countries also face high environmental pressures and have a need for vegetation monitoring. Therefore, research on remote sensing should consider how best to utilise low resolution images, such as Landsat and SPOT, which are considerably cheaper. This research modified the methodology developed in New Zealand and applied this to the context of developing countries lower spatial resolution data sources.

1.3 Aim of this research

The main objective of this research is to evaluate a range of remote sensing techniques for mapping coastal vegetation as accurately as possible, including the best combination of techniques. This vegetation mapping includes mapping the location of individual trees in New Zealand as well as calculating biomass of mangrove forests in Vietnam.

1.3.1 Specific research questions

1. What levels of segmentation are required to separate individual tree crowns/mangrove associations from other land-cover types such as grasslands, buildings, and water?
2. Which dimensionality reduction methods improve the accuracy of vegetation classification or biomass prediction?
3. Which classifier algorithms should be used for identifying coastal vegetation?
4. Does the combination of spectral and GIS derived data improve the accuracy of vegetation classification and biomass prediction?

1.4 Scope of this research

This study will use a unique combination of GIS data, remotely sensed images, OBIA with different dimensionality reduction and classification techniques that have never been used before for mapping tree species and estimating biomass. Improving the vegetation classification accuracy is the main goal of this research. The accuracy will be compared with other vegetation mapping studies conducted elsewhere in the world.

Two study areas have been chosen for this research – a coastal site in NZ for which higher spatial resolution data is available and a coastal site in Vietnam that has lower spatial resolution data sources. These two countries provided the opportunity to investigate whether the object-based approach with various classifiers is widely applicable for different types of environments and vegetation species.

Case study in New Zealand – Coromandel Peninsula

The New Zealand site is the Coromandel Peninsula. The site is characterized by different land cover types including built-up area, urban parkland/open space, sand or gravel, coastal broadleaved species of scrub or scrublands, pine forests, manuka and/or kanuka, and pohutukawa forests on the coast (Humphreys and Tyler, 1990; Weeks et al., 2009).

Pohutukawa, one of the best-known native trees in New Zealand, is a coastal species and found mainly in northern New Zealand (Bergin and Hosking, 2006; Simpson, 2005). Pohutukawa has cultural significance to Maori including medicinal uses. It has also provided timber for boat building. At present, it is used for honey production as well as cosmetic and cleaning products (Bergin and Hosking, 2006; Simpson, 2005). Regarding its ecological and environmental functions, it helps stabilize soil on eroding or unstable areas and provides habitat and resources to plant and animal associates such as tui and bellbird (Bergin and Hosking, 2006).

Despite such benefits, the number of Pohutukawa trees has considerably declined in the past due to fires and land clearance (Bergin and Hosking, 2006; Simpson, 2005). Unfortunately, this decrease is continuing at present, mainly due to possum and herbivore browsing (Bergin and Hosking, 2006; Bylsma, 2012). Recently

Pohutukawa has been considered to be at risk from myrtle rust. Therefore, counting the trees which is the first step at monitoring impacts such as possum browsing is necessary to help managers develop appropriate conservation strategies. These tasks can be done effectively and economically using remote sensing data combined with the object-based approach to identify individual trees. A map showing individual tree locations of Pohutukawa would be a first for NZ and would generate considerable interest. It is expected that the method developed will be applicable in similar locations throughout NZ.

The Coromandel Peninsula has been chosen because: 1) LIDAR and QuickBird data sets (high spatial resolution) are available, 2) there is a range of coastal vegetation including Pohutukawa, conifers, and exotic species, and 3) it is accessible by car so that ground-truth data can be collected easily.

Case study in Vietnam – Cangio mangrove forests

The Vietnam site is the Cangio mangrove forests. The Cangio mangrove forest is located in Cangio District - one of 24 districts of Ho Chi Minh City - covering an area of about 72 000 ha. In January 2000, the Cangio mangrove forest was recognized as the first biosphere reserve in Vietnam. This reserve consists of 60% planted and 40% natural forests (Kuenzer and Tuan, 2013). There are more than 200 species of fauna and more than 52 species of flora, so it is considered to have high biodiversity (Nguyen, 2006). Besides those types of vegetation, the research area includes shrimp ponds, bare lands, and muddy flats. Mangroves in Cangio have been facing the threat of increased coastal erosion as a result of the transit of large cargo ships, the ever expanding aquaculture and salt farming activities, and the negative impacts of socio-economic transformation (Kuenzer and Tuan, 2013).

This site has been chosen because: 1) SPOT images and Digital Elevation data (DEM) are freely available; 2) there are various mangrove species; 3) there is a range of GIS data available; and 4) mangrove forest in Cangio is extensive and the methodology developed by this research can be evaluated in different environments.

1.5 Thesis structure and chapter outlines

This thesis consists of six chapters – this general introductory chapter (Chapter 1), a literature review of advanced image analysis techniques (Chapter 2), three chapters written as manuscripts for publication (Chapters 3, 4, and 5), and a concluding chapter (Chapter 6) that provides discussions and a final conclusion.

Because the research chapters 3, 4, and 5 have been submitted to different journals, they follow different specific formatting and referencing styles appropriate to each journal. However, changes have been made in the formats of the individual chapters to maintain the overall consistency of the overall thesis.

Chapter 2 – “A literature review of advanced image analysis techniques for mapping vegetation”.

Chapter 2 clarifies the advantages of OBIA compared to the traditional pixel-based approach. It also reviews different machine learning algorithms for classifying vegetation and predicting biomass. It enables the discovery of knowledge gaps in the use and combination of existing techniques that the thesis seeks to fill.

Chapter 3 - “Combining QuickBird, LiDAR, and GIS topography indices to identify a single native tree species in a complex landscape using an object-based classification approach”.

Chapter 3 is a peer-reviewed paper published as “Pham, L.T.H, Brabyn, L., Ashraf, S., 2016. Combining QuickBird, LiDAR, and GIS topography indices to identify a single native tree species in a complex landscape using an object-based classification approach. *International Journal of Applied Earth Observation and Geoinformation* 50, 187-197”. <http://dx.doi.org/10.1016/j.jag.2016.03.015>

The chapter investigates the benefits of combining a range of techniques to identify individual tree species. A QuickBird image and low point density LiDAR data for a coastal region in New Zealand were used to examine the possibility of mapping individual Pohutukawa trees, which are regarded as an iconic tree in New Zealand. This chapter shows how combining LiDAR and spectral data improves classification for Pohutukawa trees.

Chapter 4 - “An evaluation of dimensionality reduction and classification techniques for identifying tree species using integrated QuickBird imagery and LiDAR data”

Chapter 4 is a paper submitted to the “IEEE Transactions on Geoscience and Remote Sensing” Journal. This chapter investigates and compares tree species classification performance for a variety of classification schemes (Naïve Bayes, Logistic Regression, Random Forest, and Support Vector Machine), combined with various dimensionality reduction methods (Correlation-based feature selection filter, Information Gain, Wrapper methods, and Principle component analysis). This chapter concludes that the SVM and RF achieve highest classification accuracy, and dimensionality reduction should be applied prior to the classification step to make the classifier algorithms run faster and/or achieve higher classification accuracy.

Chapter 5 - “Monitoring mangrove biomass change in Vietnam using SPOT images and an object-based approach combined with machine learning algorithms”.

Chapter 5 is a peer-reviewed paper published as “Pham, L.T.H., Brabyn, L., 2017. Monitoring mangrove biomass change in Vietnam using SPOT images and an object-based approach combined with machine learning algorithms”. ISPRS Journal of Photogrammetry and Remote Sensing 128, 86 -97”. <http://dx.doi.org/10.1016/j.isprsjprs.2017.03.013>

The chapter extends the applications of an object-based approach for measuring the biomass change between 2000 and 2011 of mangrove forests in the Cangio region in Vietnam. Firstly, it uses object-based image analysis and Support Vector Machine classifier for identifying different mangrove types. Random Forest regression algorithms are then used for modelling and mapping biomass. This chapter concludes that the integration of spectral, vegetation association type, texture, and vegetation indices obtains the highest accuracy ($R^2_{\text{adj}} = 0.73$).

Chapter 6 – “Discussion and Conclusion”

This final chapter synthesises results given in previous chapters, and summarises the answers to the research questions. This chapter recaps the contribution of this

research in establishing new knowledge for remote sensing of vegetation. Limitations of this research are discussed, including suggestions for future research that address these limitations.

REFERENCES

- Álvarez-Molina, L.L., Martínez, M.L., Pérez-Maqueo, O., Gallego-Fernández, J.B., Flores, P., 2012. Richness, diversity, and rate of primary succession over 20 year in tropical coastal dunes. *Plant Ecology* 213(10), 1597-1608. <https://doi.org/10.1007/s11258-012-0114-5>
- Bergin, D., Hosking, G., 2006. Pohutukawa-ecology, establishment, growth and management. New Zealand Indigenous Tree Series No. 4. New Zealand Forest Research Institute, Rotorua.
- Bylsma, R.J., 2012. Structure, composition and dynamics of *Metrosideros excelsa* (pōhutukawa) forest, Bay of Plenty, New Zealand University of Waikato.
- Castillejo-González, I.L., López-Granados, F., García-Ferrer, A., Peña-Barragán, J.M., Jurado-Expósito, M., de la Orden, M.S., González-Audicana, M., 2009. Object- and pixel-based analysis for mapping crops and their agro-environmental associated measures using QuickBird imagery. *Computers and Electronics in Agriculture* 68(2), 207-215. <https://doi.org/10.1016/j.compag.2009.06.004>
- Humphreys, E.A., Tyler, A.M., 1990. Coromandel Ecological Region: survey report for the Protected Natural Areas Programme. Department of Conservation, Waikato Conservancy.
- Kuenzer, C., Tuan, V.Q., 2013. Assessing the ecosystem services value of Can Gio Mangrove Biosphere Reserve: Combining earth-observation- and household-survey-based analyses. *Applied Geography* 45, 167-184. <https://doi.org/10.1016/j.apgeog.2013.08.012>
- Nguyen, H.N., 2006. The environment in Ho Chi Minh City harbours, in: Wolanski, E. (Ed.), *The Environment in Asia Pacific Harbours*. Springer, Dordrecht, The Netherlands, pp. 261-291.
- Simpson, P., 2005. Pohutukawa and Rata: New Zealand's Iron-Hearted Trees. Te Papa Press, Wellington, New Zealand.
- Tanaka, N., Sasaki, Y., Mowjood, M.I.M., Jinadasa, K.B.S.N., Homchuen, S., 2007. Coastal vegetation structures and their functions in tsunami protection: experience of the recent Indian Ocean tsunami. *Landscape Ecol Eng* 3(1), 33-45. <https://doi.org/10.1007/s11355-006-0013-9>
- Wang, Y., Wang, J., 2010. Remote sensing of coastal environments: An overview, in: Wang, Y. (Ed.), *Remote Sensing of Coastal Environments*. CRC Press, Boca Raton, FL, pp. 1-24.
- Weeks, E., Newsome, P., Shepherd, J., 2009. National SPOT-5 Image Orthorectification and Reflectance Standardisation: Final Project Report Landcare Research Contract Report: LC0809/102, Palmerston North, New Zealand.
- Xie, Y., Sha, Z., Yu, M., 2008. Remote sensing imagery in vegetation mapping: a review. *Journal of Plant Ecology* 1(1), 9-23. <https://doi.org/10.1093/jpe/rtm005>

CHAPTER 2

A LITERATURE REVIEW OF ADVANCED IMAGE ANALYSIS TECHNIQUES FOR MAPPING VEGETATION

2.1 Introduction

Remote sensing techniques cover a wide range of image preparation, classification, and accuracy assessment techniques. The emergence of various remote sensing data sources requires new and advanced image processing techniques to use these data sets efficiently. An overview of different types of image analysis techniques used for mapping vegetation can be found in many articles and remote sensing text books such as Chuvieco (2016), Houborg et al. (2015), Pettorelli et al. (2014), and Wang (2009). As stated in the introduction chapter this thesis focuses on advanced image analysis techniques. Therefore this review chapter focuses on just these techniques and the methods that are common to all three chapter/papers. This includes object based classification, integration of GIS and remotely sensed data, classifiers, and accuracy assessment. The subsequent chapters/papers summarise the main points of this review in light of the restriction imposed by the publication format as well as review specialised methods that are relevant to the particular chapter/paper. These specialised methods include LiDAR processing, treetop identification, biomass estimation, allometric functions, and dimensionality reduction techniques.

2.2 Pixel-based versus object-based approach

Two common categorial image analysis approaches are pixel-based and object-based analysis (Aguirre-Gutiérrez et al., 2012). While the pixel-based analysis has long been the main approach used in remote sensing studies, the object-based image analysis has become increasingly popular over the last decade (Blaschke, 2010; Duro et al., 2012). A pixel-based analysis approach assigns an individual pixel into one category (Liu and Xia, 2010) while an object-based approach operates on objects which are groups of homogenous and contiguous pixels (Liu and Xia, 2010).

Compared to the pixel-based technique, the OBIA has many advantages. Firstly, shifting the classification units from pixels to image objects decreases the intra-class spectral variability and removes the “salt-and-pepper” problem which is usual

in pixel-based classification of high spatial resolution imagery (Gao et al., 2007; Liu and Xia, 2010; Yu et al., 2006). Secondly, the OBIA integrates various features of image objects. It can use not only the spectral properties but also spatial and contextual information into the classification process, which may be able to perform the classification more accurately (Blaschke, 2010; Blaschke et al., 2014a; Gao et al., 2007; Han et al., 2014; Ouyang et al., 2011). Thirdly, the object-based approach with multi-scale segmentation and hierarchical structure of the classification scheme will provide detailed information at different levels of landscape such as from individual trees to forests (Mishra and Crews, 2014). Thanks to these flexibility characteristics, the cost for producing many products and updating information at different levels of the landscape is reduced significantly. However, one of the drawbacks of object-based image analysis is that the segmentation process and the calculation of the topological relationships between objects can consume a large amount of computer memory (Liu and Xia, 2010; Whiteside et al., 2011). In addition, there are no objective methods to choose parameters for producing image objects (Jakubowski et al., 2013; Liu and Xia, 2010; Whiteside et al., 2011). Other disadvantages are that the software is expensive and has a steep learning curve.

Many studies showed that the OBIA performed better than the pixel-based methods using a great variety of remote sensing imagery for mapping vegetation. For example, Ouyang et al. (2011) compared pixel-based and object-based analysis using QuickBird imagery and different classification models for mapping saltmarsh plants. The results indicated that OBIA achieved higher overall accuracy (87%) than the pixel-based approach (82%). Moreover, there was no “salt and pepper” in the map created from object-based classification approaches. Ghosh and Joshi (2014) used WorldView-2 imagery and different classification algorithms to map bamboo patches in West Bengal, India. Their method combined both the OBIA and a Support Vector Machine classifier, which produced 91% accuracy while the pixel-based classification scheme was only 80% accurate. Similarly, Fu et al. (2017) showed that the object-based Random Forest algorithm improved the overall accuracy (OA) between 3%-10% when compared to pixel-based classifications for wetland vegetation using high spatial resolution Gaofen-1 satellite image, L-band PALSAR and C-band Radarsat-2 data.

The OBIA outperforms pixel-based analysis for not only high but also medium resolution satellite imagery. For instance, Whiteside et al. (2011) used ASTER data to map land cover in the tropical north of the Northern Territory of Australia. The OA of using the object-oriented approach was statistically significantly greater than that of the pixel-based approach. Similarly, Myint et al. (2008) found that an object-based approach with the lacunarity technique for Landsat Thematic Mapper data was more effective in identifying three types of mangrove species than a pixel-based classifier. The OA of the object-oriented classifier was significantly higher than that of the pixel-based classifier (94.2% and 62.8% respectively).

Although the above studies found that the OBIA obtained more accurate results than pixel-based methods, the pixel-based approach may achieve similar or sometimes more accurate classification results for certain land cover categories (Duro et al., 2012; Flanders et al., 2003). In such cases, the combination of two approaches can produce the best results. Wang et al. (2004a) demonstrated that the OA of mangrove maps created from very high-resolution IKONOS imagery was improved when combining pixel-based and object-based classifications. Similarly, Aguirre-Gutiérrez et al. (2012) compared the land cover classification results among pixel-based, object-based, and the combined object-based and pixel-based classification using medium resolution imagery (Landsat ETM⁺). The result showed that the combination method delivered the best results. Li et al. (2013) also illustrated that the hybrid of image segmentation and pixel-based classification for land cover classification outperformed the use of object-based or pixel-based approach alone.

2.3 Object-based image segmentation

A defining step in OBIA is image segmentation (Kim et al., 2009a; Lang, 2008), which divides an image into contiguous, separate and homogeneous areas. These areas are called image objects (Blaschke et al., 2004; Blaschke et al., 2014b; Duro et al., 2012), which are then classified into different categories using a range of classifiers (reviewed in the next section). The quality of segmentation will affect the accuracy of the classified image (Kim et al., 2009a; Liu and Xia, 2010). The segmenting process can produce meaningful image objects at different scales of the landscape (granularity), which enables multiple features to be extracted from a

single dataset (Burnett and Blaschke, 2003; Lang and Langanke, 2006; Mishra and Crews, 2014).

Image segmentation methods can be divided into three categories, including point-based or pixel-based (e.g. grey-level thresholding), edge-based (e.g. edge detection techniques), and region-based (Blaschke et al., 2004; Pal and Pal, 1993; Van Coillie et al., 2007). Point-based methods gather pixels in a feature space using thresholds and clusters (Yu et al., 2006). Edge-based methods determine boundaries between image objects using edge detection algorithms based on changes in values (Blaschke et al., 2004; Yu et al., 2006). Region extraction can be divided into region growing, region dividing, and their combinations (Blaschke et al., 2004; Yu et al., 2006). The region growing method starts with a set of seed pixels, which are then merged to adjacent pixels that are similar (Ke and Quackenbush, 2011). This process of growing continues until a threshold is reached, and defined by specified homogeneity criteria (Blaschke et al., 2004). For segmenting individual tree crowns, various semi- and fully-automated methods have been developed and can be generally categorized into: template matching (Korpela et al., 2007; Olofsson et al., 2006); valley following (Leckie et al., 2003); watershed segmentation (Chen et al., 2006); and region growing (Bunting and Lucas, 2006; Li et al., 2012; Zhen et al., 2014). The region growing method outperformed other methods, e.g., valley-following (Hussin et al., 2014; Larsen et al., 2011), and template matching (Larsen et al., 2011) in a mixed forest.

2.4 Combining GIS data with remotely sensed data

The OBIA provides the possibilities to integrate GIS techniques and image processing to use data effectively and improve classification. This is especially useful for situations where shape or neighbourhood relations are distinctive and spectral properties are not (Blaschke et al., 2014b). For example, old meandering river beds can have a range of land cover possibilities such as remaining water filled in by sediment or overgrown by vegetation. The mixed spectral properties in this case limits the meanders identification. However, the unchanged shape of the meander provides a unique property to distinguish it from its land cover appearance (Blaschke et al., 2014b).

The integration of GIS data with remotely sensed data has been used in many studies. Han et al. (2014) used the linkages between vegetated objects at different scales to identify land cover types in shadow areas for Moso bamboo forest. Similarly, MacFaden et al. (2012) combined multispectral imagery and LiDAR data using OBIA with contextual analysis to distinguish urban tree canopy from other land cover types. The contextual analysis in their research focused on the relationship between individual objects and their neighbours. MacFaden et al. (2012) identified tree canopy with accuracy that exceeded 90%. Yu et al. (2006) also used integrated Digital Airborne Imaging System imagery and topographic data with the object-based approach for detailed vegetation classification in Northern California. They pointed out that topographic information such as slope, aspect, and distance to water courses contributed significantly for vegetation classification besides spectral and texture features derived from airborne imagery. Likewise, Blaschke et al. (2014a) showed that the combination of difference variables from satellite images with GIS variables such as slope and flow direction derivatives can detect and delineate landslides more accurately than using a single data source.

2.5 Classification algorithms

Choosing suitable classification algorithms is important to improve classification accuracy (Lu and Weng, 2007; Otukei and Blaschke, 2010). There are two main types of classification algorithms - supervised and unsupervised classification (Lu and Weng, 2007). Commonly used supervised classification techniques include Maximum Likelihood (ML), Minimum Distance, Artificial Neural Network (ANN), and Support Vector Machine (SVM); while unsupervised methods include K-Means and ISODATA (Ghosh and Joshi, 2014; Lu and Weng, 2007). Classification algorithms are also divided into non-parametric methods such as Decision Tree (DT), ANN, and SVM, and parametric methods such as ML and K-nearest neighbour (Ghosh and Joshi, 2014; Lu and Weng, 2007; Yu et al., 2006).

The most commonly used parametric classifier in remote sensing is the ML because it is widely available in image-processing software programmes (Ghosh and Joshi, 2014; Lu and Weng, 2007). However, the parametric approach assumes that the image data are normally distributed. Such assumption is often not guaranteed, especially in complex landscapes (Löw et al., 2015; Lu and Weng, 2007). This

assumption error is more serious in circumstances where training samples are not adequate, unrepresentative, or multimode distributed (Cracknell and Reading, 2014; Lu and Weng, 2007).

In contrast to parametric classifiers, non-parametric classifiers do not need an assumption of normal distribution of the dataset (L  w et al., 2015; Lu and Weng, 2007). This flexible characteristic of non-parametric classifiers allows integration of spectral and ancillary data into a classification process. Several previous studies have shown that non-parametric classifiers can produce better results than parametric classifiers in complex landscapes (Cracknell and Reading, 2014; Ghosh and Joshi, 2014). Neural Networks, DT, SVM, and Random Forest (RF) are the most common non-parametric classifiers (L  w et al., 2015; Lu and Weng, 2007; Raczko and Zagajewski, 2017).

Many studies compare the performance between parametric classifiers and non-parametric classifiers and amongst non-parametric classifiers. There is no consensus as to which method is the best practice. In general, RF and SVM perform better than ANN and MLC, especially when there is a limited number of training samples and many different classes (Cracknell and Reading, 2014). Ghosh and Joshi (2014) compared the performance among kernel based SVM, ensemble based RF and parametric ML classifiers in both pixel-based and object-based classification approaches for mapping bamboo patches in West Bengal India with WorldView 2 imagery. They showed that SVM produced higher accuracy than RF and ML classifiers while ML classifiers ran faster than SVM and RF. Similarly, Dalponte et al. (2012) identified tree species in the Southern Alps, Italy using the fused multispectral/hyperspectral images and LiDAR data and two non-parametric classifiers (SVM and RF). Their results showed that SVM provided better results than RF. Dalponte et al. (2012) explained that the unbalanced number of training samples among tree species classes may lead to the poor performance of RF. Duro et al. (2012) mapped agricultural landscapes in western Canada using SPOT-5 HRG imagery (medium spatial resolution multi-spectral imagery). Duro et al. (2012) compared the performance between three non-parametric classifiers: DT, RF, and SVM. They found that object-based classification using the DT algorithm had lower overall classification accuracy (88.84%) than the RF (93.39%) and the SVM

(94.21%) classifiers. Furthermore, statistical assessment of the classification results showed that there were statistically significant differences between DT and SVM algorithms and DT and RF algorithms. On the other hand, Otukei and Blaschke (2010) found that DT generally performed better than classifications produced using SVM. Pal (2005) showed that both SVM and RF algorithms produced similar classification accuracies.

Because this thesis mainly uses machine learning SVM and RF algorithms, these are reviewed in detail in the following subsections. The reason why the SVM and RF are used in this thesis is explained in Chapter 3 and 5. Naïve Bayes and Logistic Regressions are reviewed in Chapter 5.

2.5.1 Support Vector Machine

The theory of SVM was developed by Vapnik (1995). The SVM algorithm determines a hyperplane that separates the dataset into a discrete number of classes (Han et al., 2012). The basic theory of SVM is explained by Vapnik (1995) and Hastie et al. (2009) using the following mathematical nomenclature: Given the training data T with N samples: $T = \{(x_1, y_1), (x_2, y_2), \dots, (x_n, y_n)\}$, where $x_i \in \mathbb{R}^d$ and $y_i \in \{-1, 1\}$, $i=1, 2, \dots, n$. With the linear data, the separating hyperplane which classifies the data input can be written as:

$$f(x) = w^T \cdot x + b = \sum_{i=1}^N (w^T x_i + b) = 0, \quad (2.1)$$

where w is a N -dimensional vector and b is a scalar.

The separating hyperplane satisfies the following constraint in order for data points to lie on the correct side of the margin:

$$y_i f(x_i) = y_i (w^T x_i + b) \geq 1, \forall i (i = 1, \dots, N). \quad (2.2)$$

The separating hyperplane which has the maximum distance between the plane and the nearest training data (or the maximum margin) is the optimal separating hyperplane. The nearest data samples that are used to define the margin are support vectors, shown as thick borders (see Figure 2.1).

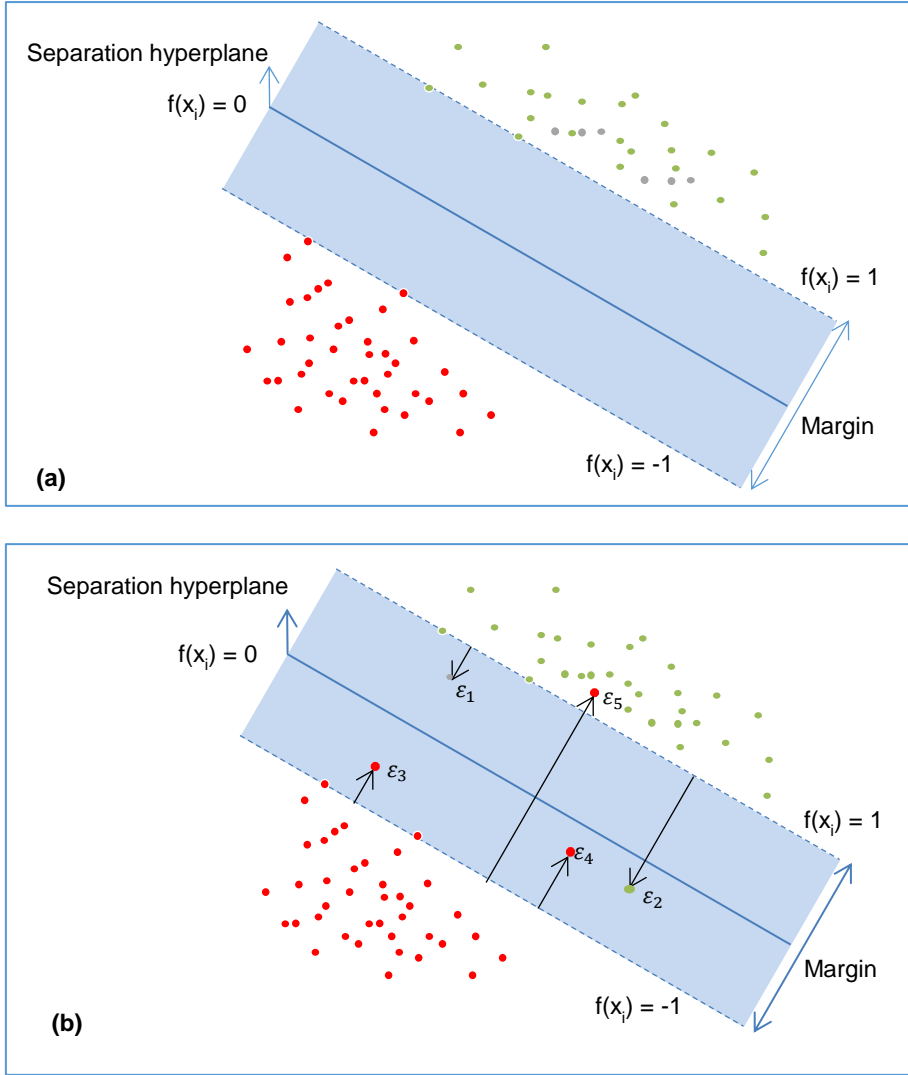


Figure 2.1. The (a) panel shows the linear SVM separable case while the (b) panel shows the linearly non-separable case. Source: adapted from Hastie et al. (2009).

Geometrically, the margin is equal to $\frac{2}{\|w\|}$. To maximize the distance between the plane and the nearest training data, $\|w\|$ should be minimized. Therefore, the optimal separating hyperplane for classifying two different categories of data can be obtained as a solution to the following optimization problem:

$$\min_{w,b} \|w\| \quad (2.3)$$

subject to the constraint (2.2)

When introducing the slack variables ϵ_i to intensify the generalization, the optimization problem is modified to:

$$\min_{w,b}(\|w\|) \text{ subject to } \begin{cases} y_i(w^T x_i + b) \geq 1 - \varepsilon_i, \forall i (i = 1, \dots, N), \\ \varepsilon_i \geq 0, \sum \varepsilon_i \leq \text{constant} \end{cases} \quad (2.4)$$

The slack variables measure the distance between the margin and the data point that lies beyond the correct margin. The problem (2.4) is quadratic with linear inequality constraints, therefore it is a convex optimization problem. For computational convenience, (2.4) is re-expressed in the equivalent form:

$$\min_{w,b} \left(\frac{1}{2} \|w\|^2 \right) + C \sum_{i=1}^N \varepsilon_i \quad (2.5)$$

$$\text{subject to } \varepsilon_i \geq 0, y_i(w^T x_i + b) \geq 1 - \varepsilon_i, \forall i,$$

where the parameter C replaces the constant in (2.4)

To optimize (2.5), the Lagrange (primal) function is applied:

$$L(w, b, \varepsilon_i) = \frac{1}{2} \|w\|^2 + C \sum_{i=1}^N \varepsilon_i - \sum_{i=1}^N \alpha_i [y_i(w^T x_i + b) - (1 - \varepsilon_i)] - \sum_{i=1}^N \mu_i \varepsilon_i \quad (2.6)$$

Setting the derivatives of L with respect to w , b , and ε_i to zero, we get:

$$w = \sum_{i=1}^N \alpha_i y_i x_i, \quad (2.7)$$

$$0 = \alpha_i y_i, \quad (2.8)$$

$$\alpha_i = C - \mu_i, \forall i, \quad (2.9)$$

Substituting (2.7), (2.8), (2.9) into (2.6), we get the Lagrangian dual problem:

$$\text{maximize } L(\alpha) = \sum_{i=1}^N \alpha_i - \frac{1}{2} \sum_{i=1}^N \sum_{j=1}^N \alpha_i \alpha_j y_i y_j x_i x_j \quad (2.10)$$

$$\text{subject to } 0 \leq \alpha_i \leq C,$$

$$\sum_{i=1}^N \alpha_i y_i = 0$$

The coefficients α_i is obtained by solving the dual optimization problem. Then, the decision function is define by:

$$f(x) = \text{sign}(\sum_{i,j=1}^N \alpha_i y_i (x_i x_j) + b) \quad (2.11)$$

In the nonlinear SVM classification, the nonlinear vector function $\phi(x) = (\phi_1(x), \dots, \phi_m(x))$ is used to map the input data into a higher dimensional feature space:

$$f(x) = w^T \phi(x) + b \quad (2.12)$$

The Lagrangian dual problem is given by:

$$L(\alpha) = \sum_{i=1}^N \alpha_i - \frac{1}{2} \sum_{i=1}^N \sum_{j=1}^N \alpha_i \alpha_j y_i y_j \phi^T(x_i) \phi(x_j) \quad (2.13)$$

The decision function is written as:

$$f(x) = \text{sign} \left(\sum_{i,j=1}^N \alpha_i y_i \left(\phi^T(x_i) \cdot \phi(x_j) \right) + b \right) \quad (2.14)$$

The high dimensional feature space can cause computational problem. To solve this problem, the kernel function K is used where:

$$K(x_i, x_j) = \phi^T(x_i) \cdot \phi(x_j), \quad (2.15)$$

When applying the kernel function, (2.14) becomes:

$$f(x) = \text{sign} \left(\sum_{i,j=1}^N \alpha_i y_i K(x_i, x_j) + b \right) \quad (2.16)$$

2.5.2 *Random Forest*

RF is an ensemble method that combines multiple decision trees and obtains results by aggregating the predictions from all individual trees (majority votes for classification, average for regression). Random forest was developed by Breiman (2001a). The advantages of RF compared to other tree ensemble methods are: (1) high accuracy for prediction outcomes, (2) robustness to outliers and noise, (3) fast computation speed, and (4) ability to estimate the importance of predictor variables (Cutler et al., 2007; Rodriguez-Galiano et al., 2012). In addition, RF can use a large number of predictor variables (Breiman, 2001a; Chaudhary et al., 2015). These characteristics led to the use of RF for this research.

RF is built using bagging (bootstrap aggregating) with random predictor selection (Breiman, 2001a). The process involves the following steps:

- (1) Given the training dataset of size k , bagging generates n new training datasets D_i ($i = 1, 2, \dots, n$) - the same size as the original dataset - by picking data randomly with replacement from the original dataset. This is called a bootstrap sample. Some data points in the original dataset can be used more than once to generate a bootstrap sample while others may never be used (Belgiu and Drăguț, 2016).
- (2) The bootstrap samples are then used to build decision trees (*ntree*). To construct a decision tree, a random subset of the predictors (*mtry*) is used to determine the best split at each node of the tree (Breiman, 2001a). Such a

random predictive variable selection reduces correlation among trees, which decreases bias (Breiman, 2001a; Prasad et al., 2006). The trees are grown to maximum size and not pruned, hence the computation is light (Rodriguez-Galiano et al., 2012).

(3) The prediction at a target point x results from majority votes (for classification) and average (for regression) from the predictions of all trees. It is usual for 2/3 of data points from the original dataset to be included in a bootstrap sample ('in bag' data) while the 1/3 remaining data set is excluded from the bootstrap sample – known as 'out-of-bag' (OOB) data (Rodriguez-Galiano et al., 2012). The OOB data are used to calculate a prediction error, known as the OOB error estimate, by contrasting the predictions from the in-bag data and the OOB data (Poulos and Camp, 2010). The OOB samples are also used to measure the variable importance (the prediction strength of each variable) by changing randomly the values of a given variable in the OOB samples. The increase of OOB error from these changes are averaged over all trees and is a measure of the importance of the variable (Hastie et al., 2009).

2.6 Accuracy assessment

The error matrix is the most commonly used approach for classification accuracy assessment (Comber et al., 2012; Foody, 2002; Lu and Weng, 2007). An error matrix is a square array of rows and columns in which columns express the reference data and rows represent the classification produced from remotely sensed data (Congalton and Green, 2008; Lillesand et al., 2014). Important accuracy measures such as overall accuracy and kappa coefficient can be derived from the error matrix (Congalton and Green, 2008). The advantage of overall accuracy is its easy interpretation as a proportion of the correctly classified sample units to the total number of the sample units (Congalton and Green, 2008). The Kappa coefficient is considered as a powerful method for assessing statistical difference between classifications (Congalton, 1991; Congalton and Green, 2008).

Three additional indices are useful to evaluate the performance of the classifications. These include quantity disagreement (QD), allocation disagreement (AD), and total disagreement (TD) developed by Pontius Jr and Millones (2011). The quantity disagreement is defined as the difference in the proportions of the categories

between the reference map and the predicted map. The allocation disagreement represents the amount of difference between the reference map and the predicted map, based on the spatial allocation of the categories. Total disagreement is the sum of the quantity disagreement and the allocation disagreement.

Studies assessing the performance of different classifiers often use the same testing and training samples (Duro et al., 2012; Foody, 2004). Therefore, the samples are not independent and a statistical comparison using Kappa coefficient which requires independent samples is inappropriate (Foody, 2004). In such case, using McNemar's test, a non-parametric test based on confusion matrixes and on the binary distinction between correct and incorrect class allocations is suggested (Foody, 2004; Pal and Foody, 2010).

$$\chi^2 = \frac{(f_{12} - f_{21})^2}{f_{12} + f_{21}}$$

in which f_{12} and f_{21} , respectively, are the number of points correctly identified by one classifier and not the other.

2.7 Conclusion

There are now a wide range of image analysis techniques to consider. This review has highlighted the development of object based techniques as an advancement over pixel based techniques. OBIA can be used with both remotely sensed data and GIS derived data to improve classification. In considering OBIA it is necessary to determine the appropriate segmentation parameters and classifiers. There are now a wide range of classifiers to choose from that go beyond consideration of supervised versus non supervised techniques. Machine learning is a relatively new classifier technique used for remote sensing, and there is a wide range of machine learning techniques to choose from. Research that tests the performance of these different techniques as well as different combinations of techniques and parameters is necessary.

REFERENCES

- Aguirre-Gutiérrez, J., Seijmonsbergen, A.C., Duivenvoorden, J.F., 2012. Optimizing land cover classification accuracy for change detection, a combined pixel-based and object-based approach in a mountainous area in Mexico. *Applied Geography* 34, 29-37. <https://doi.org/10.1016/j.apgeog.2011.10.010>
- Belgiu, M., Drăguț, L., 2016. Random forest in remote sensing: A review of applications and future directions. *ISPRS Journal of Photogrammetry and Remote Sensing* 114, 24-31. <https://doi.org/10.1016/j.isprsjprs.2016.01.011>
- Blaschke, T., 2010. Object based image analysis for remote sensing. *ISPRS Journal of Photogrammetry and Remote Sensing* 65(1), 2-16. <https://doi.org/10.1016/j.isprsjprs.2009.06.004>
- Blaschke, T., Burnett, C., Pekkarinen, A., 2004. Image segmentation methods for object-based analysis and classification, in: de Jong, S.M., van der Meer, F.D. (Eds.), *Remote Sensing Image Analysis: Including the Spatial Domain*. Springer, Dordrecht, pp. 211-236.
- Blaschke, T., Feizizadeh, B., Hölbling, D., 2014a. Object-based image analysis and digital terrain analysis for locating landslides in the Urmia Lake basin, Iran. *IEEE Journal of Selected Topics in Applied Earth Observations and Remote Sensing* 7(12), 4806-4817. <https://doi.org/10.1109/JSTARS.2014.2350036>
- Blaschke, T., Hay, G.J., Kelly, M., Lang, S., Hofmann, P., Addink, E., Queiroz Feitosa, R., van der Meer, F., van der Werff, H., van Coillie, F., Tiede, D., 2014b. Geographic object-based image analysis – towards a new paradigm. *ISPRS Journal of Photogrammetry and Remote Sensing* 87, 180-191. <https://doi.org/10.1016/j.isprsjprs.2013.09.014>
- Breiman, L., 2001a. Random forests. *Machine Learning* 45(1), 5-32. <https://doi.org/10.1023/A:1010933404324>
- Bunting, P., Lucas, R., 2006. The delineation of tree crowns in Australian mixed species forests using hyperspectral Compact Airborne Spectrographic Imager (CASI) data. *Remote Sensing of Environment* 101(2), 230-248. <https://doi.org/10.1016/j.rse.2005.12.015>
- Burnett, C., Blaschke, T., 2003. A multi-scale segmentation/object relationship modelling methodology for landscape analysis. *Ecological Modelling* 168(3), 233-249. [https://doi.org/10.1016/S0304-3800\(03\)00139-X](https://doi.org/10.1016/S0304-3800(03)00139-X)
- Chaudhary, N., Sharma, A.K., Agarwal, P., Gupta, A., Sharma, V.K., 2015. 16S classifier: a tool for fast and accurate taxonomic classification of 16S rRNA hypervariable regions in metagenomic datasets. *PloS One* 10(2), e0116106. <https://doi.org/10.1371/journal.pone.0116106>
- Chen, Q., Baldocchi, D., Gong, P., Kelly, M., 2006. Isolating individual trees in a savanna woodland using small footprint lidar data. *Photogrammetric Engineering & Remote Sensing* 72(8), 923-932. <https://doi.org/10.14358/PERS.72.8.923>
- Chuvieco, E., 2016. *Fundamentals of Satellite Remote Sensing: An Environmental Approach*, 2nd ed. CRC press, Boca Raton, FL.
- Comber, A., Fisher, P., Brunson, C., Khmag, A., 2012. Spatial analysis of remote sensing image classification accuracy. *Remote Sensing of Environment* 127(Supplement C), 237-246. <https://doi.org/https://doi.org/10.1016/j.rse.2012.09.005>

- Congalton, R.G., 1991. A review of assessing the accuracy of classifications of remotely sensed data. *Remote Sensing of Environment* 37(1), 35-46. [https://doi.org/10.1016/0034-4257\(91\)90048-B](https://doi.org/10.1016/0034-4257(91)90048-B)
- Congalton, R.G., Green, K., 2008. *Assessing the Accuracy of Remotely Sensed Data: Principles and Practices*. CRC Press, Boca Raton, FL.
- Cracknell, M.J., Reading, A.M., 2014. Geological mapping using remote sensing data: A comparison of five machine learning algorithms, their response to variations in the spatial distribution of training data and the use of explicit spatial information. *Computers & Geosciences* 63, 22-33. <https://doi.org/10.1016/j.cageo.2013.10.008>
- Cutler, D.R., Edwards, T.C., Beard, K.H., Cutler, A., Hess, K.T., Gibson, J., Lawler, J.J., 2007. Random forests for classification in ecology. *Ecology* 88(11), 2783-2792. <https://doi.org/10.1890/07-0539.1>
- Dalponte, M., Bruzzone, L., Gianelle, D., 2012. Tree species classification in the Southern Alps based on the fusion of very high geometrical resolution multispectral/hyperspectral images and LiDAR data. *Remote Sensing of Environment* 123, 258-270. <https://doi.org/10.1016/j.rse.2012.03.013>
- Duro, D.C., Franklin, S.E., Dubé, M.G., 2012. A comparison of pixel-based and object-based image analysis with selected machine learning algorithms for the classification of agricultural landscapes using SPOT-5 HRG imagery. *Remote Sensing of Environment* 118, 259-272. <https://doi.org/10.1016/j.rse.2011.11.020>
- Flanders, D., Hall-Beyer, M., Pereverzoff, J., 2003. Preliminary evaluation of eCognition object-based software for cut block delineation and feature extraction. *Canadian Journal of Remote Sensing* 29(4), 441-452.
- Foody, G.M., 2002. Status of land cover classification accuracy assessment. *Remote Sensing of Environment* 80(1), 185-201. [https://doi.org/10.1016/S0034-4257\(01\)00295-4](https://doi.org/10.1016/S0034-4257(01)00295-4)
- Foody, G.M., 2004. Thematic map comparison: Evaluating the statistical significance of differences in classification accuracy. *Photogrammetric Engineering & Remote Sensing* 70(5), 627-634.
- Fu, B., Wang, Y., Campbell, A., Li, Y., Zhang, B., Yin, S., Xing, Z., Jin, X., 2017. Comparison of object-based and pixel-based Random Forest algorithm for wetland vegetation mapping using high spatial resolution GF-1 and SAR data. *Ecological Indicators* 73, 105-117. <https://doi.org/10.1016/j.ecolind.2016.09.029>
- Gao, Y., Mas, J., Niemeyer, I., Marpu, P., Palacio, J., 2007. Object-based image analysis for mapping land-cover in a forest area, 5th International Symposium: Spatial Data Quality, Enschede, The Netherlands, pp. 13-15.
- Ghosh, A., Joshi, P., 2014. A comparison of selected classification algorithms for mapping bamboo patches in lower Gangetic plains using very high resolution WorldView 2 imagery. *International Journal of Applied Earth Observation and Geoinformation* 26, 298-311. <https://doi.org/10.1016/j.jag.2013.08.011>
- Han, J., Kamber, M., Pei, J., 2012. *Data Mining: Concepts and Techniques*, 3rd ed. Morgan Kaufmann, Boston, MA.
- Han, N., Du, H., Zhou, G., Sun, X., Ge, H., Xu, X., 2014. Object-based classification using SPOT-5 imagery for Moso bamboo forest mapping. *International Journal of Remote Sensing* 35(3), 1126-1142. <https://doi.org/10.1080/01431161.2013.875634>

- Hastie, T.J., Tibshirani, R.J., Friedman, J.H., 2009. *The Elements of Statistical Learning: Data Mining, Inference, and Prediction*. Springer, New York, NY.
- Houborg, R., Fisher, J.B., Skidmore, A.K., 2015. Advances in remote sensing of vegetation function and traits. *International Journal of Applied Earth Observation and Geoinformation* 43, 1-6. <https://doi.org/10.1016/j.jag.2015.06.001>
- Hussin, Y., Gilani, H., Leeuwen, L., Murthy, M.S.R., Shah, R., Baral, S., Tsendbazar, N.-E., Shrestha, S., Shah, S., Qamer, F., 2014. Evaluation of object-based image analysis techniques on very high-resolution satellite image for biomass estimation in a watershed of hilly forest of Nepal. *Appl Geomat* 6(1), 59-68. <https://doi.org/10.1007/s12518-014-0126-z>
- Jakubowski, M.K., Li, W., Guo, Q., Kelly, M., 2013. Delineating individual trees from Lidar data: A comparison of vector-and raster-based segmentation approaches. *Remote Sensing* 5(9), 4163-4186. <https://doi.org/10.3390/rs5094163>
- Ke, Y., Quackenbush, L.J., 2011. A review of methods for automatic individual tree-crown detection and delineation from passive remote sensing. *International Journal of Remote Sensing* 32(17), 4725-4747. <https://doi.org/10.1080/01431161.2010.494184>
- Kim, M., Madden, M., Warner, T.A., 2009a. Forest type mapping using object-specific texture measures from multispectral IKONOS imagery: Segmentation quality and image classification issues. *Photogrammetric Engineering and Remote Sensing* 75(7), 819-829.
- Korpela, I., Dahlin, B., Schäfer, H., Bruun, E., Haapaniemi, F., Honkasalo, J., Ilvesniemi, S., Kuutti, V., Linkosalmi, M., Mustonen, J., 2007. Single-tree forest inventory using lidar and aerial images for 3D treetop positioning, species recognition, height and crown width estimation, *Proceedings of ISPRS Workshop on Laser Scanning*, pp. 227-233.
- Lang, S., 2008. Object-based image analysis for remote sensing applications: Modeling reality—dealing with complexity, in: Blaschke, T., Lang, S., Hay, G.J. (Eds.), *Object-Based Image Analysis*. Springer-Verlag, Berlin, pp. 3-27.
- Lang, S., Langanke, T., 2006. Object-based mapping and object-relationship modeling for land use classes and habitats. *Photogrammetrie Fernerkundung Geoinformation* 2006(1), 5.
- Larsen, M., Eriksson, M., Descombes, X., Perrin, G., Brandtberg, T., Gougeon, F.A., 2011. Comparison of six individual tree crown detection algorithms evaluated under varying forest conditions. *International Journal of Remote Sensing* 32(20), 5827-5852. <https://doi.org/10.1080/01431161.2010.507790>
- Leckie, D., Gougeon, F., Hill, D., Quinn, R., Armstrong, L., Shreenan, R., 2003. Combined high-density lidar and multispectral imagery for individual tree crown analysis. *Canadian Journal of Remote Sensing* 29(5), 633-649. <https://doi.org/10.5589/m03-024>
- Li, W., Guo, Q., Jakubowski, M.K., Kelly, M., 2012. A new method for segmenting individual trees from the lidar point cloud. *Photogrammetric Engineering & Remote Sensing* 78(1), 75-84.
- Li, X., Meng, Q., Gu, X., Jancso, T., Yu, T., Wang, K., Mavromatis, S., 2013. A hybrid method combining pixel-based and object-oriented methods and its application in Hungary using Chinese HJ-1 satellite images. *International*

- journal of remote sensing 34(13), 4655-4668.
<https://doi.org/10.1080/01431161.2013.780669>
- Lillesand, T., Kiefer, R.W., Chipman, J., 2014. Remote sensing and image interpretation. John Wiley & Sons, Hoboken, NJ.
- Liu, D., Xia, F., 2010. Assessing object-based classification: advantages and limitations. Remote Sensing Letters 1(4), 187-194.
<https://doi.org/10.1080/01431161003743173>
- Löw, F., Conrad, C., Michel, U., 2015. Decision fusion and non-parametric classifiers for land use mapping using multi-temporal RapidEye data. ISPRS Journal of Photogrammetry and Remote Sensing 108, 191-204.
<https://doi.org/10.1016/j.isprsjprs.2015.07.001>
- Lu, D., Weng, Q., 2007. A survey of image classification methods and techniques for improving classification performance. International Journal of Remote Sensing 28(5), 823-870. <https://doi.org/10.1080/01431160600746456>
- MacFaden, S.W., O'Neil-Dunne, J.P.M., Royar, A.R., Lu, J.W.T., Rundle, A.G., 2012. High-resolution tree canopy mapping for New York City using LIDAR and object-based image analysis. J Appl Remote Sens 6(1), 063567-063561-063567-063523. <https://doi.org/10.1117/1.JRS.6.063567>
- Mishra, N.B., Crews, K.A., 2014. Mapping vegetation morphology types in a dry savanna ecosystem: integrating hierarchical object-based image analysis with Random Forest. International Journal of Remote Sensing 35(3), 1175-1198. <https://doi.org/10.1080/01431161.2013.876120>
- Myint, S.W., Giri, C.P., Wang, L., Zhu, Z., Gillette, S.C., 2008. Identifying mangrove species and their surrounding land use and land cover classes using an object-oriented approach with a lacunarity spatial measure. GIScience & Remote Sensing 45(2), 188-208.
<https://doi.org/10.2747/1548-1603.45.2.188>
- Olofsson, K., Wallerman, J., Holmgren, J., Olsson, H., 2006. Tree species discrimination using Z/I DMC imagery and template matching of single trees. Scandinavian Journal of Forest Research 21(S7), 106-110.
<https://doi.org/10.1080/14004080500486955>
- Otukei, J., Blaschke, T., 2010. Land cover change assessment using decision trees, support vector machines and maximum likelihood classification algorithms. International Journal of Applied Earth Observation and Geoinformation 12, S27-S31. <https://doi.org/10.1016/j.jag.2009.11.002>
- Ouyang, Z.-T., Zhang, M.-Q., Xie, X., Shen, Q., Guo, H.-Q., Zhao, B., 2011. A comparison of pixel-based and object-oriented approaches to VHR imagery for mapping saltmarsh plants. Ecological Informatics 6(2), 136-146.
<https://doi.org/10.1016/j.ecoinf.2011.01.002>
- Pal, M., 2005. Random forest classifier for remote sensing classification. International Journal of Remote Sensing 26(1), 217-222.
<https://doi.org/10.1080/01431160412331269698>
- Pal, M., Foody, G.M., 2010. Feature selection for classification of hyperspectral data by SVM. IEEE Transactions on Geoscience and Remote Sensing 48(5), 2297-2307. <https://doi.org/10.1109/TGRS.2009.2039484>
- Pal, N.R., Pal, S.K., 1993. A review on image segmentation techniques. Pattern recognition 26(9), 1277-1294. [https://doi.org/10.1016/0031-3203\(93\)90135-J](https://doi.org/10.1016/0031-3203(93)90135-J)
- Pettorelli, N., Lurance, W.F., O'Brien, T.G., Wegmann, M., Nagendra, H., Turner, W., 2014. Satellite remote sensing for applied ecologists: opportunities and

- challenges. *Journal of Applied Ecology* 51(4), 839-848.
<https://doi.org/10.1111/1365-2664.12261>
- Pontius Jr, R.G., Millones, M., 2011. Death to Kappa: Birth of quantity disagreement and allocation disagreement for accuracy assessment. *International Journal of Remote Sensing* 32(15), 4407-4429.
<https://doi.org/10.1080/01431161.2011.552923>
- Poulos, H.M., Camp, A.E., 2010. Decision support for mitigating the risk of tree induced transmission line failure in utility rights-of-way. *Environmental Management* 45(2), 217-226. <https://doi.org/10.1007/s00267-009-9422-5>
- Prasad, A.M., Iverson, L.R., Liaw, A., 2006. Newer classification and regression tree techniques: bagging and random forests for ecological prediction. *Ecosystems* 9(2), 181-199.
- Raczko, E., Zagajewski, B., 2017. Comparison of support vector machine, random forest and neural network classifiers for tree species classification on airborne hyperspectral APEX images. *European Journal of Remote Sensing* 50(1), 144-154. <https://doi.org/10.1080/22797254.2017.1299557>
- Rodriguez-Galiano, V.F., Ghimire, B., Rogan, J., Chica-Olmo, M., Rigol-Sanchez, J.P., 2012. An assessment of the effectiveness of a random forest classifier for land-cover classification. *ISPRS Journal of Photogrammetry and Remote Sensing* 67, 93-104. <https://doi.org/10.1016/j.isprsjprs.2011.11.002>
- Van Coillie, F.M.B., Verbeke, L.P.C., De Wulf, R.R., 2007. Feature selection by genetic algorithms in object-based classification of IKONOS imagery for forest mapping in Flanders, Belgium. *Remote Sensing of Environment* 110(4), 476-487. <https://doi.org/10.1016/j.rse.2007.03.020>
- Vapnik, V.N., 1995. *The Nature of Statistical Learning Theory*. Springer-Verlag, New York, NY.
- Wang, L., Sousa, W.P., Gong, P., 2004a. Integration of object-based and pixel-based classification for mapping mangroves with IKONOS imagery. *International Journal of Remote Sensing* 25(24), 5655-5668.
<https://doi.org/10.1080/014311602331291215>
- Wang, Y., 2009. *Remote Sensing of Coastal Environments*. CRC Press, Boca Raton, FL.
- Whiteside, T.G., Boggs, G.S., Maier, S.W., 2011. Comparing object-based and pixel-based classifications for mapping savannas. *International Journal of Applied Earth Observation and Geoinformation* 13(6), 884-893.
<https://doi.org/10.1016/j.jag.2011.06.008>
- Yu, Q., Gong, P., Clinton, N., Biging, G., Kelly, M., Schirokauer, D., 2006. Object-based detailed vegetation classification with airborne high spatial resolution remote sensing imagery. *Photogrammetric Engineering and Remote Sensing* 72(7), 799-811.
- Zhen, Z., Quackenbush, L.J., Zhang, L., 2014. Impact of tree-oriented growth order in marker-controlled region growing for individual tree crown delineation using Airborne Laser Scanner (ALS) data. *Remote Sensing* 6(1), 555-579.
<https://doi.org/10.3390/rs6010555>

CHAPTER 3

COMBINING QUICKBIRD, LIDAR, AND GIS TOPOGRAPHY INDICES TO IDENTIFY A SINGLE NATIVE TREE SPECIES IN A COMPLEX LANDSCAPE USING AN OBJECT-BASED CLASSIFICATION APPROACH

This chapter was published as following: “Pham, L.T.H., Brabyn, L., Ashraf, S., 2016. Combining QuickBird, LiDAR, and GIS topography indices to identify a single native tree species in a complex landscape using an object-based classification approach. International Journal of Applied Earth Observation and Geoinformation 50, 187-197”. <https://doi.org/10.1016/j.jag.2016.03.015>

Abstract

There are now a wide range of techniques that can be combined for image analysis. These include the use of object-based classifications rather than pixel-based classifiers, the use of LiDAR to determine vegetation height and vertical structure, as well terrain variables such as topographic wetness index and slope that can be calculated using GIS. This research investigates the benefits of combining these techniques to identify individual tree species. A QuickBird image and low point density LiDAR data for a coastal region in New Zealand was used to examine the possibility of mapping Pohutukawa trees which are regarded as an iconic tree in New Zealand. The study area included a mix of buildings and vegetation types. After image and LiDAR preparation, single tree objects were identified using a range of techniques including: a threshold of above ground height to eliminate ground based objects; Normalised Difference Vegetation Index and elevation difference between the first and last return of LiDAR data to distinguish vegetation from buildings; geometric information to separate clusters of trees from single trees, and treetop identification and region growing techniques to separate tree clusters into single tree crowns. Important feature variables were identified using Random Forest, and the Support Vector Machine provided the classification. The combined techniques using LiDAR and spectral data produced an overall accuracy of 85.4% (Kappa 80.6%). Classification using just the spectral data produced an overall accuracy of 75.8% (Kappa 67.8%). The research findings demonstrate how the combining of LiDAR and spectral data improves classification for Pohutukawa trees.

Keywords: Object-based classification; Pohutukawa; Random Forest; Support Vector Machine, QuickBird; LiDAR

3.1 Introduction

It is often important to map single tree species, such as when a tree has high ecological or cultural significance, and requires intensive management because it is under threat. Pohutukawa (*Metrosideros excelsa* Sol. ex Gaertn) is such a tree in New Zealand because it has been subject to fires and land clearance, and more recently possum browsing (Bylsma et al., 2014). Pohutukawa is a multi-stemmed tree up to 25m high with large rounded crowns growing in northern coastal regions of New Zealand. Providing accurate information about the distribution of this species is necessary to help managers decide on appropriate conservation strategies.

Remote sensing and image analysis is advancing quickly with the capture of high spatial resolution data, which includes multispectral images as well as LiDAR. There have also been advances in data analysis techniques, including object based image analysis (OBIA), combining GIS terrain analysis, and advanced classifier algorithms. In the past, remote sensing of vegetation has focused on identifying broad vegetation classes, but advances in data and analysis techniques make it possible to identify specific vegetation species. LiDAR data produces accurate information on the vertical vegetation structure, which has been used for tree species classification (Kim et al., 2009b; Ørka et al., 2009). LiDAR has also been combined with multispectral information to identify species (Cho et al., 2012; Dalponte et al., 2012).

OBIA has become increasingly popular over the last decade (Blaschke, 2010) because it provides a higher accuracy of classification compared to traditional pixel-based approaches (Ouyang et al., 2011). OBIA integrates spectral properties and spatial and contextual information into the classification process (Blaschke, 2010; Han et al., 2014), and can be combined with multi-scale analysis to classify at regional and individual tree scales (Blaschke, 2010).

An important first step in OBIA is image segmentation which divides an image into contiguous, separate and homogeneous areas called image objects (Blaschke et al., 2004). For segmenting individual tree crowns, various automated methods have been developed and include: template matching (Korpela et al., 2007; Olofsson et al., 2006); valley following (Leckie et al., 2003); watershed segmentation (Chen et al., 2006); and region growing (Bunting and Lucas, 2006; Zhen et al., 2014). For some crown delineation algorithms the prior detection of treetops is required, which often uses the local maximum filtering technique with fixed or variable window sizes (Chen et al., 2006; Zhen et al., 2014). The local maximum technique is based

on the assumption that treetops have the highest reflectance (multispectral images) or the highest elevation value (LiDAR data) within a tree crown. Using variable window sizes to identify treetops provides higher accuracy than a fixed window size (Gebreslasie et al., 2011).

The region growing method for crown delineation has outperformed other methods such as valley-following (Hussin et al., 2014) and template matching (Larsen et al., 2011) in both mixed and dense forests. The region growing method starts with a set of seed pixels (treetops), which are then merged to adjacent pixels that are similar (Ke and Quackenbush, 2011). This process of growing continues until a threshold is reached, and defined by specified homogeneity criteria (Blaschke et al., 2004).

In this study, the support vector machine (SVM), a non-parametric classifier, was used because the number of training samples was small. With small training data sets, the SVM is the preferred classifier because it has good generalization ability (Mountrakis et al., 2011). In addition, a non-parametric classifier does not need an assumption of a normal distribution of the dataset; thus it is suitable for the integration of non-spectral data into a classification process (Lu and Weng, 2007). SVM can also produce more accurate classification results than other traditional parametric classifiers in a complex landscape (Dalponte et al., 2009). SVM algorithm finds the best decision boundary that separates the dataset into discrete classes with minimal misclassification (Mountrakis et al., 2011). A SVM can be nonlinear and linear, however, the nonlinear SVM is proving to be more accurate for nonlinear, complex classification problems (Izenman, 2008). An important pre-process for SVM is selecting relevant features, which improves the classification accuracy and computational efficiency (Huang and Wang, 2006).

Although recent studies on tree species mapping have used a combination of multispectral and LiDAR data with OBIA (and produced promising results), the combined technique requires further testing on a range of species, contexts, and input data, including the inclusion of additional GIS generated feature objects, such as the terrain wetness index. It is clear that humans use surrounding context information when manually identifying individual trees from an image, and it is well known that water is a key driver of vegetation distribution. It therefore makes sense that topographical indices well established in the GIS and ecological literature are included. This study therefore combines LiDAR and QuickBird imagery to: (1) develop an OBIA workflow for segmentation and classification of Pohutukawa

trees, and (2) identify which object features are important based on classification accuracy. For comparison other broad classes of vegetation are also classified.

3.2 Materials

3.2.1 Study area

The research area is the Eastern side of the Coromandel region (see Figure 3.1) at between 36°48'30"S to 36°47'30"S latitude, and 175°38'30"E and 175°47'30"E longitude. The total area of the study site is 1277.76 ha. The site is characterized by different land cover types including built-up area, urban parkland/open space, and both coniferous and broadleaf species.

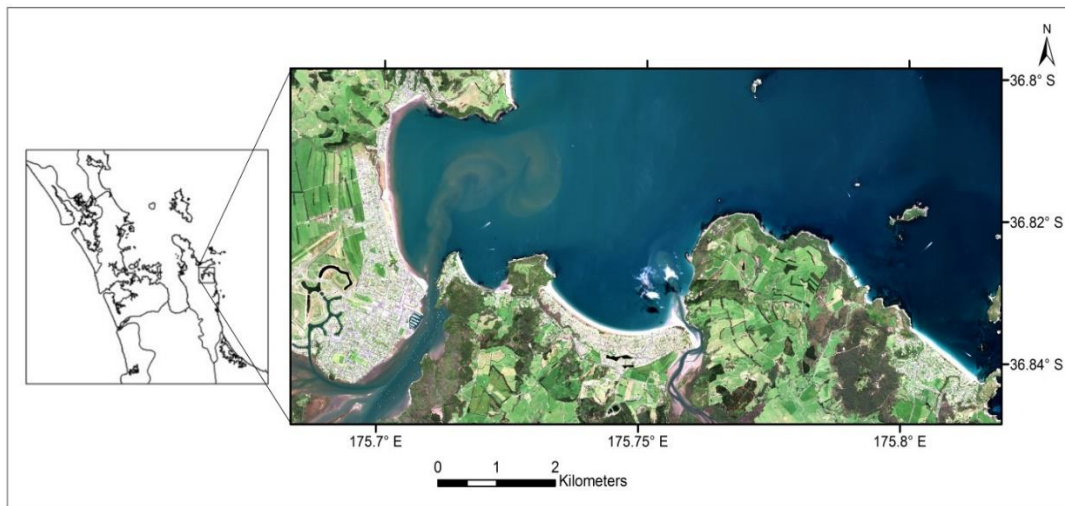


Figure 3.1. QuickBird image of the Coromandel study area. The coordinate is in NZTM2000 projection system.

3.2.2 Field data collection

Details of field data collected are shown in Table 3.1. The position of 560 trees was randomly selected and the species type recorded. Of these trees, 320 (57%) were used as training data and the remaining were used for accuracy assessment. Tree heights and crown diameters (mean of the N–S and E–W directions) of 90 trees were measured to determine the relationship between these variables, which are used for the treetop algorithm. These crowns were also manually mapped, which was required for assessing the segmentation accuracy.

Table 3.1. Ground-truthed data

a) Training and validation datasets

Species	No. of crowns for training data	No. of crowns for validation data
Pohutukawa	80	60
Other broadleaf species	80	60
Coniferous species	80	60
Manuka	80	60

b) Descriptive statistics of tree height and crown size from field inventory data

	Minimum	Median	Mean	Maximum	Standard deviation
Tree height (m)	2.32	13.04	13.61	34.55	4.95
Crown size (m)	2.78	14.58	15.14	28.04	4.49

3.2.3 Image data

Two main data sets were used – a QuickBird image and a LiDAR point cloud. The QuickBird multispectral image was captured on November 5th, 2010 (Figure 3.1), and had a panchromatic band (450-900nm) with 0.6m spatial resolution, and four multispectral bands - blue (450–520 nm), green (520–600 nm), red (630–690 nm), and NIR (760–900 nm) - with 2.4m spatial resolution. The LiDAR data set was captured during Feb and March, 2013 using NZAM's Optech 3100EA LiDAR system (flight height 1,300 metres above lowest ground and scan angle of 22 degrees either side of nadir). The outgoing laser pulse rate was 70kHz and the mirror scan frequency was 34 Hz. The maximum returns for each pulse was four and the average point density was 1.2 point/m².

3.3 Methods

Figure 3.2 provides an overview of the method developed and a detailed description and justification of the five main steps is discussed further in the following sections.

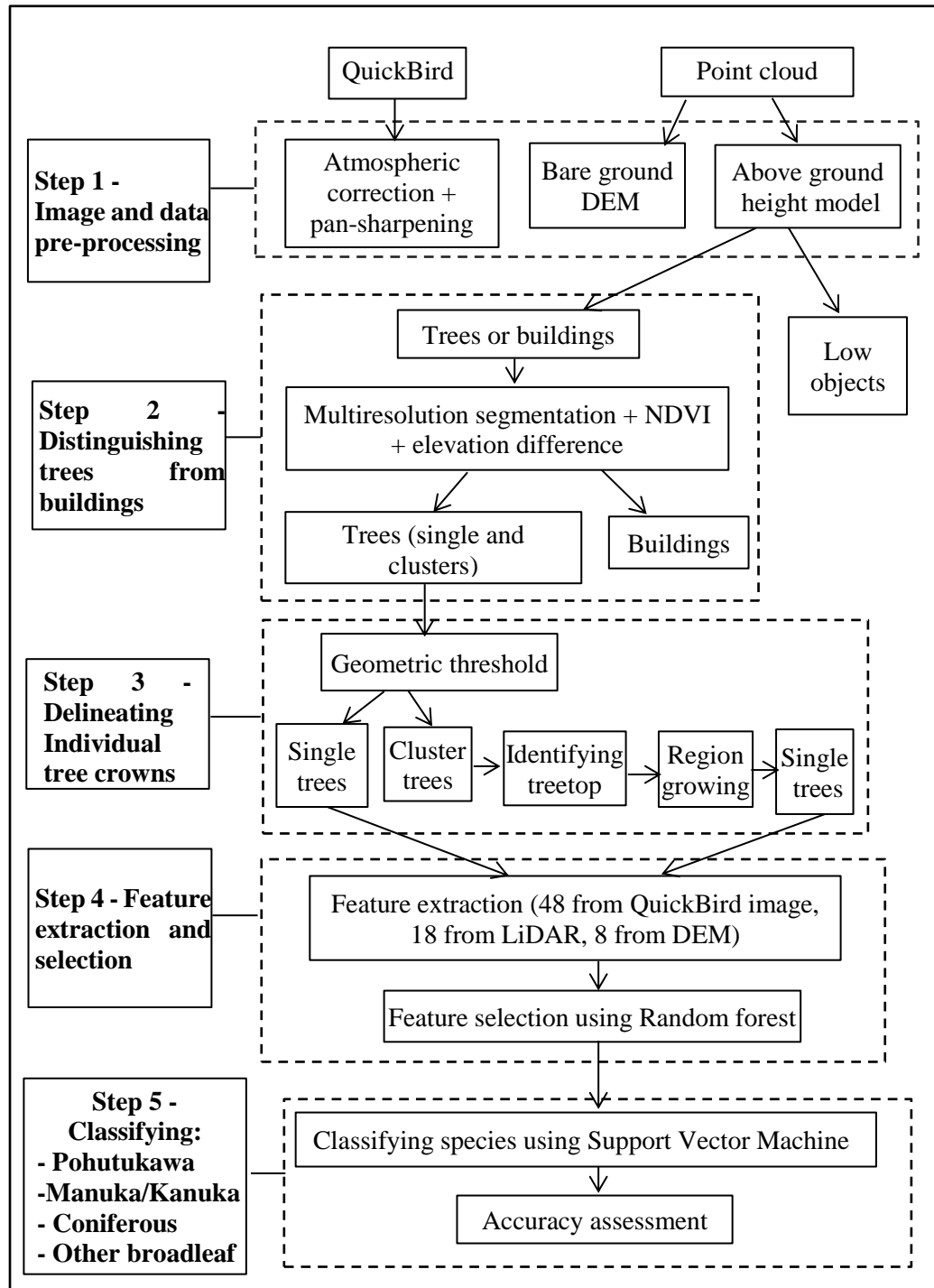


Figure 3.2. Workflow of tree species classification

3.3.1 Step 1 - Image and data pre-processing

The QuickBird image was atmospherically corrected using the Atmospheric Correction Algorithm, ATCOR-3 developed by Richter and Schläpfer (2014). The hue-saturation-intensity method was chosen for panchromatic sharpening because

it has been proven to obtain the best balance between the spectral and spatial information for QuickBird imagery (Arenas-Castro et al., 2012).

A 1m spatial resolution DEM was created using LAS2DEM in LAsTools (<http://rapidlasso.com>, version 6.1.7601). The LiDAR point cloud data was also used to derive a height above bare ground model (Figure 3.3), which involved removing “data pits”. Data pits are caused by the laser beams penetrating to a lower branch or the ground before generating the first return (Khosravipour et al., 2014). Data pits in the height model of the canopy decrease the tree detection accuracy if the tree detection is based on the identification of local maxima in the canopy height model. The data pits were removed using the method developed by Khosravipour et al. (2014), which works by: 1) creating a standard canopy height model (CHM) from all first returns, and a partial CHM from only the first returns meeting or exceeding defined height thresholds; and then (2) merging both CHMs based on the highest value. This method provides a higher accuracy for tree detection than the Gaussian smoothing, and can be easily implemented in the LAsTools.

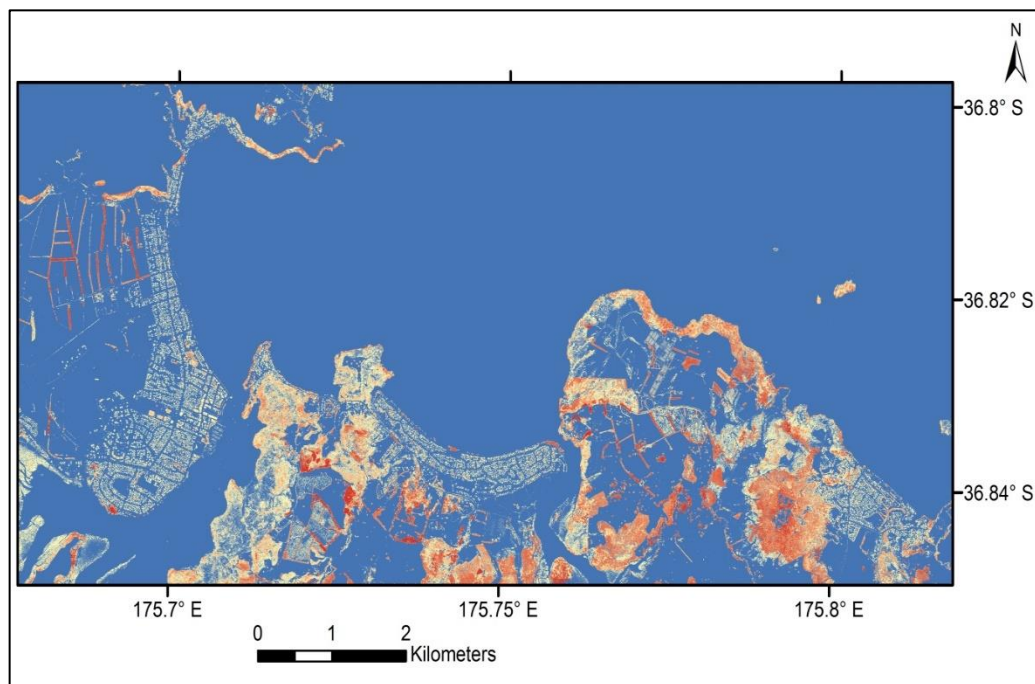


Figure 3.3. The LiDAR derived height above bare ground model

3.3.2 *Step 2 - Distinguishing trees from buildings*

Low land-cover types, such as grasslands, shrubs, bare ground, and coastal sand were identified using the above bare ground height model (with the value lower than 2m) and excluded because they are not trees. The process for distinguishing trees from buildings first used the multi-resolution segmentation function in eCognition to create image objects of trees and buildings. The four bands from the Quickbird image and the above bare ground height model were used as the input layers for this process (Ke et al., 2010). The average size of the image objects created was specified as a segmentation scale parameter, which affects the accuracy of the later image classification (Kim et al., 2011). A large segmentation scale results in buildings and neighbour trees being segmented into one object, while a small scale separates buildings into too many objects (Chen and Gao, 2014). A scale of 20 was selected based on comparing the segmentation quality of different parameter values.

A combination of elevation difference (calculated from LiDAR penetration) and NDVI (calculated from the QuickBird image) were used to distinguish tree objects from building objects. Figure 3.4 shows the decision steps that were used. Trees allow laser pulses to penetrate gaps between leaves (Chen and Gao, 2014), therefore the elevation value of the first return is significantly different to the last return for tree objects. For building roofs these values are the same and can therefore be used to distinguish the trees (Chen and Gao, 2014). NDVI was also used to improve the classification between trees and buildings because elevation difference can be similar for dense vegetation and buildings.

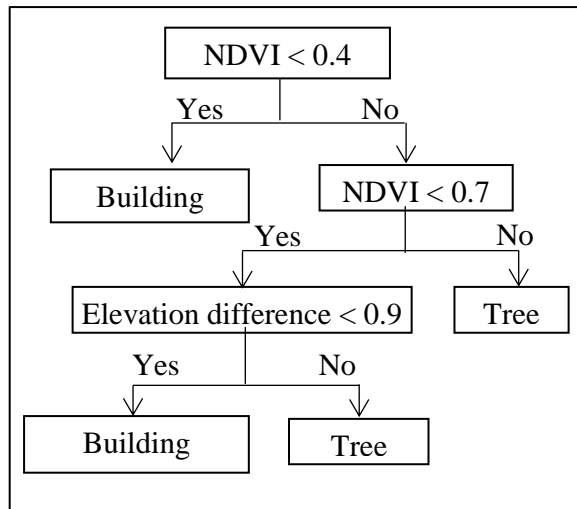


Figure 3.4. Decision steps for distinguishing trees and buildings

3.3.3 Step 3 - Delineating individual tree crowns

3.3.3.1 Separating individual tree crowns from cluster crowns

The trees identified in Step 2 could either be an individual tree crown or a cluster of crowns. To differentiate individual crowns from crown clusters, the eCognition geometric object features include elliptic fit, ratio of length to width, and area were applied. Using reference crowns from the field data, thresholds of these geometric parameters were used to distinguish individual crowns from crown clusters. The elliptic fit describes how closely an object fits into an ellipse of a similar area (Trimble Germany GmbH, 2015a) and has a value from 0 to 1. A perfect circle has an elliptic fit value equal to 1. As most of the tree crowns in the research area had a relatively circular shape, a high elliptic fit threshold of > 0.65 was used. The ratio of length to width was useful to identify single crowns which were symmetrical and not elongated; therefore a threshold of < 2.2 was used. A width threshold of the objects was used to limit the possible extent of the individual crowns and was calculated from the relationship between tree height and crown size shown in Figure 3.5. Equation (1) shows the mathematical relationship using a nonlinear regression calculated with STATA (version 11.2).

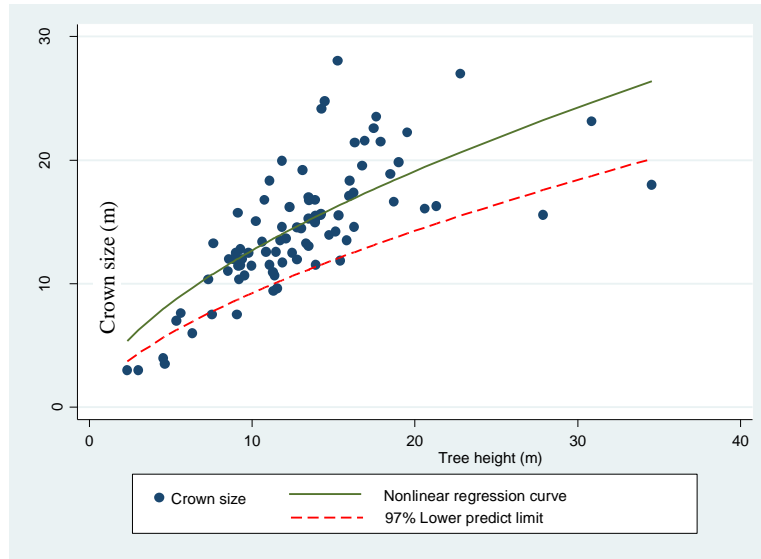


Figure 3.5. The relationship between tree crown size and height

The Equation (1) shows the nonlinear relationship between tree height and crown size:

$$\text{Crown size} = 2.6125 + \text{tree height}^{(0.665)} \quad (1)$$

3.3.3.2 Splitting cluster crowns into individual crowns

This sub-step involved first identifying treetops as seed points and then growing these points into individual tree crowns using the eCognition functions - Image Object Fusion algorithm and Parent Process Object (see Figure 3.6 for an illustration of the result).

Treetop points were identified by applying the method of Chen et al. (2006). First a canopy maxima model (CMM) is calculated in ArcMap using a focal neighbourhood maximum height value with variable window sizes. The variable window sizes were determined by the 97% lower prediction limit of the regression curve between tree height and crown size (see Figure 3.5). A smoothed CMM was then generated using Gaussian filtering with a standard deviation of 1 to further remove non-treetop local maxima. A condition statement was used to identify pixels where the height above ground equalled the maximum values. These pixels were then converted to point features.

The treetop points were expanded into individual crowns using the eCognition functions - Image Object Fusion and Parent Process Object. These functions grew

the treetop points (seeds) by merging the immediate neighbouring pixels which have lower height value than the original seeds if the region generated satisfied the following conditions: (1) the crown area is less than or equal to the area of a circle with the diameter defined by the equation (1); (2) The elliptic fit is higher than 0.65 so the crown delineated has a circular shape; (3) the ratio of length to width is less than 2.2 so the crown generated is symmetrical and not elongated. The growing stopped when there was no candidate that can combine with the seed to satisfy these criteria.

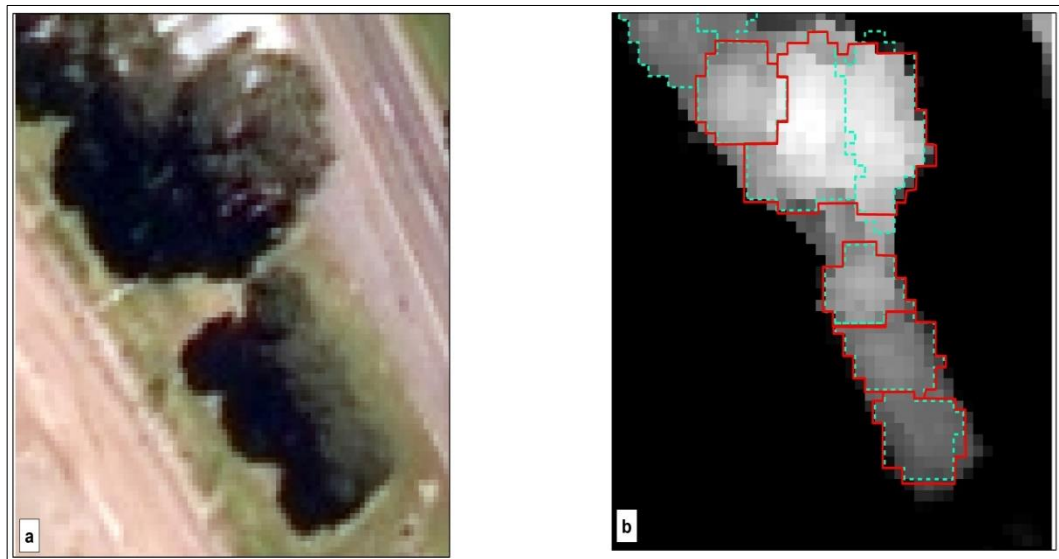


Figure 3.6. a) A subset image showing crown overlap. b) Segmentation of the image - red polygons represent the ground reference crowns and the blue polygons representing automatic segmentation

3.3.4 Step 4 - Feature extraction and selection

Table 3.2 lists the features extracted for each tree crown and considered for classification. Apart from the topographic variables, which were calculated in ArcGIS, eCognition was used to generate the other features from Quickbird and LiDAR data using mostly standard functions. The texture features were calculated using Haralick's algorithms, which included Grey-Level Co-occurrence (GLCM) and Gray-Level Difference Vector features (GLDV). The relative height percentiles were calculated as the height percentile of laser returns divided by the maximum height of laser returns within individual tree crowns.

The topographical wetness index (TWI) used Beven and Kirkby (1979) formula and is as follows:

$$TWI = \ln(\alpha/\tan\beta)$$

where α = area value calculated as (flow accumulation + 1) x (cell size) and β is the slope expressed in radians.

Table 3.2. Image object features used for classifications

Categories	Input layers	Object features	No of features
Spectral	<ul style="list-style-type: none"> • Blue • Green • Red • Nir 	<ul style="list-style-type: none"> - Mean of each layer - Standard deviation of each layer - Texture variables of each layer: GLCM mean, GLCM standard deviation, GLCM correlation, GLCM homogeneity, GLCM contrast, GLCM dissimilarity, GLCM entropy, GLDV mean, GLDV contrast, GLDV entropy 	48
Height	Point cloud LiDAR data	<ul style="list-style-type: none"> - h_{mean1}: mean height of all returns within each tree crown - h_{mean2}: mean height of first returns within each tree crown - h_{max}: maximum height of all returns within each tree crown - h_{min}: minimum height of all returns within each tree crown - reh_{10}: Relative 10th height percentile of all returns within each tree crown - reh_{25}: Relative 25th height percentile of all returns within each tree crown - reh_{50}: Relative 50th height percentile of all returns within each tree crown - reh_{75}: Relative 75th height percentile of all returns within each tree crown - reh_{90}: Relative 90th height percentile of all returns within each tree crown - h_{st}: standard deviation of all returns within each tree crown - h_{coef}: coefficient of variation of all returns within each tree crown 	11
Intensity	Point cloud LiDAR data	<ul style="list-style-type: none"> - i_{mean1}: mean intensity of all returns within each tree crown - i_{mean2}: mean intensity of first returns within each tree crown - i_{max}: maximum intensity of all returns within each tree crown - i_{min}: minimum intensity of all returns within each tree crown - i_{st1}: standard deviation of all returns within each tree crown - i_{st2}: standard deviation of first returns within each tree crown - i_{coef}: coefficient of variation of all returns within each tree crown 	7
Topographic	<ul style="list-style-type: none"> • DEM • Slope • Aspect • TWI 	<ul style="list-style-type: none"> - Mean of each layer - Standard deviation of each layer 	8

The Random Forest (RF) algorithm in the R statistical package (R Core Team, 2015) was used for selecting relevant features. This algorithm is a classifier consisting of a set of randomly generated decision trees and each tree contributes with a single vote for the most frequent class. This algorithm calculates the importance of each feature, which is based on the mean decrease in classification accuracy if the values of this feature are randomly altered in the out-of-bag (OOB) samples, while keeping all the other features constant (Hastie et al., 2009). The higher the mean decrease in accuracy when a feature is altered, the more relevant that feature is for the classification (Archer and Kimes, 2008).

The two main parameters for RF are the number of trees in the forest (*ntree*) and number of variables considered for splitting at each tree node (*mtry*). These parameters were optimized and selected based on the lowest OOB estimate of error rate for *mtry* and the stability of OOB error rate for *ntree* (Adelabu and Dube, 2015; Breiman, 2001a). The *ntree* value was tested from 10 – 1000 trees with intervals of 50, while *mtry* was tested using all values with a single interval - ranging from 1 to 74 for both LiDAR and QuickBird data used and ranging from 1 to 48 values for only QuickBird data used. Figures 3.7a and 3.7b showed the OOB error rates were stable after *ntree* = 300 and the optimal *mtry* = 12 with only the QuickBird data used. These values are 300 and 18, respectively when both QuickBird and LiDAR data were used (Figures 3.8a and 3.8b).

After running RF with the selected *ntree* and *mtry*, only features that met both the following criteria were used as input variables for the SVM algorithm: 1) had positive values of mean decrease accuracy and, 2) the values exceeded the absolute negative values (Strobl et al., 2009).

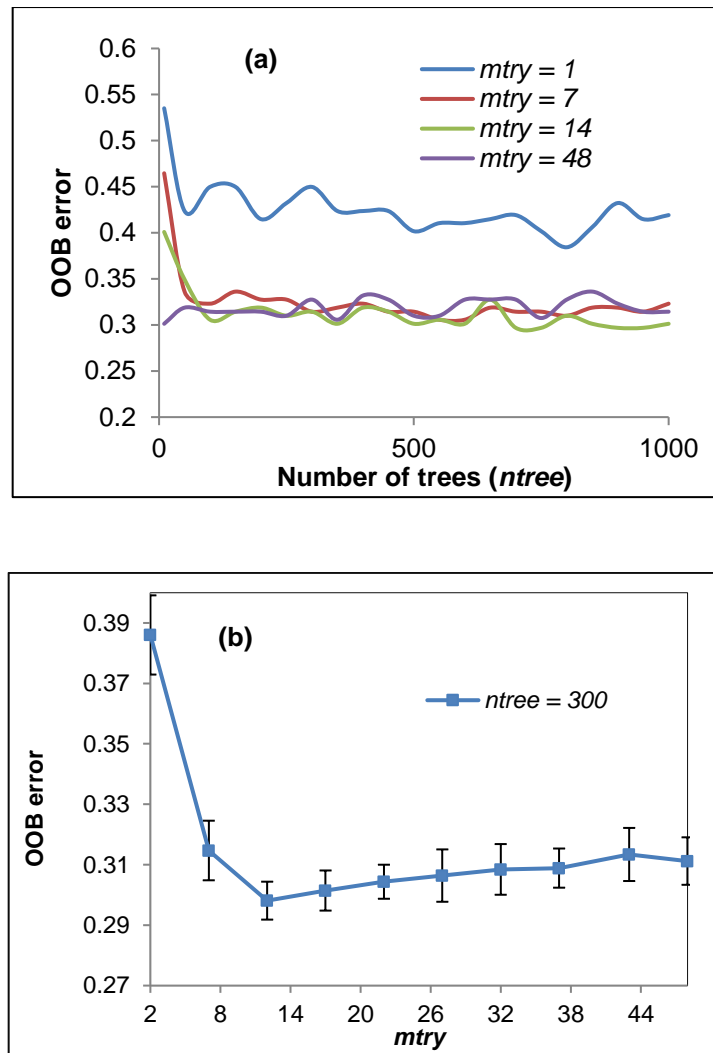


Figure 3.7. The effect of different *ntree* and *mtry* values on the performance of RF measured by OOB estimate of error rate using only QuickBird data

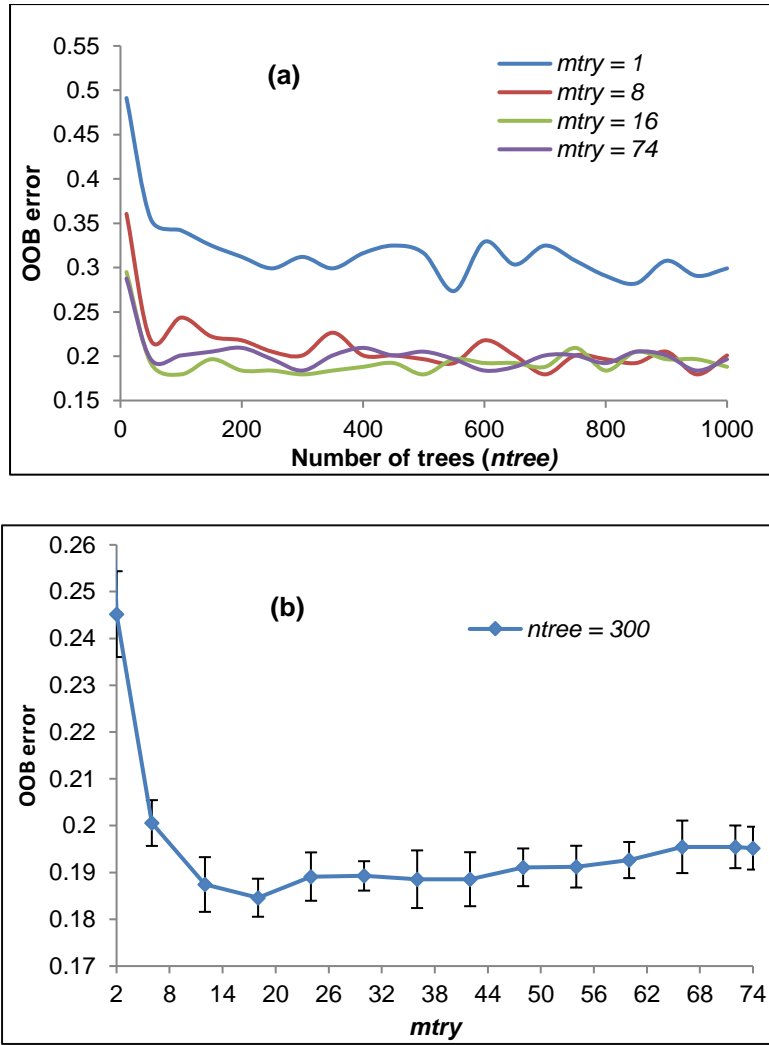


Figure 3.8. The effect of different $ntree$ and $mtry$ values on the performance of RF measured by OOB estimate of error rate using both QuickBird and LiDAR data.

Of the 74 features derived from a combination of QuickBird and LiDAR data, 32 features were selected as inputs for the SVM classifier. When only QuickBird was used, 18 features from a total of 48 were chosen for the SVM classifier.

Figures 3.9a and 3.9b show the average decrease in accuracy for eleven of the most important features from only multispectral data and a combination of multispectral and LiDAR data.

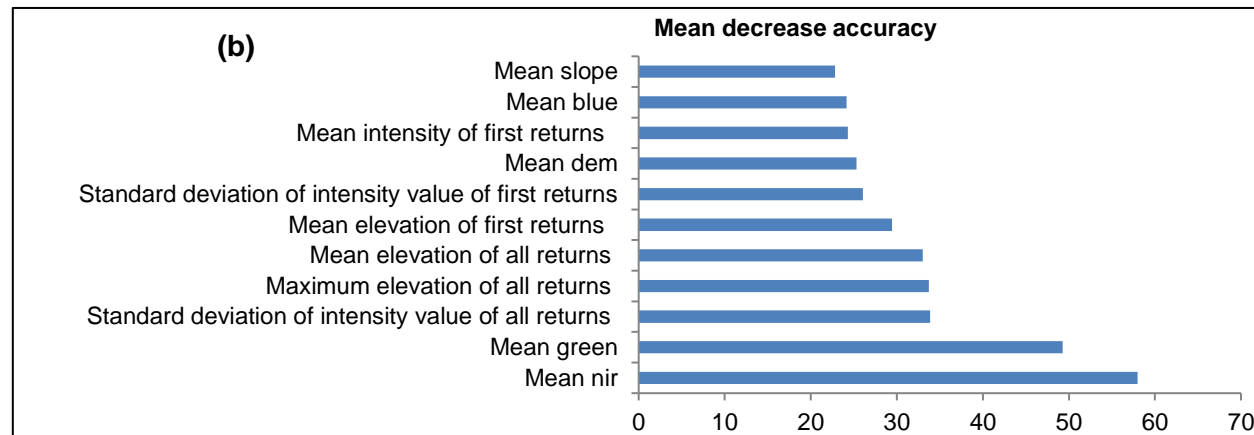
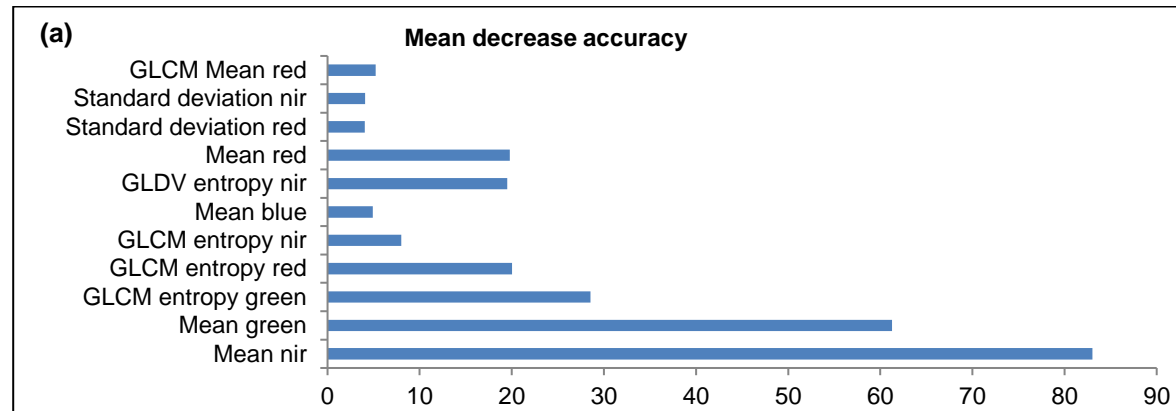


Figure 3.9. The importance of different features measured by mean decrease accuracy (a) using spectral data (b) using both spectral and LiDAR data.

3.3.5 Step 5- Classification and accuracy assessment

The eCognition SVM classifier was applied to the selected features using the radial basis kernel function. This classifier was trained using two parameters: 1) cost of constraint violation (C) and, 2) gamma. The open source LIBSVM tools (version 3.20), developed by Chang and Lin (2011) was used to determine C and gamma.

Four classifications were conducted in this study. These included classifications using LiDAR and QuickBird data with and without RF feature selection; and classifications using only QuickBird data with and without RF feature selection.

The accuracy of both the segmentation and the classification was assessed against reference data collected in the field. The accuracy of the segmentation was measured using the closeness to an ideal segmentation result represented by D (Equation 2) developed by Clinton et al. (2010). D is calculated from over-segmentation (Equation 3) and under-segmentation (Equation 4). The higher the D value, the more the mismatch between reference objects and segments.

$$D = \sqrt{\frac{Oversegmentation_{ij}^2 + Undersegmentation_{ij}^2}{2}} \quad (2)$$

$$Oversegmentation_{ij} = 1 - \frac{area(x_i \cap y_j)}{area(x_i)} \quad (3)$$

$$Undersegmentation_{ij} = 1 - \frac{area(x_i \cap y_j)}{area(y_j)} \quad (4)$$

Where: x_i is the reference polygons relative, and y_j is the set of image segments that are relevant to reference polygons x_i

The accuracy metrics were reported using producer's (PA) and user's accuracies (UA), overall accuracy (OA), the overall Kappa coefficient of agreement (K) and conditional Kappa value for each category (K_1). Furthermore, three additional indices were used to evaluate the performance of the classifications. These included quantity disagreement (QD), allocation disagreement (AD), and total disagreement (TD) developed by Pontius Jr and Millones (2011). The quantity disagreement is defined as the difference in the proportions of the categories between the reference map and the predicted map. The allocation disagreement represents the amount of difference between the reference map and the predicted map, based on the spatial

allocation of the categories. Total disagreement is the sum of the quantity disagreement and the allocation disagreement. The training and testing sets were different, but the same sets were used for developing each classification. Because the same sets of data were used for each classification, the McNemar's test was conducted to determine whether the different classification results were statistically different (Foody, 2004).

3.4 Results and Discussions

The over- and under-segmentation was 0.27 and 0.34 respectively for the crown delineation. The D value was 0.31. The segmentation accuracy was 69%. This is a similar accuracy to the study of Hussin et al. (2014), which obtained 68% segmentation accuracy for mixed forest in Nepal.

Tables 3.3a and 3.3b compare the accuracy of using both spectral and LiDAR data with just spectral data (both have feature selection), and Tables 3.4a and 3.4b provide the same comparison but without feature selection. Overall, the best result was achieved using both spectral and LiDAR data, and feature selection (Table 3.3a). This improvement is reflected in both the Kappa index, the OA, AD and TD, as well as the UA and PA percentages across all the vegetation classes. Combining spectral and LiDAR data improved the classification regardless of whether feature selection was used - the highest increase in Kappa % index was 12.8 (z value = 4.2) and the largest decrease in total disagreement % was 9.6. Having feature selection increased the Kappa % index by 6.7 (z value = 5.4) and decreased total disagreement and allocation disagreement by 5% and 5.4%, respectively when both spectral and LiDAR data were used. Similarly, using feature selection for just multispectral data also increased the Kappa % value by 5.0 (z value = 2.3) and decreased total disagreement and allocation disagreement by 3.7% and 7.9% respectively.

Table 3.3. Confusion matrix of classification accuracies obtained through RF feature selection and SVM classifier

(a) Confusion matrix of classification accuracies obtained through RF feature selection and SVM classifier using both spectral and LiDAR data

Class	Reference data				
	Pohu	Other	Co	Ma	UA(%)
Pohu	49	3	2	6	81.7
Other	8	56	5	7	73.7
Co	0	0	53	0	100
Ma	3	1	0	47	92.2
PA(%)	81.7	93.3	88.3	78.3	
K ₁ (%)	75.6	90.2	85	72.5	
OA(%)	85.4				
K (%)	80.6				
QD(%)	6.6				
AD(%)	7.9				
TD(%)	14.6				

(b) Confusion matrix of classification accuracies obtained through RF feature selection and SVM classifier using just spectral data

Class	Reference data				
	Pohu	Other	Co	Ma	UA(%)
Pohu	41	6	4	9	68.3
Other	16	53	7	11	60.9
Co	1	0	49	1	96.1
Ma	2	1	0	39	92.9
PA(%)	68.3	88.3	81.7	65	
K ₁ (%)	57.8	81.7	76.7	57.6	
OA(%)	75.8				
K (%)	67.8				
QD(%)	11.3				
AD(%)	12.9				
TD(%)	24.2				

Class key: Pohu, pohutukawa; Other, other broadleaf species; Co, coniferous species; Ma, manuka/kanuka.

Table 3.4. Confusion matrix of classification accuracies obtained through SVM classifier without feature selection

(a) Confusion matrix of classification accuracies obtained through SVM classifier using both spectral and LiDAR data with all 74 features

Class	Reference data				
	Pohu	Other	Co	Ma	UA(%)
Pohu	45	1	7	11	70.3
Other	12	53	2	4	74.6
Co	0	3	51	1	92.7
Ma	3	3	0	44	88
PA(%)	75	88.3	85	73.3	
K ₁ (%)	65.9	83.4	80.5	66.3	
OA(%)	80.4				
K (%)	73.9				
QD(%)	6.3				
AD(%)	13.3				
TD(%)	19.6				

(b) Confusion matrix of classification accuracies obtained through SVM classifier using just spectral data with all 48 features

Class	Reference data				
	Pohu	Other	Co	Ma	UA(%)
Pohu	38	12	8	7	58.5
Other	15	47	2	8	65.3
Co	4	1	47	4	83.9
Ma	3	0	3	41	87.2
PA(%)	63.3	78.3	78.3	68.3	
K ₁ (%)	49.7	69	71.7	60.6	
OA(%)	72.1				
K (%)	62.8				
QD(%)	7.1				
AD(%)	20.8				
TD(%)	27.9				

Class key: Pohu, pohutukawa; Other, other broadleaf species; Co, coniferous species; Ma, manuka/kanuka.

Pohutukawa was difficult to accurately identify compared to other general vegetation classes (other broadleaf, and conifer) but was similar to the more specific Manuka/Kanuka class. This is reflected in the kappa % values for each class (K_1).

3.4.1 *The contribution of different features*

Figure 3.9 (mean decrease accuracy) and Figure 3.10 (spectral reflectance) show that the green and near infrared bands were the most valuable for discriminating between vegetation classes. Figures 3.9b, 3.11, and 3.12 show that the LiDAR-derived features, in particular, the standard deviation of the intensity and height features also made a strong contribution to classifying different species. Topographic features, especially mean slope and mean DEM were more valuable than texture information.

Similarly to previous studies, this result emphasizes the important role of the green region (Adelabu and Dube, 2015; Alonzo et al., 2014) and the NIR (Adelabu and Dube, 2015; Clark et al., 2005) in tree species discrimination. The reason may be the variations in pigment contents, and the structural carbohydrates among the tree species. There is a close relationship between pigment contents such as chlorophyll, carotenoid, anthocyanin and xanthophyll content and the green band reflectance. The NIR reflectance also has a relationship with cellulose and other structural carbohydrates (Ustin et al., 2009; Vin et al., 2011).

Concerning LiDAR-derived features, the standard deviation of intensity values were the most useful for differentiating between tree species. Figure 3.11 shows that Pohutukawa has a higher standard deviation of intensity values than the other tree species. These high values could be because the majority of the samples (75%) were taken from mature Pohotukawa trees, which have large gaps between the branches. This is similar to research by Holmgren and Persson (2004) who also found that standard deviation of intensity is one of the most important variables affecting species classification of spruce and pine trees.

The maximum height of all returns also contributes an important role for identifying different species. The Coniferous species had the highest maximum height of all returns; therefore this feature is useful for differentiating between Coniferous species from others (see Figure 3.12). This supports Dalponte et al. (2012) research,

which also found that the addition of the maximum height of low density LiDAR data increased the classification accuracy.

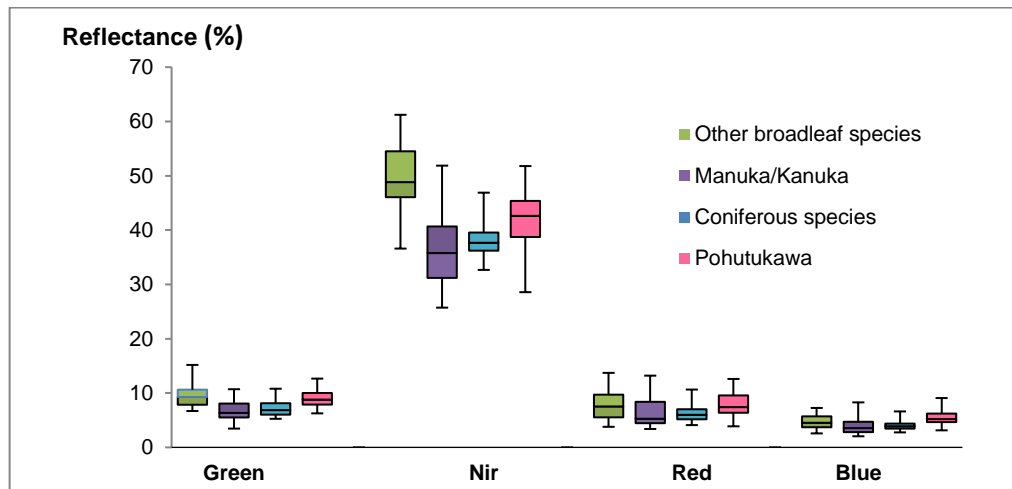


Figure 3.10. Box-and-whisker plot showing the statistics of reflectance of different tree species across 4 multi-spectral bands

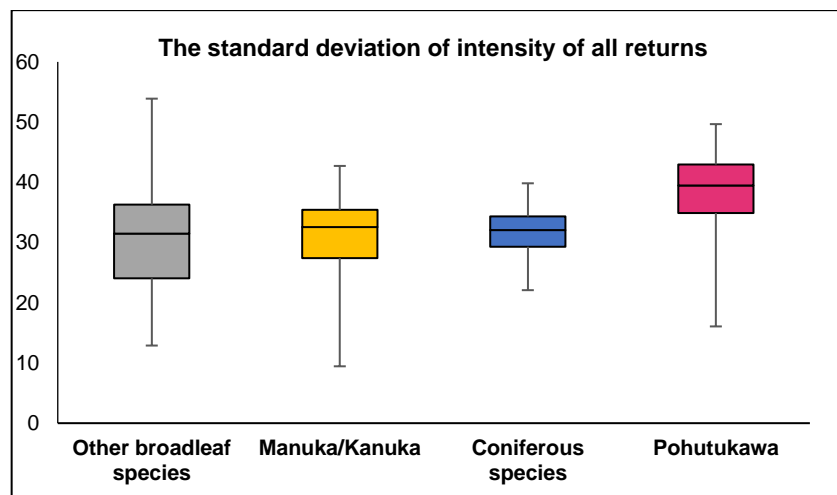


Figure 3.11. Box-and-whisker plot showing the statistics of the standard deviation of intensity of all returns of different tree species

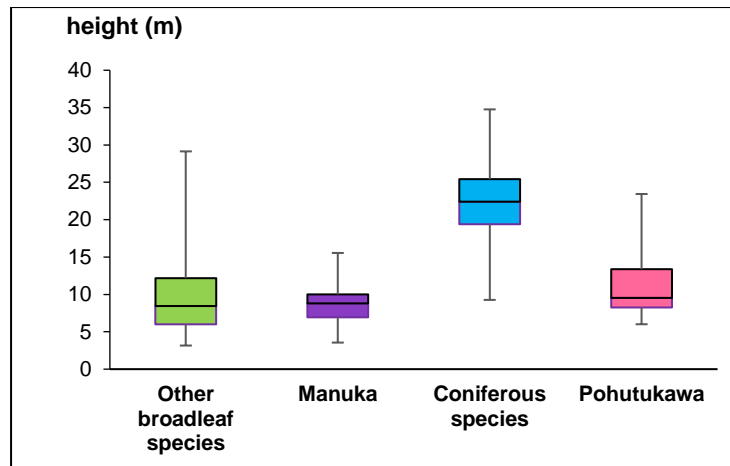


Figure 3.12. Box-and-whisker plot showing the statistics of the maximum height of all returns of different tree species

3.5 Conclusion

The goal of this research was to develop a method to distinguish single trees of Pohutukawa, from a mix of other trees and structures, and experiment with a range of techniques and data sets to determine the best method. Using a combination of spectral and LiDAR data has been shown that Pohutukawa trees can be identified with a kappa accuracy of 75.6%. The method developed has used a range of techniques that goes well beyond basic spectral classification and has shown the improvements that can be gained from also considering terrain context (based on slope, elevation, and wetness), tree height, canopy shape, and branch density (based on LiDAR return intensity). The method is explicitly described in this paper and is therefore reproducible. The study area chosen to demonstrate the method was a large area containing a complex mix of vegetation and infrastructure, therefore the method will be transferable to other areas, which are likely to be less complex in the land-cover mix. This research supports the growth of combining GIS and image analysis techniques to produce sophisticated multi-stepped methods.

There are many different steps in the method that could be improved with future research. For example, this research used Random Forest for feature selection; however there are many other algorithms for feature selection that could be experimented with, including principle component analysis, linear discriminant analysis, and genetic algorithms. Identifying treetops is important because errors in treetop detection can lead to under-segmentation (omission errors) or over-

segmentation (commission error). Clinton et al. (2010) have also highlighted this issue because the object segmentation affects the feature information submitted to the classifier. Combining LiDAR and spectral data could also improve treetop identification and object segmentation. Individual tree segmentation could be improved by using a simultaneous growth, which will overcome problems associated with the order of growth specified in the sequential growth algorithm (Zhen et al., 2014).

Humans can accurately identify individual tree specimens such as Pohutukawa trees in the field and also from detailed images. It is clear that the human brain does not just consider spectral information when identifying individual trees, but uses a range of information such as the surrounding context, density of branches, canopy shape, and height. All this information is now available in digital form due to the addition of LiDAR and GIS analysis, as well as image analysis functions. This research has shown how this information can be used together to produce more accurate results. With additional research computers will be just as accurate as the human brain, but have the added advantage of 24/7 processing power which can analyse large areas consistently.

Acknowledgments

The reviewers have made useful suggestions which have been incorporated into this paper. The New Zealand Aid Programme provided financial assistance to pursue this research.

REFERENCES

- Adelabu, S., Dube, T., 2015. Employing ground and satellite-based QuickBird data and random forest to discriminate five tree species in a Southern African Woodland. *Geocarto International* 30(6), 457-471. <https://doi.org/10.1080/10106049.2014.885589>
- Alonzo, M., Bookhagen, B., Roberts, D.A., 2014. Urban tree species mapping using hyperspectral and lidar data fusion. *Remote Sensing of Environment* 148, 70-83. <https://doi.org/10.1016/j.rse.2014.03.018>
- Archer, K.J., Kimes, R.V., 2008. Empirical characterization of random forest variable importance measures. *Computational Statistics & Data Analysis* 52(4), 2249-2260. <https://doi.org/10.1016/j.csda.2007.08.015>
- Arenas-Castro, S., Julien, Y., Jiménez-Muñoz, J.C., Sobrino, J.A., Fernández-Haeger, J., Jordano-Barbudo, D., 2012. Mapping wild pear trees (*Pyrus bourgaeana*) in Mediterranean forest using high-resolution QuickBird satellite imagery. *International Journal of Remote Sensing* 34(9-10), 3376-3396. <https://doi.org/10.1080/01431161.2012.716909>
- Beven, K.J., Kirkby, M.J., 1979. A physically based, variable contributing area model of basin hydrology / Un modèle à base physique de zone d'appel variable de l'hydrologie du bassin versant. *Hydrological Sciences Bulletin* 24(1), 43-69. <https://doi.org/10.1080/02626667909491834>
- Blaschke, T., 2010. Object based image analysis for remote sensing. *ISPRS Journal of Photogrammetry and Remote Sensing* 65(1), 2-16. <https://doi.org/10.1016/j.isprsjprs.2009.06.004>
- Blaschke, T., Burnett, C., Pekkarinen, A., 2004. Image segmentation methods for object-based analysis and classification, in: de Jong, S.M., van der Meer, F.D. (Eds.), *Remote Sensing Image Analysis: Including the Spatial Domain*. Springer, Dordrecht, pp. 211-236.
- Breiman, L., 2001a. Random forests. *Machine Learning* 45(1), 5-32. <https://doi.org/10.1023/A:1010933404324>
- Bunting, P., Lucas, R., 2006. The delineation of tree crowns in Australian mixed species forests using hyperspectral Compact Airborne Spectrographic Imager (CASI) data. *Remote Sensing of Environment* 101(2), 230-248. <https://doi.org/10.1016/j.rse.2005.12.015>
- Bylsma, R.J., Clarkson, B.D., Efford, J.T., 2014. Biological flora of New Zealand 14: *Metrosideros excelsa*, pōhutukawa, New Zealand Christmas tree. *New Zealand Journal of Botany* 52(3), 365-385. <https://doi.org/10.1080/0028825x.2014.926278>
- Chang, C.-C., Lin, C.-J., 2011. LIBSVM: A library for support vector machines. *ACM Transactions on Intelligent Systems and Technology (TIST)* 2(3), 1-27. <https://doi.org/10.1145/1961189.1961199>
- Chen, Q., Baldocchi, D., Gong, P., Kelly, M., 2006. Isolating individual trees in a savanna woodland using small footprint lidar data. *Photogrammetric Engineering & Remote Sensing* 72(8), 923-932. <https://doi.org/10.14358/PERS.72.8.923>
- Chen, Z., Gao, B., 2014. An object-based method for urban land cover classification using airborne lidar data. *IEEE Journal of Selected Topics in Applied Earth Observations and Remote Sensing* 7(10), 4243-4254. <https://doi.org/10.1109/Jstars.2014.2332337>

- Cho, M.A., Mathieu, R., Asner, G.P., Naidoo, L., van Aardt, J., Ramoelo, A., Debba, P., Wessels, K., Main, R., Smit, I.P.J., Erasmus, B., 2012. Mapping tree species composition in South African savannas using an integrated airborne spectral and LiDAR system. *Remote Sensing of Environment* 125(0), 214-226. <https://doi.org/10.1016/j.rse.2012.07.010>
- Clark, M.L., Roberts, D.A., Clark, D.B., 2005. Hyperspectral discrimination of tropical rain forest tree species at leaf to crown scales. *Remote Sensing of Environment* 96(3-4), 375-398. <https://doi.org/10.1016/j.rse.2005.03.009>
- Clinton, N., Holt, A., Scarborough, J., Yan, L., Gong, P., 2010. Accuracy assessment measures for object-based image segmentation goodness. *Photogrammetric Engineering & Remote Sensing* 76(3), 289-299.
- Dalponte, M., Bruzzone, L., Gianelle, D., 2012. Tree species classification in the Southern Alps based on the fusion of very high geometrical resolution multispectral/hyperspectral images and LiDAR data. *Remote Sensing of Environment* 123, 258-270. <https://doi.org/10.1016/j.rse.2012.03.013>
- Dalponte, M., Bruzzone, L., Vescovo, L., Gianelle, D., 2009. The role of spectral resolution and classifier complexity in the analysis of hyperspectral images of forest areas. *Remote Sensing of Environment* 113(11), 2345-2355. <https://doi.org/10.1016/j.rse.2009.06.013>
- Foody, G.M., 2004. Thematic map comparison: Evaluating the statistical significance of differences in classification accuracy. *Photogrammetric Engineering & Remote Sensing* 70(5), 627-634.
- Gebreslasie, M.T., Ahmed, F.B., Van Aardt, J.A.N., Blakeway, F., 2011. Individual tree detection based on variable and fixed window size local maxima filtering applied to IKONOS imagery for even-aged Eucalyptus plantation forests. *International Journal of Remote Sensing* 32(15), 4141-4154.
- Han, N., Du, H., Zhou, G., Sun, X., Ge, H., Xu, X., 2014. Object-based classification using SPOT-5 imagery for Moso bamboo forest mapping. *International Journal of Remote Sensing* 35(3), 1126-1142. <https://doi.org/10.1080/01431161.2013.875634>
- Hastie, T.J., Tibshirani, R.J., Friedman, J.H., 2009. *The Elements of Statistical Learning: Data Mining, Inference, and Prediction*. Springer, New York, NY.
- Holmgren, J., Persson, A., 2004. Identifying species of individual trees using airborne laser scanner. *Remote Sensing Of Environment* 90(4), 415-423. [https://doi.org/10.1016/S0034-4257\(03\)00140-8](https://doi.org/10.1016/S0034-4257(03)00140-8)
- Huang, C.-L., Wang, C.-J., 2006. A GA-based feature selection and parameters optimization for support vector machines. *Expert Systems with Applications* 31(2), 231-240. <https://doi.org/10.1016/j.eswa.2005.09.024>
- Hussin, Y., Gilani, H., Leeuwen, L., Murthy, M.S.R., Shah, R., Baral, S., Tsendbazar, N.-E., Shrestha, S., Shah, S., Qamer, F., 2014. Evaluation of object-based image analysis techniques on very high-resolution satellite image for biomass estimation in a watershed of hilly forest of Nepal. *Appl Geomat* 6(1), 59-68. <https://doi.org/10.1007/s12518-014-0126-z>
- Izenman, A.J., 2008. *Modern Multivariate Statistical Techniques*. Springer, New York, NY.
- Ke, Y., Quackenbush, L.J., 2011. A review of methods for automatic individual tree-crown detection and delineation from passive remote sensing. *International Journal of Remote Sensing* 32(17), 4725-4747. <https://doi.org/10.1080/01431161.2010.494184>

- Ke, Y., Quackenbush, L.J., Im, J., 2010. Synergistic use of QuickBird multispectral imagery and LIDAR data for object-based forest species classification. *Remote Sensing of Environment* 114(6), 1141-1154. <https://doi.org/10.1016/j.rse.2010.01.002>
- Khosravipour, A., Skidmore, A.K., Isenburg, M., Wang, T., Hussin, Y.A., 2014. Generating pit-free canopy height models from airborne Lidar. *Photogrammetric Engineering & Remote Sensing* 80(9), 863-872. <https://doi.org/10.14358/PERS.80.9.863>
- Kim, M., Warner, T.A., Madden, M., Atkinson, D.S., 2011. Multi-scale GEOBIA with very high spatial resolution digital aerial imagery: Scale, texture and image objects. *International Journal of Remote Sensing* 32(10), 2825-2850. <https://doi.org/10.1080/01431161003745608>
- Kim, S., McGaughey, R.J., Andersen, H.-E., Schreuder, G., 2009b. Tree species differentiation using intensity data derived from leaf-on and leaf-off airborne laser scanner data. *Remote Sensing of Environment* 113(8), 1575-1586. <https://doi.org/10.1016/j.rse.2009.03.017>
- Korpela, I., Dahlin, B., Schäfer, H., Bruun, E., Haapaniemi, F., Honkasalo, J., Ilvesniemi, S., Kuutti, V., Linkosalmi, M., Mustonen, J., 2007. Single-tree forest inventory using lidar and aerial images for 3D treetop positioning, species recognition, height and crown width estimation, *Proceedings of ISPRS Workshop on Laser Scanning*, pp. 227-233.
- Larsen, M., Eriksson, M., Descombes, X., Perrin, G., Brandtberg, T., Gougeon, F.A., 2011. Comparison of six individual tree crown detection algorithms evaluated under varying forest conditions. *International Journal of Remote Sensing* 32(20), 5827-5852. <https://doi.org/10.1080/01431161.2010.507790>
- Leckie, D., Gougeon, F., Hill, D., Quinn, R., Armstrong, L., Shreenan, R., 2003. Combined high-density lidar and multispectral imagery for individual tree crown analysis. *Canadian Journal of Remote Sensing* 29(5), 633-649. <https://doi.org/10.5589/m03-024>
- Lu, D., Weng, Q., 2007. A survey of image classification methods and techniques for improving classification performance. *International Journal of Remote Sensing* 28(5), 823-870. <https://doi.org/10.1080/01431160600746456>
- Mountrakis, G., Im, J., Ogole, C., 2011. Support vector machines in remote sensing: A review. *ISPRS Journal of Photogrammetry and Remote Sensing* 66(3), 247-259. <https://doi.org/10.1016/j.isprsjprs.2010.11.001>
- Olofsson, K., Wallerman, J., Holmgren, J., Olsson, H., 2006. Tree species discrimination using Z/I DMC imagery and template matching of single trees. *Scandinavian Journal of Forest Research* 21(S7), 106-110. <https://doi.org/10.1080/14004080500486955>
- Ørka, H.O., Næsset, E., Bollandsås, O.M., 2009. Classifying species of individual trees by intensity and structure features derived from airborne laser scanner data. *Remote Sensing of Environment* 113(6), 1163-1174. <https://doi.org/10.1016/j.rse.2009.02.002>
- Ouyang, Z.-T., Zhang, M.-Q., Xie, X., Shen, Q., Guo, H.-Q., Zhao, B., 2011. A comparison of pixel-based and object-oriented approaches to VHR imagery for mapping saltmarsh plants. *Ecological Informatics* 6(2), 136-146. <https://doi.org/10.1016/j.ecoinf.2011.01.002>
- Pontius Jr, R.G., Millones, M., 2011. Death to Kappa: Birth of quantity disagreement and allocation disagreement for accuracy assessment.

- International Journal of Remote Sensing 32(15), 4407-4429.
<https://doi.org/10.1080/01431161.2011.552923>
- R Core Team, 2015. R: A language and environment for statistical computing.
- Richter, R., Schläpfer, D., 2014. ATCOR-2/3 user guide, version 8.3. 1. Zurich, Switzerland.
- Strobl, C., Malley, J., Tutz, G., 2009. An introduction to recursive partitioning: Rationale, application and characteristics of classification and regression trees, bagging and random forests. *Psychological Methods* 14(4), 323-348.
<https://doi.org/10.1037/a0016973>
- Trimble Germany GmbH, 2015a. Trimble Documentation: eCognition Developer 9.1 Reference Book. Trimble Germany GmbH, Munich, Germany.
- Ustin, S., Jacquemoud, S., Palacios-Orueta, A., Li, L., Whiting, M., 2009. Remote sensing based assessment of biophysical indicators for land degradation and desertification, in: Röder, A., Hill, J. (Eds.), *Recent Advances in Remote Sensing and Geoinformation, Processing for Land Degradation Assessment*. CRC Press, Boca Raton, FL, pp. 15-44.
- Vin, A., Gitelson, A.A., 2011. Sensitivity to Foliar Anthocyanin Content of Vegetation Indices Using Green Reflectance. *Geoscience and Remote Sensing Letters, IEEE* 8(3), 464-468.
<https://doi.org/10.1109/LGRS.2010.2086430>
- Zhen, Z., Quackenbush, L.J., Zhang, L., 2014. Impact of tree-oriented growth order in marker-controlled region growing for individual tree crown delineation using Airborne Laser Scanner (ALS) data. *Remote Sensing* 6(1), 555-579.
<https://doi.org/10.3390/rs6010555>

CHAPTER 4

AN EVALUATION OF DIMENSIONALITY REDUCTION AND CLASSIFICATION TECHNIQUES FOR IDENTIFYING TREE SPECIES USING INTEGRATED QUICKBIRD IMAGERY AND LIDAR DATA

Abstract

The objective of this research was to investigate and compare tree species classification performance for a variety of classification schemes (Naïve Bayes, Logistic Regression, Random Forest, and Support Vector Machine), combined with various dimensionality reduction methods (Correlation-based feature selection filter, Information Gain, Wrapper methods, and Principal Component Analysis). Two primary data sets were used - QuickBird and LiDAR, as well as derived topography data. When dimensionality reduction was used prior to classification, only the Naïve Bayes (NB) classifier had a significant improvement in accuracy. SVM and RF had the best classification accuracy, and this was achieved without dimensionality reduction. The overall accuracy (OA) of SVM and RF were 88.2% and 87.2% (Kappa 0.84 and 0.83) respectively, followed closely by LR (OA: 84.8%, Kappa: 0.79) and more distantly by NB (OA: 79%, Kappa: 0.72).

Key words: Tree species, Dimensionality reduction, Naïve Bayes, Logistic Regression, Random Forest, Support Vector Machine

4.1 Introduction

Information on the spatial distribution of tree species, especially for species that have high ecological and cultural significance as well as under threat, is important for managers and policy makers when deciding on appropriate conservation strategies. Pohutukawa (*Metrosideros excelsa* Sol. ex Gaertn) is such a tree in New Zealand which has been subject to fires and land clearance, and more recently possum browsing (Bylsma et al., 2014). Pohutukawa is a multi-stemmed tree up to 25m high with large rounded crowns growing in northern coastal regions of New Zealand.

Many studies have combined spectral information derived from multispectral or hyperspectral images with height information derived from LiDAR data, which has

improved classification accuracy of tree species (Ke et al., 2010; Pham et al., 2016b). Having diverse information from multiple data sets results in more features for classification. However, not all features are useful for classification and can decrease the classification performance. Dimensionality reduction methods are used to reduce the redundancy and irrelevance of some features as a pre-processing step. This improves the classification accuracy and reduces computation demand (Xue et al., 2014). Dimensionality reduction methods can be categorized as feature extraction and feature selection (Fassnacht et al., 2014a). Feature extraction uses a transformation of the original features into a lower dimensional space, while the feature selection process selects a subset from the original features (Fassnacht et al., 2014a; Widodo et al., 2007).

Although previous studies have compared various classifiers combined with dimensionality reduction methods for tree species classification (Fassnacht et al., 2014b; Pal and Foody, 2010), they only used a single dataset and compared two machine learning algorithms: Random Forest and Support Vector Machines. Hence, this paper examines and compares the performance of a larger variety of machine learning algorithms, combined with a wide range of dimensionality reduction methods. This study also uses 74 features extracted from QuickBird and LiDAR data, and a complex mixed landscape environment instead of a boreal forest.

In addition, the performance of the classifiers were compared with different levels of sample training data. Ideally, it is preferable to have high classification performance with a low sample size to reduce field work and computation. The training data ranged from 10 to 125 samples per class.

4.2 Materials

4.2.1 *Study area and data sets*

The research area was the eastern side of the Coromandel region (36°48'30"S to 36°55'30"S latitude, and 175°38'30"E and 175°48'30"E longitude). The site is characterized by different land cover types including built-up areas, urban parkland/open space, and both coniferous and broadleaf species. This research focuses on identifying four important tree species/types in the Coromandel region: Pohutukawa, Manuka/Kanuka, other broadleaf species, and coniferous species.

A QuickBird image and a LiDAR point cloud were used. The QuickBird image was captured on November 5th 2010, and has a panchromatic band (450-900nm; 0.6m spatial resolution) and four multispectral bands - blue (450–520 nm), green (520–600 nm), red (630–690 nm), and NIR (760–900 nm) - with 2.4m spatial resolution. The QuickBird image was atmospherically corrected using the Atmospheric Correction Algorithm (ATCOR-3) developed by Richter and Schläpfer (2014). The hue-saturation-intensity method was chosen for panchromatic sharpening to increase the spatial resolution of the multispectral bands (to 0.6m spatial resolution). The LiDAR data set was captured during February and March, 2013. The maximum number of returns for each pulse was four and the average point density was 1.2 point/m².

For training and comparing the classification performance of various feature selection and classification techniques, a ground-truth dataset was collected. There were a total 500 trees identified, 125 trees for each type of the four tree species/types in the region. To evaluate the effects of dimensionality reduction methods on classifiers, a range of training set sizes, including 10, 25, 50, 75, 100, and 125 samples per class were used. This range is commonly used in remote sensing studies (Ma et al., 2017; Pal and Foody, 2010). The supervised resampling filter in the WEKA data mining package version 3.8 (Frank et al., 2016) was used to synthesise small training sets from larger dataset containing ground truth information.

4.3 Methods

Figure 4.1 provides an overview of the method developed. Identification of tree species using information derived from QuickBird and LiDAR data includes two main procedures. First, image segmentation - which divides an image into contiguous, separate and homogeneous areas; these areas are called image objects. In the context of this paper, these image objects are individual trees. The second step classified these image objects into different species/types.

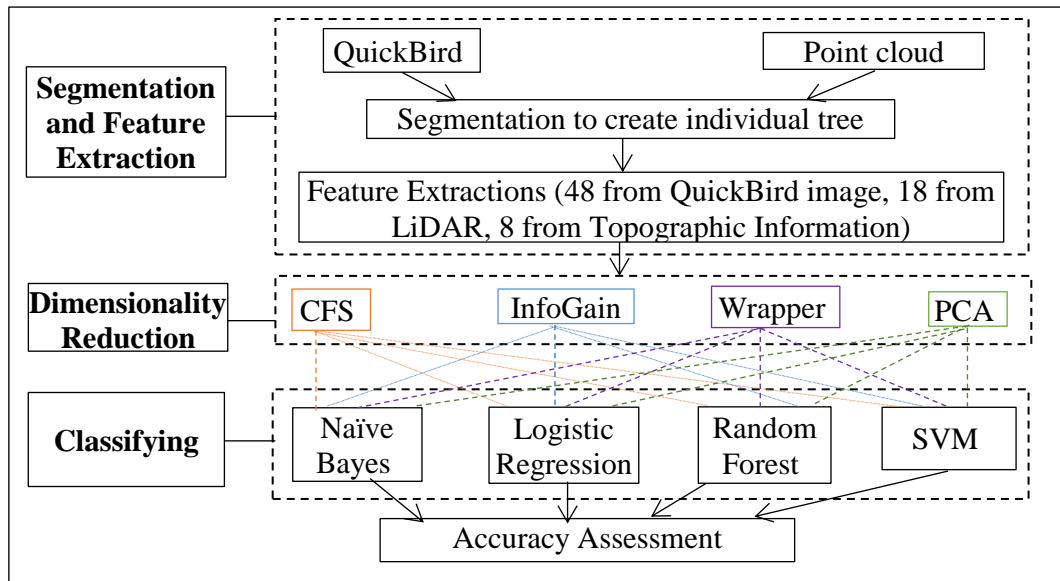


Figure 4.1. Work flow of mapping tree species using dimensionality reduction and classification techniques.

The Methods section only focuses on dimensionality reduction and classification methods because these are the subject of this research. The procedures used to segment individual trees and extract image features from the image objects are described in Pham et al. (2016b). Figure 4.2 illustrates the individual crown trees obtained from the segmentation process. The object features investigated for classification are listed in Table 4.1.

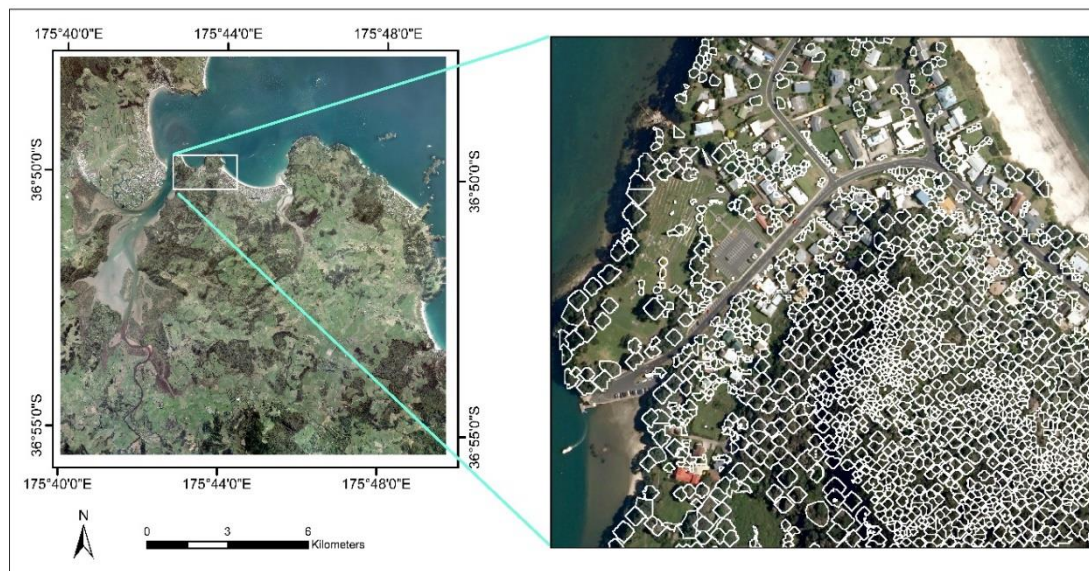


Figure 4.2. Individual tree crowns are represented by polygons.

Table 4.1. Image object features were used for classifications

. Categories	Input layers	Object features	No of features
Spectral	<ul style="list-style-type: none"> • Blue • Green • Red • Nir 	<ul style="list-style-type: none"> - Mean of each layer - Standard deviation of each layer - Texture variables of each layer: GLCM mean, GLCM standard deviation, GLCM correlation, GLCM homogeneity, GLCM contrast, GLCM dissimilarity, GLCM entropy, GLDV mean, GLDV contrast, GLDV entropy 	48
Height	Point cloud LiDAR data	<ul style="list-style-type: none"> - h_{mean1}: mean height of all returns within each tree crown - h_{mean2}: mean height of first returns within each tree crown - h_{max}: maximum height of all returns within each tree crown - h_{min}: minimum height of all returns within each tree crown - reh_{10}: Relative 10th height percentile of all returns within each tree crown - reh_{25}: Relative 25th height percentile of all returns within each tree crown - reh_{50}: Relative 50th height percentile of all returns within each tree crown - reh_{75}: Relative 75th height percentile of all returns within each tree crown - reh_{90}: Relative 90th height percentile of all returns within each tree crown - h_{st}: standard deviation of all returns within each tree crown - h_{coef}: coefficient of variation of all returns within each tree crown 	11
Intensity	Point cloud LiDAR data	<ul style="list-style-type: none"> - i_{mean1}: mean intensity of all returns within each tree crown - i_{mean2}: mean intensity of first returns within each tree crown - i_{max}: maximum intensity of all returns within each tree crown - i_{min}: minimum intensity of all returns within each tree crown - i_{st1}: standard deviation of all returns within each tree crown - i_{st2}: standard deviation of first returns within each tree crown - i_{coef}: coefficient of variation of all returns within each tree crown 	7
Topographic	<ul style="list-style-type: none"> • DEM • Slope • Aspect • TWI 	<ul style="list-style-type: none"> - Mean of each layer - Standard deviation of each layer 	8

4.3.1 *Dimensionality reduction methods*

As mentioned previously, dimensionality reduction methods can be divided into feature selection and feature extraction. The feature selection methods will be presented first, followed by feature extraction. These methods were implemented using the WEKA data mining package (Frank et al., 2016).

4.3.1.1 *Feature selection methods*

Two common feature selection methods will be used in this research: filter and wrapper methods.

4.3.1.1.1 *Filter methods*

Filter methods use feature ranking to select variables. A metric is used to compute the feature score, and then all features with a score below a user defined threshold are removed (Chandrashekar and Sahin, 2014; Saeys et al., 2007). The advantages of filter methods are that they are computationally cheaper than wrapper methods and operate independently of the choice of classifier (Galelli et al., 2014). Consequently, only a single iteration of filtering needs to be run, and then different classifiers can be assessed using the reduced feature set (Bolón-Canedo et al., 2013; Saeys et al., 2007). The disadvantage of filter methods is that dependencies among features are not taken into account because each feature is considered in isolation, which leads to some relevant features be eliminated (Galelli et al., 2014). For example, an important feature, which is less informative individually but highly discriminative when combined with others, could be removed (Bolón-Canedo et al., 2013). This issue can be overcome by multivariate filter methods such as Correlation-based feature selection, but at the cost of being slower and less scalable than univariate methods (Bolón-Canedo et al., 2013).

Two filter methods were used in this research: Correlation-based feature selection and Information gain.

4.3.1.1.1.1 *Correlation-based feature selection filter (CFS)*

CFS is a multivariate filter algorithm that uses a correlation based heuristic evaluation function (Hall, 1999) to select a subset of features. These features are

individually correlated with the class but uncorrelated with each other. The CFS's feature subset evaluation function is described by Hall (1999) as following:

$$M_s = \frac{k\overline{r_{cf}}}{\sqrt{k+k(k-1)\overline{r_{ff}}}}$$

Where M_s is the heuristic “merit” of a feature subset S containing k features, $\overline{r_{cf}}$ is the mean feature-class correlation, and $\overline{r_{ff}}$ is the average feature-feature inter-correlation.

4.3.1.1.1.2 Information Gain (InfoGain)

Information gain is a metric for univariate filters which ranks features based on information value (also called entropy). The information gain value of a feature is a measure of the amount of uncertainty that is reduced for a target class when this feature is used. Features with higher information gain values have a greater probability of improving the classification (Rogers et al., 2015).

The formula for entropy and information gain are:

$$\text{Entropy} = \sum_{i=1}^n (-p_i \log_2 p_i) \quad (\text{Shannon and Weaver, 1949; Witten and Frank, 2005})$$

with p_i being the probability of class i .

$$\text{Information gain (Class, Attribute)} = \text{Entropy (Class)} - \text{Entropy (Class | Attribute)}$$

4.3.1.1.2 Wrapper methods

Wrapper methods employ search algorithms to extract the relevant feature sets and evaluate these feature sets by using a machine learning algorithm with cross validation (Witten and Frank, 2005). Search algorithms can be broadly classified as sequential selection algorithms (SS) and heuristic search algorithms (Chandrashekar and Sahin, 2014). Forward selection and backward elimination are examples of SS. The SS starts either with no features and then sequentially adds features, or all features and then sequentially removes features, until the classification performance stops improving (Witten and Frank, 2005). The heuristic search algorithms explore the space of possible subsets of the original feature space, keeping track of the best performing subset as measured by cross validation (Chandrashekar and Sahin, 2014). Genetic Algorithms and Particle Swarm Optimisation are two common heuristic search algorithms.

The main disadvantage of Wrapper methods is the high computational costs associated with training and testing several models, which is required to evaluate each subset. In addition, using classifier performance in the subset selection has a risk of overfitting. Using classification accuracy for the subset selection can lead to an inappropriate feature subset with high accuracy but poor generalization capacity (Chandrashekar and Sahin, 2014). Using cross validation, rather than a single training and testing set, helps to mitigate this.

4.3.1.2 Feature extraction method - Principal component analysis (PCA)

PCA is one of the most popular feature extraction methods used in machine learning (Uğuz, 2011). The first step is to find the principal components of the dataset. This is done by computing the covariance matrix of the data, and then performing an eigen-decomposition.

That is, finding the eigenvectors and associated eigenvalues of the covariance matrix (Abdi and Williams, 2010). The size of each eigenvalue indicates the significance of the relationship represented by the corresponding eigenvector (Widodo et al., 2007). Once principal components have been obtained, a linear transformation can be constructed by concatenating the most informative eigenvectors into a matrix. By multiplying vectors from the original feature space by this matrix, the dimensionality of the data can be reduced while retaining most of the information.

4.3.2 Classification techniques

In this research, a range of classification algorithms were compared, including: Naïve Bayes (NB), Logistic Regression (LR), Random Forest (RF), and Support Vector Machine (SVM). All of these methods were implemented in the WEKA data mining package (version 3.8).

4.3.2.1 Naïve Bayes classifier (NB)

The Naïve Bayes classifier uses Bayes' theorem to predict a new instance, and assumes that the predictive variables are independent given the output class (Duda and Hart, 1973; Pham et al., 2016a; Soria et al., 2011). The Naïve Bayes formula

calculates the un-normalized posterior probabilities of each class using the following equation:

$$P(c|x_1, x_2, \dots, x_n) = \frac{\prod_{i=1}^n P(x_i|c)P(c)}{P(x_1, x_2, \dots, x_n)}$$

where $P(\cdot)$ refers to the probability; x_1, x_2, \dots, x_n are conditionally independent attributes given the class variable c . The instance is then categorized into the class associated with the highest un-normalized probability value.

4.3.2.2 Logistic Regression classifier (LR)

Logistic Regression classifiers are linear models for solving binary classification problems (Cox, 1958). Because the data we considered contained more than two classes, we selected one of the several generalisations to multiclass data. Namely, multinomial logistic regression, which also goes by the name of softmax regression (Bishop, 2007). This method builds a set of binary logistic regression models, each corresponding to a different class. Each of these models can then be used to compute a score indicating how likely a novel instance is to belong to each class. By normalising this vector of scores one can produce a categorical distribution over the possible classes. To make a prediction, one simply selects the class corresponding to the highest probability. Similar to building logistic regression models, these softmax regression models can be trained by minimising the negative log-likelihood of the model parameters through the use of numerical optimisation algorithms.

4.3.2.3 Random Forest classifier (RF)

A Random Forest is an ensemble method that combines multiple decision trees by aggregating their predictions and treating them as votes (Breiman, 2001a). Each tree is built from a bootstrap sample generated by sampling data randomly with replacement from the original dataset. A random subset of the features is used when determining the best split at each node of the tree - a technique known as feature bagging (Liaw and Wiener, 2002; Rodriguez-Galiano et al., 2012). New instances are classified based on the majority vote of the decision trees in the ensemble.

On average, two-thirds of the data points in the original dataset are included in each bootstrap sample, and are known as the ‘in bag’ data, while the remaining one-third

of the data excluded from the bootstrap sample is known as the ‘out-of-bag’ (OOB) data (Rodriguez-Galiano et al., 2012). The OOB data are used to estimate the prediction error, known as the OOB error estimate, by contrasting the predictions from the in-bag data and the OOB data (Poulos and Camp, 2010). The OOB samples are also used to measure the importance of each variable by randomly changing the values of a given variable in the OOB samples. The variable importance is positively correlated with the change in OOB error (Hastie et al., 2009).

Two parameters – *mtry* (the number of predictors) and *ntree* (the number of classification trees) – need to be specified. Choosing good values for *mtry* and *ntree* is necessary to build a RF model with a low OOB error. These two parameters were identified using the multi-search scheme in WEKA.

4.3.2.4 Support Vector Machines classifier (SVM)

SVM algorithm, formally developed by Vapnik (1995), implicitly maps the original training data into a higher dimensional vector space, through the use of a kernel function, where the maximum margin separating hyperplane is used to classify the input data (Han et al., 2012; Rodrigues and de la Riva, 2014). In this research, the Gaussian radial basis function (RBF) was used as the kernel function. Given the training data T with n samples: $T = \{(x_1, y_1), (x_2, y_2), \dots, (x_n, y_n)\}$, $x_i \in R^d$ and $y_i \in \{-1, 1\}$, $i=1, 2, \dots, n$, the SVM classification model can be written as:

$$f(x) = \text{sign}\left(\sum_{i,j=1}^n \alpha_i y_i K(x_i, x_j) + b\right)$$

where K is the kernel function, α_i is a Lagrange multiplier, and b is a scalar bias term.

The RBF-SVM was used in this research for many reasons. First, the RBF kernel can deal with the situation where the relationship between the class labels and features is non-linear. Consequently, the RBF-SVM proves to be more accurate for nonlinear, complex classification problems (Izenman, 2008). Second, the RBF kernel has fewer tuning parameters than the polynomial and the sigmoid kernels. It is known that the number of tuning parameters affects the complexity of model selection. There are only two parameters required for a RBF-SVM: the regularisation coefficient (C) and the kernel smoothness (γ). The multi-search function in WEKA was used to find a good assignment for these two parameters.

Values in the set 2^i with $i = -10, -9, \dots, 15$ were considered for C , and 2^i with $i = -8, -2, \dots, 8$ for γ .

4.3.3 *Validation and comparison method*

To obtain a reliable result for each algorithm, a 10-fold cross-validation was performed on the entire data set and repeated 5 times. For each 10-fold cross-validation process, the data set was first divided into ten equal-sized parts or folds. Then 10 iterations of training and validation were performed. With each iteration a different fold was held out for validation and the remaining nine folds were used for training the classification model.

In this research, the overall accuracy (OA) and the Kappa coefficient of agreement were used to measure the accuracy of each classifier. For comparing different classifiers, the corrected paired t-test (Nadeau and Bengio, 2003) with a significance level of 0.05 was used.

4.4 **Results and Discussions**

Since this research compares four different classifiers combined with four different dimensionality reduction methods, and six different levels of sampling, a total of 96 unique combinations are analysed. The performances of these combinations were compared using the paired t-test. This produced a large number of results and it is not practical to present them all. Instead, three sets of comparisons are used to present the results. First, the performance of the four different classifiers combined with the four different dimensionality reduction (DR) methods are compared. These overall accuracies are also compared with just the performance of each classifier alone without using dimensionality reduction. The results showed that dimensionality reduction only improved the NB classifier. Second, the performance of the different classifiers is then compared using a range of sample sizes and no dimensionality reduction. The best performances varied with sample size, however SVM had the best performance when sample size was over 25. Third, the best combinations of classifier and DR (or No DR) are presented using different sample sizes. The best combination was SVM with No DR when the sample size was 50 or above.

4.4.1 *Comparison of dimensionality reduction and non-dimensionality reduction for the different classifiers*

Table 4.2 and Figure 4.3 show the performance of each classifier (NB, LR, RF, and SVM) with 125 training samples per class combined with four different dimensionality reduction (DR) methods and no dimensionality reduction (no DR). Table 4.2 also shows the paired t-test results when the combination of each classifier and DR is compared with just the classifier (no DR). The DR methods only improved the accuracy significantly for the NB classifier, and this was only using the CFS and Wrapper methods (see Table 4.2). This is because of the sensitivity of NB to redundant and irrelevant features (Fong et al., 2015). DR techniques did not improve the performance of RF, and when RF was used with PCA it actually reduced the accuracy. This result is in line with Dalponte et al. (2013) and is observed regardless of the training set size. RF performs an implicit feature selection or feature weighting in its learning process, therefore reducing the number of input features does not enhance the classification performance (Dalponte et al., 2013). Dimensionality reduction also did not improve SVM performance, even when the training set size was small.

Table 4.2. Comparison between four different classifiers combined with four different DR methods and no DR. Paired t-test (corrected) between the use of DR and no DR at 0.05 significance level from 10-fold CV repeated 5 times. Note: (b) and (w) denote that the result was statistically better or worse respectively than the no DR, while (-) denotes that there was no significant difference.

Classifiers	Dimensionality Reduction method	OA (%)
Naïve Bayes	CFS	77.7 (b)
	InfoGain	72.9 (-)
	PCA	75.7 (-)
	Wrapper NB + Linear Forward Selection	79.0 (b)
	No DR	71
Logistic Regression	CFS	83.5 (-)
	InfoGain	83.9 (-)
	PCA	81.6 (-)
	Wrapper LR + Linear Forward Selection	84.1 (-)
	No DR	84.8
Random Forest	CFS	85.3 (-)
	InfoGain	86.2 (-)
	PCA	78.6 (w)
	Wrapper RF + Linear Forward Selection	87.0 (-)
	No DR	87.2
Support Vector Machine	CFS	85.9 (-)
	InfoGain	85.8 (-)
	PCA	84.9 (w)
	Wrapper SVM + Linear Forward Selection	87.0 (-)
	No DR	88.2

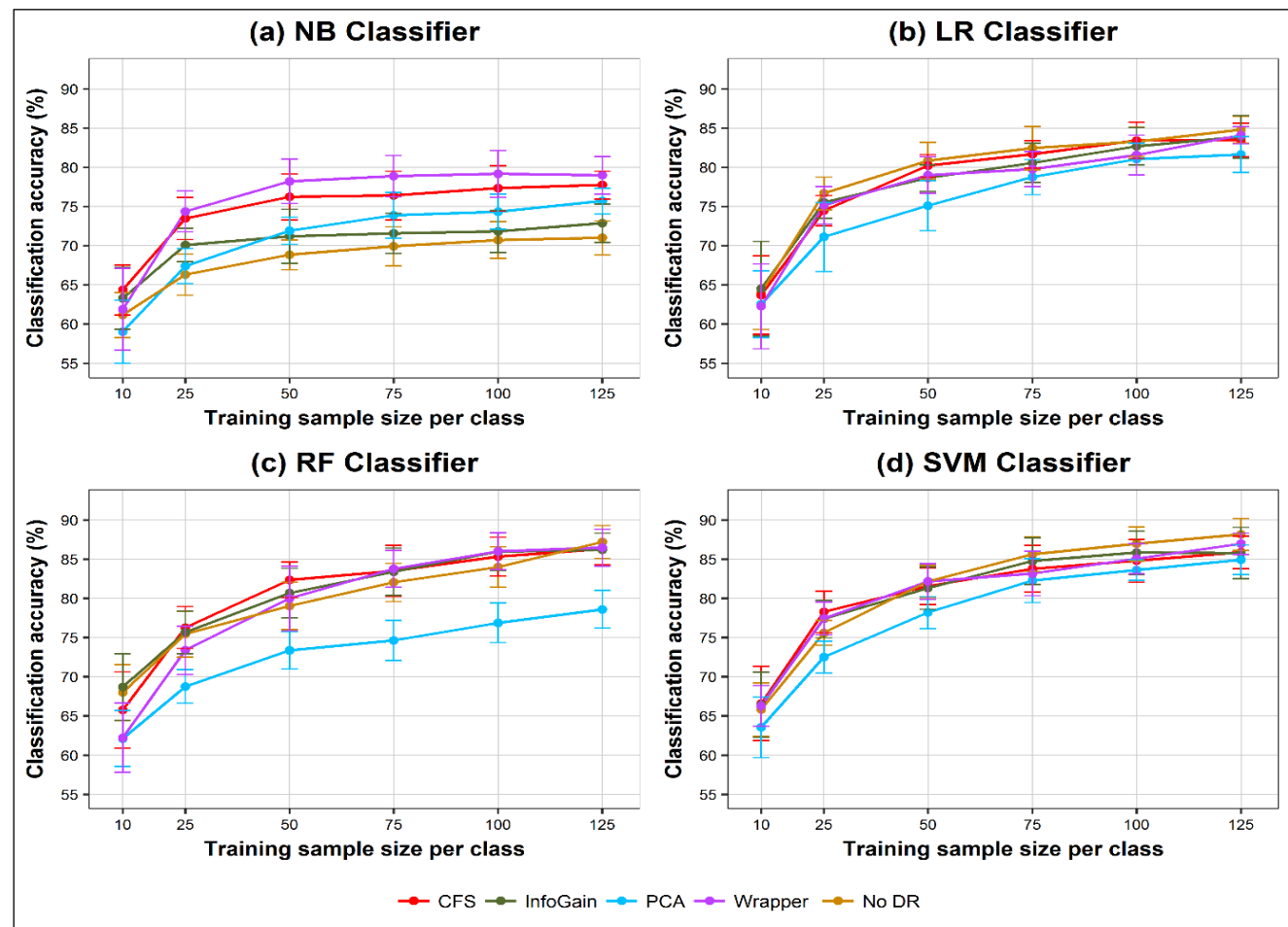


Figure 4.3. Classification accuracy (OA) of NB, LR, RF, and SVM with different DR and no DR using a range of training samples per class

4.4.2 Comparing the performance of different classifiers using different training sample sizes and no DR

Figure 4.3 also shows the effect of training sample size on classification performance. Figure 4.4, for visual convenience, only compares the classifiers without DR. The performance improves with increasing sample sizes and this research does not show the level of sampling where there is no incremental improvement in performance. Notably, the accuracy of the Naïve Bayes classifier increases much slower than the other methods once the sample sizes are over 50. Ng and Jordan (2002) provide some theoretical reasoning for why this might be. Table 4.3 supports these finding by showing the individual overall accuracies (OA) and Kappa statistics (K). Table 4.3 also shows what comparisons are statistically significant.

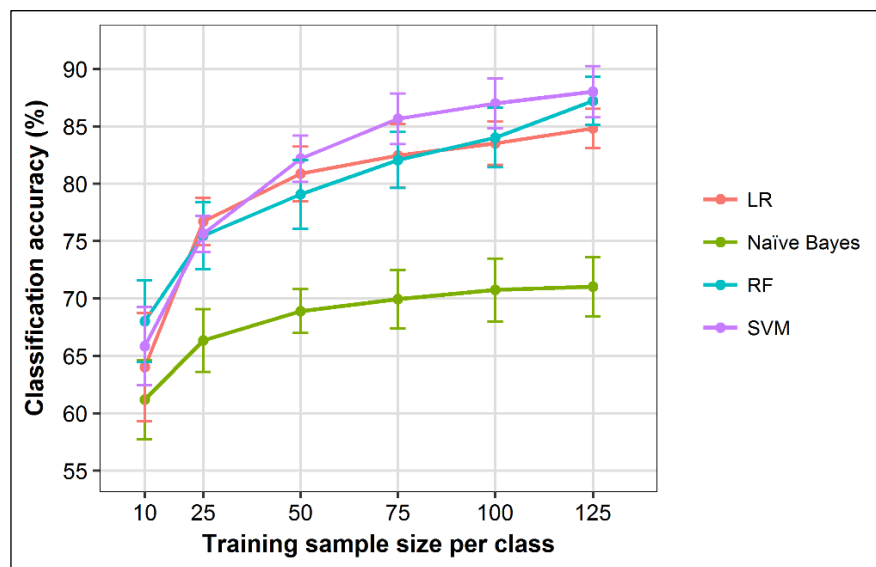


Figure 4.4. Classification accuracy (OA) of NB, LR, RF, and SVM with different training sizes per class with no DR

Table 4.3. Comparing NB, LR, RF, and SVM using all features and different training set sizes with 10-fold CV repeated 5 times and paired t-tester (corrected) at 0.05 significance level. Note: Bolded OA and Kappa scores indicate the highest performance, b and w denote the result is statistically better or worse than the classifier compared; while - denotes there is no significant difference between classifiers.

Training size	Classifier	OA (%)	Kappa	Paired t-test results			
				NB	LR	RF	SVM
10 samples per class	NB	61.2	0.48	NB	-	w	-
	LR	64.0	0.52	-	LR	-	-
	RF	68.0	0.57	b	-	RF	-
	SVM	65.8	0.54	-	-	-	SVM
25 samples per class	NB	67.3	0.56	NB	w	w	w
	LR	76.7	0.69	b	LR	-	-
	RF	75.4	0.67	b	-	RF	-
	SVM	75.6	0.67	b	-	-	SVM
50 samples per class	NB	67.9	0.57	NB	w	w	w
	LR	80.8	0.74	b	LR	-	-
	RF	79.0	0.72	b	-	RF	-
	SVM	82.2	0.76	b	-	-	SVM
75 samples per class	NB	69.9	0.60	NB	w	w	w
	LR	82.4	0.77	b	LR	-	-
	RF	82.0	0.76	b	-	RF	-
	SVM	85.6	0.81	b	-	-	SVM
100 samples per class	NB	70.7	0.61	NB	w	w	w
	LR	83.3	0.78	b	LR	-	w
	RF	84.0	0.79	b	-	RF	-
	SVM	87.0	0.83	b	b	-	SVM
125 samples per class	NB	71.0	0.61	NB	w	w	w
	LR	84.8	0.79	b	LR	-	w
	RF	87.2	0.83	b	-	RF	-
	SVM	88.2	0.84	b	b	-	SVM

4.4.3 Comparing the performance of the best combinations of classifier and DR (or no DR)

Table 4.4 and Figure 4.5 compares the performance of each classifier when combined with the best DR (or no DR) that suits each classifier for a particular training sample size. For each combination of sample size and classification algorithm, we selected the DR (or no DR) that performed best in the previous experiments. When the training sample size is 25 or less there is no difference in performance of the different classifiers when these are combined with the most suitable DR (or no DR). When the sample size is 50 or greater, SVM is better than NB. SVM also has higher performance than RF when sample size is large but this

is not significant. RF is better than SVM when the sample size is 10 but this is also not significant.

These results are consistent with other research, where SVM outperformed other parametric classifiers (Tien Bui et al., 2012). These results confirm the research of Dalponte et al. (2013), where there was no significant difference between SVM and RF classifiers. RFs and SVMs are both capable of approximating arbitrary nonlinear functions, with the accuracy of this approximation constrained by the regularisation parameters of each scheme.

For LR, although in general its OA and Kappa were lower than RF, no statistically significant difference was found. This trend does not extend to the comparison with SVM, where LR was statistically significantly worse than SVM when the sample size is 125. The ability of these nonlinear methods to outperform Logistic Regression provides some evidence that there is an inherent nonlinear relationship between the input features and the log odds of the output target variable. This is something that can be difficult to verify in practice because of the high dimensionality of the data. When many features are present in a dataset, visualisation becomes difficult and standard goodness-of-fit tests for linear models are known to be ineffective (Breiman, 2001b).

Table 4.4. Comparing the best classification accuracy of NB, LR, RF, and SVM and different training set sizes with 10-fold CV repeated 5 times and paired t-tester (corrected) at 0.05 significance level. Note: Bolded OA and Kappa scores indicate the highest performance, b and w denote that the result is statistically significantly better or worse respectively than the classifier compared; while - denotes there is no significant difference between classifiers.

Training size	Classifier + DR (or no DR)	OA (%)	Kappa	Paired t-test results			
				NB	LR	RF	SVM
10 samples	NB + CFS	64.4	0.52	NB	-	-	-
	LR + InfoGain	64.5	0.53	-	LR	-	-
	RF + InfoGain	68.7	0.58	-	-	RF	-
	SVM + CFS	66.6	0.56	-	-	-	SVM
25 samples	NB+ Wrapper	74.3	0.66	NB	-	-	-
	LR + no DR	76.7	0.69	-	LR	-	-
	RF + CFS	76.3	0.68	-	-	RF	-
	SVM +CFS	77.4	0.70	-	-	-	SVM
50 samples	NB+ Wrapper	77.2	0.71	NB	-	w	w
	LR + no DR	80.8	0.74	-	LR	-	-
	RF + CFS	82.4	0.76	b	-	RF	-
	SVM + no DR	82.4	0.76	b	-	-	SVM
75 samples	NB+ Wrapper	77.7	0.71	NB	-	w	w
	LR + no DR	82.4	0.77	-	LR	-	-
	RF + CFS	83.8	0.78	b	-	RF	-
	SVM + no DR	85.6	0.81	b	-	-	SVM
100 samples	NB+ Wrapper	78.3	0.72	NB	w	w	w
	LR + CFS	83.6	0.78	b	LR	-	-
	RF + Wrapper	86.7	0.81	b	-	RF	-
	SVM + no DR	87.0	0.83	b	-	-	SVM
125 samples	NB+ Wrapper	79.0	0.72	NB	w	w	w
	LR + no DR	84.8	0.79	b	LR	-	w
	RF + no DR	87.2	0.83	b	-	RF	-
	SVM + no DR	88.2	0.84	b	b	-	SVM

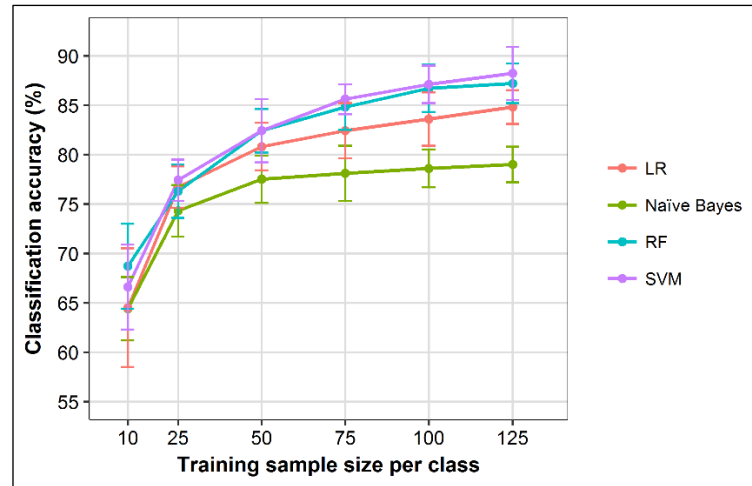


Figure 4.5. The classification accuracy of the best combination of classifier and DR (or no DR) for different training sample size per class. Note: the DR (or no DR) changes with the sample size.

4.5 Conclusion

This study has provided further evidence that SVM and RF are the best classification algorithms compared to other machine learning algorithms when using integrated data sets for identifying tree species. The results suggest that SVM or RF should be used when high accuracy is required for tree species classification.

The four DR methods did not improve the accuracy of SVM and RF, and only improved the accuracy of NB. However, the benefit of using a DR method in combination with classifiers is that it reduces computation, and thus speeds up the modelling process. This research does not show that DR methods significantly decrease the accuracy of classifiers, therefore they can be applied prior to classification with all four classifiers to accelerate the model fitting process — particularly when the sample size is large. Among the various feature selection methods, the CFS approach should be used when speed is important because it is much faster than Wrapper methods. The CFS is also more convenient than the InfoGain method because the CFS method does not need the user to select the number of desired features, while the InfoGain does.

Although Naïve Bayes was the worst classifier in terms of classification accuracy, when the sample size was small, it achieved similar accuracies to the other classifiers. This is congruent with the conclusions made by Ng and Jordan (2002), where it is shown that generative models have a tendency to outperform

discriminative models when sample sizes are small. The additional benefit of NB is that it is simple and fast compared to LR, RF, and SVM because it does not require tuning parameters for training. The performance of NB also improves with the feature selection methods. Future research could investigate the performance of other generative model, such as Bayesian Networks, that could potentially be more sample efficient than discriminative models such as LR, RF, and SVM.

The range of classifiers as well as the different data pre-processing techniques that are available are increasingly complicating image classification methods. When these techniques are combined, there are a large number of potential outcomes. It is important to investigate these combination and outcomes for different applications. This research has systematically researched a range of classifiers and dimensionality reduction methods for tree species classification to provide a clear picture of how these techniques perform and the trade-offs associated with different sampling intensity. This type of research is important for guiding future tree species classification using remote sensing data.

REFERENCES

- Abdi, H., Williams, L.J., 2010. Principal component analysis. *Wiley Interdisciplinary Reviews: Computational Statistics* 2(4), 433-459. <https://doi.org/10.1002/wics.101>
- Bishop, C.M., 2007. *Pattern Recognition and Machine Learning*. Springer, New York, NY.
- Bolón-Canedo, V., Sánchez-Marono, N., Alonso-Betanzos, A., 2013. A review of feature selection methods on synthetic data. *Knowledge and Information Systems* 34(3), 483-519. <https://doi.org/10.1007/s10115-012-0487-8>.
- Breiman, L., 2001a. Random forests. *Machine Learning* 45(1), 5-32. <https://doi.org/10.1023/A:1010933404324>
- Bylsma, R.J., Clarkson, B.D., Efford, J.T., 2014. Biological flora of New Zealand 14: *Metrosideros excelsa*, pōhutukawa, New Zealand Christmas tree. *New Zealand Journal of Botany* 52(3), 365-385. <https://doi.org/10.1080/0028825x.2014.926278>
- Chandrashekar, G., Sahin, F., 2014. A survey on feature selection methods. *Computers & Electrical Engineering* 40(1), 16-28. <https://doi.org/10.1016/j.compeleceng.2013.11.024>
- Cox, D.R., 1958. The regression analysis of binary sequences. *Journal of the Royal Statistical Society. Series B (Methodological)* 20(2), 215-242.
- Dalponte, M., Ørka, H.O., Gobakken, T., Gianelle, D., Næsset, E., 2013. Tree species classification in boreal forests with hyperspectral data. *IEEE Transactions on Geoscience and Remote Sensing* 51(5), 2632-2645. <https://doi.org/10.1109/TGRS.2012.2216272>
- Duda, R.O., Hart, P.E., 1973. *Pattern Classification and Scene Analysis*. John Wiley, New York, NY.
- Fassnacht, F.E., Hartig, F., Latifi, H., Berger, C., Hernández, J., Corvalán, P., Koch, B., 2014a. Importance of sample size, data type and prediction method for remote sensing-based estimations of aboveground forest biomass. *Remote Sensing of Environment* 154, 102-114. <https://doi.org/10.1016/j.rse.2014.07.028>
- Fassnacht, F.E., Neumann, C., Förster, M., Buddenbaum, H., Ghosh, A., Clasen, A., Joshi, P.K., Koch, B., 2014b. Comparison of feature reduction algorithms for classifying tree species with hyperspectral data on three central European test sites. *IEEE Journal of Selected Topics in Applied Earth Observations and Remote Sensing* 7(6), 2547-2561. <https://doi.org/10.1109/Jstars.2014.2329390>
- Fong, S., Zhuang, Y., Liu, K., Zhou, S., 2015. Classifying forum questions using PCA and machine learning for improving online CQA, *International Conference on Soft Computing in Data Science*, Putrajaya, Malaysia, pp. 13-22.
- Frank, E., Hall, M.A., Witten, I.H., 2016. *The WEKA Workbench*. Online Appendix for "Data Mining: Practical Machine Learning Tools and Techniques", 4th ed. Morgan Kaufmann, Cambridge, MA.
- Galelli, S., Humphrey, G.B., Maier, H.R., Castelletti, A., Dandy, G.C., Gibbs, M.S., 2014. An evaluation framework for input variable selection algorithms for environmental data-driven models. *Environmental Modelling & Software* 62, 33-51. <https://doi.org/10.1016/j.envsoft.2014.08.015>

- Hall, M.A., 1999. Correlation-Based Feature Selection for Machine Learning (Unpublished PhD thesis). University of Waikato, Hamilton, New Zealand.
- Han, J., Kamber, M., Pei, J., 2012. Data Mining: Concepts and Techniques, 3rd ed. Morgan Kaufmann, Boston, MA.
- Hastie, T.J., Tibshirani, R.J., Friedman, J.H., 2009. The Elements of Statistical Learning: Data Mining, Inference, and Prediction. Springer, New York, NY.
- Izenman, A.J., 2008. Modern Multivariate Statistical Techniques. Springer, New York, NY.
- Ke, Y., Quackenbush, L.J., Im, J., 2010. Synergistic use of QuickBird multispectral imagery and LIDAR data for object-based forest species classification. *Remote Sensing of Environment* 114(6), 1141-1154. <https://doi.org/10.1016/j.rse.2010.01.002>
- Liaw, A., Wiener, M., 2002. Classification and regression by random forest. *R News* 2(3), 18-22.
- Ma, L., Fu, T., Blaschke, T., Li, M., Tiede, D., Zhou, Z., Ma, X., Chen, D., 2017. Evaluation of feature selection methods for object-based land cover mapping of unmanned aerial vehicle imagery using random forest and support vector machine classifiers. *ISPRS International Journal of Geo-Information* 6(2), ARTN 51. <https://doi.org/10.3390/ijgi6020051>
- Nadeau, C., Bengio, Y., 2003. Inference for the generalization error. *Machine Learning* 52(3), 239-281. <https://doi.org/10.1023/A:1024068626366>.
- Ng, A.Y., Jordan, M.I., 2002. On discriminative vs. generative classifiers: A comparison of logistic regression and naive bayes. *Adv Neur In* 2, 841-848.
- Pal, M., Foody, G.M., 2010. Feature selection for classification of hyperspectral data by SVM. *IEEE Transactions on Geoscience and Remote Sensing* 48(5), 2297-2307. <https://doi.org/10.1109/TGRS.2009.2039484>
- Pham, B.T., Pradhan, B., Tien Bui, D., Prakash, I., Dholakia, M.B., 2016a. A comparative study of different machine learning methods for landslide susceptibility assessment: A case study of Uttarakhand area (India). *Environmental Modelling & Software* 84, 240-250. <https://doi.org/10.1016/j.envsoft.2016.07.005>.
- Pham, L.T., Brabyn, L., Ashraf, S., 2016b. Combining QuickBird, LiDAR, and GIS topography indices to identify a single native tree species in a complex landscape using an object-based classification approach. *International Journal of Applied Earth Observation and Geoinformation* 50, 187-197. <https://doi.org/10.1016/j.jag.2016.03.015>
- Poulos, H.M., Camp, A.E., 2010. Decision support for mitigating the risk of tree induced transmission line failure in utility rights-of-way. *Environmental Management* 45(2), 217-226. <https://doi.org/10.1007/s00267-009-9422-5>
- Richter, R., Schläpfer, D., 2014. ATCOR-2/3 user guide, version 8.3. 1. Zurich, Switzerland.
- Rodrigues, M., de la Riva, J., 2014. An insight into machine-learning algorithms to model human-caused wildfire occurrence. *Environmental Modelling & Software* 57, 192-201. <https://doi.org/10.1016/j.envsoft.2014.03.003>
- Rodriguez-Galiano, V.F., Ghimire, B., Rogan, J., Chica-Olmo, M., Rigol-Sanchez, J.P., 2012. An assessment of the effectiveness of a random forest classifier for land-cover classification. *ISPRS Journal of Photogrammetry and Remote Sensing* 67, 93-104. <https://doi.org/10.1016/j.isprsjprs.2011.11.002>
- Rogers, B., Qiao, Y., Gung, J., Mathur, T., Burge, J.E., 2015. Using text mining techniques to extract rationale from existing documentation, in: Gero, J.S.,

- Hanna, S. (Eds.), Design Computing and Cognition '14. Springer International Publishing, Cham, pp. 457-474.
- Saeys, Y., Inza, I., Larrañaga, P., 2007. A review of feature selection techniques in bioinformatics. *Bioinformatics*.
<https://doi.org/10.1093/bioinformatics/btm344>
- Shannon, C.E., Weaver, W., 1949. The Mathematical Theory of Communication. University of Illinois Press, Urbana, IL.
- Soria, D., Garibaldi, J.M., Ambrogi, F., Biganzoli, E.M., Ellis, I.O., 2011. A ‘non-parametric’ version of the naive Bayes classifier. *Knowledge-Based Systems* 24(6), 775-784. <https://doi.org/10.1016/j.knosys.2011.02.014>
- Tien Bui, D., Pradhan, B., Lofman, O., Revhaug, I., 2012. Landslide susceptibility assessment in Vietnam using support vector machines, decision tree, and Naive Bayes Models. *Mathematical Problems in Engineering* 2012, 1-26.
<https://doi.org/10.1155/2012/974638>
- Uğuz, H., 2011. A two-stage feature selection method for text categorization by using information gain, principal component analysis and genetic algorithm. *Knowledge-Based Systems* 24(7), 1024-1032.
<https://doi.org/10.1016/j.knosys.2011.04.014>
- Vapnik, V.N., 1995. The Nature of Statistical Learning Theory. Springer-Verlag, New York, NY.
- Widodo, A., Yang, B.-S., Han, T., 2007. Combination of independent component analysis and support vector machines for intelligent faults diagnosis of induction motors. *Expert Systems with Applications* 32(2), 299-312.
<https://doi.org/10.1016/j.eswa.2005.11.031>
- Witten, I.H., Frank, E., 2005. Data Mining: Practical machine learning tools and techniques. Morgan Kaufmann, Cambridge, MA.
- Xue, B., Zhang, M., Browne, W.N., 2014. Particle swarm optimisation for feature selection in classification: Novel initialisation and updating mechanisms. *Applied Soft Computing* 18, 261-276.
<https://doi.org/10.1016/j.asoc.2013.09.018>

CHAPTER 5

MONITORING MANGROVE BIOMASS CHANGE IN VIETNAM USING SPOT IMAGES AND AN OBJECT-BASED APPROACH COMBINED WITH MACHINE LEARNING ALGORITHMS

This chapter was published as following as “Pham, L.T.H., Brabyn, L., 2017. Monitoring mangrove biomass change in Vietnam using SPOT images and an object-based approach combined with machine learning algorithms”. ISPRS Journal of Photogrammetry and Remote Sensing 128, 86 -97”. <http://dx.doi.org/10.1016/j.isprsjprs.2017.03.013>

Abstract

Mangrove forests are well-known for their provision of ecosystem services and capacity to reduce carbon dioxide concentrations in the atmosphere. Mapping and quantifying mangrove biomass is useful for the effective management of these forests and maximizing their ecosystem service performance. The objectives of this research were to model, map, and analyse the biomass change between 2000 and 2011 of mangrove forests in the Cangio region in Vietnam. SPOT 4 and 5 images were used in conjunction with object-based image analysis and machine learning algorithms. The study area included natural and planted mangroves of diverse species. After image preparation, three different mangrove associations were identified using two levels of image segmentation followed by a Support Vector Machine classifier and a range of spectral, texture and GIS information for classification. The overall classification accuracy for the 2000 and 2011 images were 77.1% and 82.9%, respectively. Random Forest regression algorithms were then used for modelling and mapping biomass. The model that integrated spectral, vegetation association type, texture, and vegetation indices obtained the highest accuracy ($R^2_{\text{adj}} = 0.73$). Among the different variables, vegetation association type was the most important variable identified by the Random Forest model. Based on the biomass maps generated from the Random Forest, total biomass in the Cangio mangrove forest increased by 820,136 tons over this period, although this change varied between the three different mangrove associations.

Keywords: Mangrove; Biomass change; Object-based; Random Forest; Support Vector Machine

5.1 Introduction

Mangrove forests provide a wide range of ecological and socio-economic functions. One of their important roles is global climate change mitigation through carbon sequestration. Mangroves are well-known as highly effective carbon sinks when compared with terrestrial forests in the tropics (Donato et al., 2011). However, the extent of mangrove forests worldwide has declined considerably, mainly due to human activities such as shrimp farm expansions and urbanization (Giri et al., 2015). Mangroves in Vietnam have faced the same decline, and have decreased from 408,500 ha in 1943 to 155,290 ha in 2000 (Viet Nam Environment Protection Agency, 2005). Mangroves in the Càngio have been facing the threat of increased coastal erosion as a result of three anthropogenic factors: the waves from large cargo ships, ever expanding aquaculture and salt farming activities, and the negative impacts of socio-economic transformation (Kuenzer and Tuan, 2013). At present, information on the extent and biomass of mangrove forests in Vietnam is deficient. Effective methods to provide such information are necessary to understand how above-ground biomass (AGB) changes in time and space. This information could then be used for effective mangrove management.

There are two common approaches for AGB estimation: field measurements and remote sensing (Lu, 2006; Tian et al., 2014). Although the traditional field inventory method is often the most accurate estimation approach, it is costly, time-consuming, and difficult to apply for large areas. Compared to field measurements, remote sensing can efficiently obtain data on inaccessible regions and provide large and repetitive coverage (Bergen and Dobson, 1999). Therefore, remote sensing is a viable data source for estimating AGB at large scales (Lu, 2006; Proisy et al., 2007; Tian et al., 2014). When linked with biomass inventory data, AGB can be measured using remote sensing data combined with statistical models. Biomass inventory data can be obtained by using the allometric models available for tree species, which are based on input parameters such as diameter at breast height and tree height measured in the field.

There is a range of promising approaches for biomass estimation that use new remote sensing data sources. These include synthetic aperture radars (Bergen and Dobson, 1999; Hamdan et al., 2014; Le Toan et al., 1992; Proisy et al., 2000; Simard

et al., 2006) and light detection and ranging (LiDAR) (Drake et al., 2002; Feliciano et al., 2014; Lefsky et al., 2002; Popescu et al., 2011). Compared to optical sensors, these types of data sets have the advantage of penetrability through forest canopy to get tree trunk information. Therefore, biomass estimation can achieve higher accuracy because the trunks may contain over 60% of the above-ground biomass (Bergen and Dobson, 1999). Especially, for radar data sets, they are also weather independent; while for LiDAR data sets, they overcome the saturation problem which limits the usefulness of optical and radar data in regions with high biomass levels (Chen, 2013). The disadvantages of LiDAR data sets are their cost to capture and their limited spectral resolution (Chen, 2013).

This research focuses on optical images for monitoring biomass change because there are new techniques available to improve the biomass estimation accuracy; and fundamentally, they are the only cost effective solution for use in developing countries, where the majority of the world's mangrove forests exists. They are also the only solution for retrospectively estimating biomass over the past decades because archived images are available. Optical data sets that have been used for measuring biomass in mangrove forests include Landsat and SPOT (Hamdan et al., 2013), IKONOS (Proisy et al., 2007), ALOS AVNIR-2 (Wicaksono et al., 2016), and GeoEye-1 (Jachowski et al., 2013). These optical data sets are available at various spatial, spectral, and temporal resolutions. However, the accuracy of the biomass estimates using optical sensor data is compromised in overcast weather and by factors such as forest stand complexity and shadows caused by canopy and topography (Lu et al., 2014). These limiting factors can be reduced through the use of object-based analysis and textural images (Lu et al., 2014). Addink et al. (2007) showed that object-based image analysis for biomass estimation provides higher accuracy than a pixel-based approach. In addition, because different mangrove species have their own allometric models, AGB accuracy can be improved by using species maps and species-specific allometric relationships (Chen et al., 2012).

Different parametric and non-parametric statistical models have been used for predicting mangrove biomass. Compared to parametric methods, the prediction accuracy of the non-parametric approaches is often better because they do not make assumptions about the distribution of the data (Tian et al., 2014). Therefore, the non-parametric approaches are preferred (Jachowski et al., 2013). One of the most

common non-parametric methods that has been used for mangrove biomass estimation is the Random Forest algorithm (Mutanga et al., 2012), which is discussed in the Methods Section.

Although previous research has used an object-based approach for estimating biomass in different forest types (Charoenjit et al., 2015; Kajisa et al., 2009), it has primarily focused on estimating biomass at a specific time. There have not been many published research projects that use an object-based approach for monitoring forest biomass change over a period of time. This research addresses this knowledge gap using the Cangio mangrove forest of Vietnam as a study area. The specific objectives of this research include: (1) mapping mangrove associations in the Cangio mangrove forest in 2000 and 2011 using object-based classification; (2) establishing a relationship between mangrove biomass and indices derived from SPOT4 and SPOT5 images using Random Forest models; and (3) quantifying and analysing mangrove biomass changes between 2000 and 2011.

5.2 Materials

5.2.1 Study area

The Cangio mangrove forest is located in Cangio District (see Figure 5.1) - one of 24 districts of Ho Chi Minh City - covering an area of about 72 000 ha. In January 2000, the Cangio mangrove forest was recognized as the first biosphere reserve in Vietnam. This reserve consists of 60% planted and 40% natural forests (Kuenzer and Tuan, 2013). There are more than 200 species of fauna and more than 52 species of flora, so it is considered to have high biodiversity (Nguyen, 2006). There are three main floral associations (Luong et al., 2015). The first of these is the *Avicennia alba* – *Sonneratia alba* association (Association I), which is often found along estuaries, riverbanks, and watery, muddy flats. This association is dominated by *Avicennia alba* and *Sonneratia alba* or mixed with *Avicennia officinalis*, *Rhizophora mucronata*, and *Sonneratia caseolaris*. These species are tolerant of high salinity and are able to grow on unstable soil (Kuenzer and Tuan, 2013). The second association is mainly *Rhizophora apiculata* (Association II), which is located on stable land and covering large areas of the Cangio mangrove forest. The remaining association (Association III or mixed species) is found on higher ground and stable clay and contains small tree/shrub species such as *Phoenix paludosa*,

Ceriops zippeliana, *Xylocarpus granatum*, and *Lumnitzera racemosa*. Besides these vegetation associations, the research area includes shrimp ponds, bare lands, and muddy flats.

Although the research area has different types of mangrove species, this research used the association of the dominant species as described above because the resolution of the SPOT images was not high enough to identify each specific species (Wang et al., 2004a). This approach has been used by Chen et al. (2012) due to the strong correlation between forest stand biomass and prevailing species.

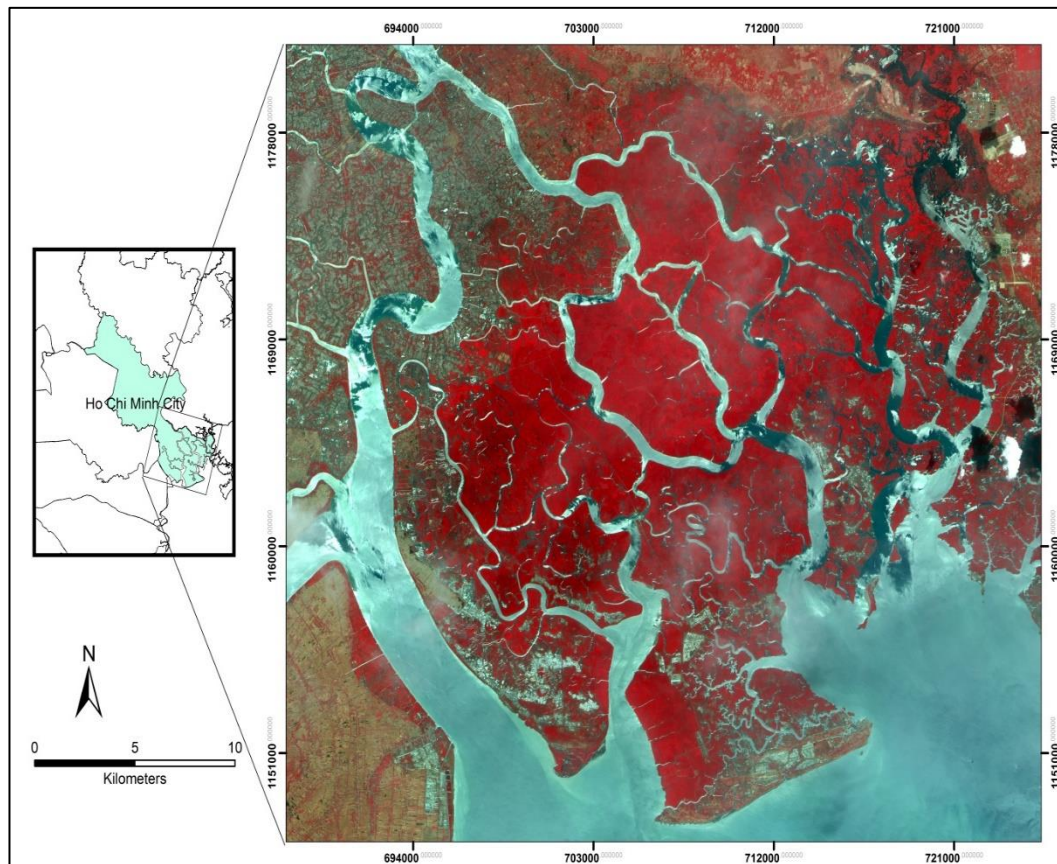


Figure 5.1. SPOT4 image of the Cangio study area. The coordinate is in WGS 1984 UTM zone 48N projection system.

5.2.2 Field data collection

The GPS position and mangrove floral associations were collected for 525 points distributed over the study area. Of these 525 points, 60% were used for classification training, and the remaining 40% were used for validation.

Plot locations for biomass estimation were selected using a stratified random sampling approach, based on the classification maps generated from this research and the management zones issued by the HCMC Forest Protection Department. The sample plots covered the three floral associations described previously and included a wide range of age classes and stand densities. A total of 140 plots – 30m x 30m, were measured and of these a third were collected in 2000 and the remaining collected during 2016. The diameter at breast height (DBH) of each living tree with a DBH greater than 5 cm was recorded for each plot. The DBH records of 98 (70%) plots were then used for biomass model training, and the remaining plots (42) were used for validation.

The above-ground biomass of each plot was calculated from five species-specific allometric equations for the Cangio mangrove forest. For species where the allometric equation was unknown, a generic allometric equation developed by Komiyama et al. (2005) was used. Table 5.1 provides details on the species-specific allometric equations, and Table 5.2 provides the descriptive statistics of the generated biomass results.

Table 5.1. Species-specific biomass allometric equations for the Cangio mangrove forest

Species	Biomass allometric equation (kg)
<i>Rhizophora apiculata</i>	$W = 0.3482 \times (\text{DBH})^{2.2965}$ (Nam, 2011b)
<i>Avicennia alba</i>	$W = 0.128 \times (\text{DBH})^{2.417}$ (Nam, 2003)
<i>Lumnitzera racemosa</i>	$W = 0.0157 \times (\text{DBH})^{2.36238}$ (Nam, 2011a)
<i>Ceriops zippeliana</i>	$W = 0.20792 \times (\text{DBH})^{2.407}$ (Binh and Nam, 2014)
<i>Phoenix paludosa</i>	$W = (-1.5857 + 1.6962 \times \sqrt{\text{DBH}})^2$ (Sang, 2011)

W: Dry biomass (kg)

Table 5.2. Descriptive statistics of biomass plots

Vegetation association	No. of plots	Biomass (ton/ha)				Tree density	
		Min	Max	Mean	Standard deviation	Min no. of trees	Max no. of trees
Association I	30	42	324	72	35	90	450
Association II	75	58	596	276	52	57	400
Association III	35	30	347	134	68	102	1092

5.2.3 *Image data*

Two orthorectified satellite images were obtained for this research - a SPOT4 image captured on 26th March, 2000, and a SPOT5 image captured on 24th February, 2011. Both images have four multispectral bands, each with 10m spatial resolution. These bands are green (500-590 nm), red (610-680 nm), near infrared (NIR, 780-890 nm), and mid infrared (MIR, 1580 -1750 nm).

5.3 **Methods**

The procedures for predicting biomass with the object-based image analysis involved two main steps: (1) identifying the three mangrove associations with two-level segmentation and a Support Vector Machine for classification, and (2) estimating biomass using the Random Forest algorithm with a range of object features - spectral, texture, vegetation indices, and vegetation association type. Figure 5.2 provides an overview of the method developed. A detailed description and justification of the main steps are discussed further in the following sections.

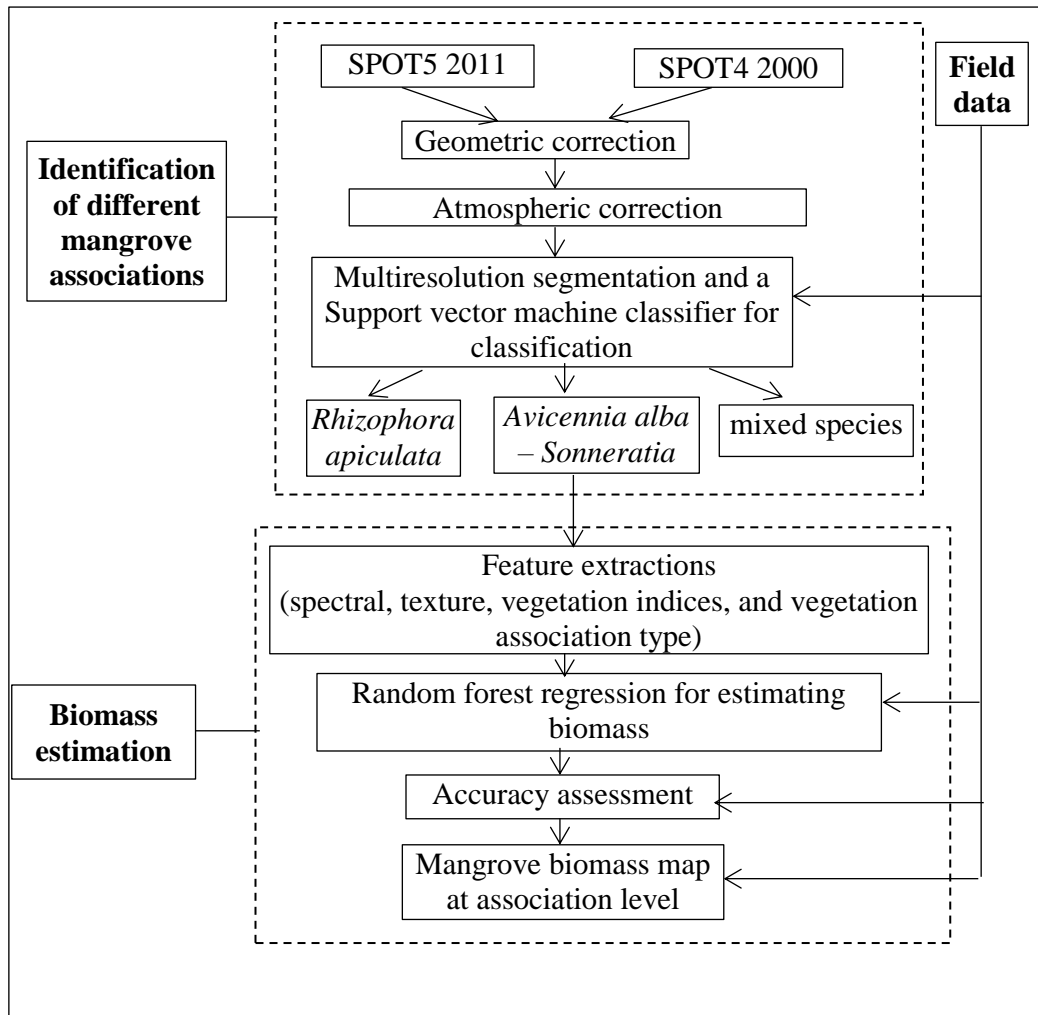


Figure 5.2. A workflow of estimating ABG in the Cangio mangrove forest from SPOT data and ground inventory data.

5.3.1 Image data pre-processing

The pre-processing first involved geo-referencing the images to the topographic map of Ho Chi Minh City at a scale of 1:5000. This process used 30 control points, the first order polynomial transformation, and the nearest neighbour resampling algorithm for each image. The nearest neighbour resampling method was selected because it maintains the original pixel values of the images (Wicaksono et al., 2016). The root-mean-square error for the geo-referencing was less than 0.5 pixels (5 m). Digital numbers of the images were then converted into radiance values. Lastly, the images were atmospherically corrected to obtain surface reflectance using the Fast Line-of-sight Atmospheric Analysis of Hypercubes (FLAASH) module of ENVI software.

5.3.2 *Classifying different mangrove associations*

As mentioned in Section 5.2.1, the study area is a heterogeneous landscape which includes water bodies (river channels and shrimp ponds), non-vegetation types (bare land, muddy flats, and roads), and different mangrove associations. Therefore, water and non-vegetation types were identified and excluded prior to distinguishing different mangrove associations. An object-based approach with a two-level segmentation was used to identify different land cover types because it provided greater accuracy than pixel-based approaches for mangrove forests (Myint et al., 2008). The object-based image analysis includes two main steps: (1) image segmentation which divides an image into contiguous, separate, and homogeneous areas and (2) image classification (Blaschke, 2010). In this research, the multi-resolution segmentation algorithm in eCognition Developer 9.1 was used for the two levels of segmentation. This is a region-growing technique that starts with single pixels as image objects and then merges them with their neighbours based on relative homogeneity criteria (Trimble Germany GmbH, 2015b). This homogeneity criterion comprises spectral and shape criteria where shape is composed of smoothness and compactness.

5.3.2.1 *Level 1: Masking of water and non-vegetation regions*

A first level segmentation was used to distinguish between water and other features. This used the four bands from the SPOT images, with an equal weight of one for all bands. The scale parameter, which determines the size of the image objects created, was set to one so that small objects such as roads and channels could be identified and excluded. The spectral information contributes more to the identification of the homogeneous regions than the shape information, therefore the shape parameter was set to a low value (0.1). To set the weighting of smoothness and compactness equally, compactness was set to 0.5. These shape and compactness values were constant for the second level of segmentation.

After segmentation, objects with a mean Normalized Difference Water Index (NDWI) higher than zero and a Normalized Difference Vegetation Index (NDVI) less than 0.3 were classified as water. The NDWI was calculated from the green and MIR bands (Ji et al., 2009), and the NDVI was calculated from the red and near infra-red bands.

Rivers needed to be distinguished from shrimp pond objects because distance between vegetation and the river was required for later analysis of mangrove associations. Water objects with a length larger than 2 km were assigned as river objects, and then merged.

The remaining objects were either non-vegetation or vegetation. Vegetation was distinguished from non-vegetation by using a NDVI threshold greater than 0.3.

5.3.2.2 Level 2: Identifying three mangrove associations

This second level was used for segmenting vegetation and then classifying vegetation into three mangrove associations (referred to in Section 5.2.1).

For segmentation, input layers included all four spectral bands and a DEM layer. Adding topographic information for segmenting can result in higher accuracy for vegetation classification than the use of spectral information alone (Ke et al., 2010). The layer weight was set at one for each input layer except the NIR band, which was set at four because vegetation reflectance is more differentiated in this band (Chemura et al., 2015). After visually comparing the segmentation quality of different parameter values, the scale parameter was set at three. At this scale the average object size was 0.8 ha, which is similar with the average patch size in the field inventory.

After segmentation, a Support Vector Machine (SVM) algorithm was used to classify different mangrove associations. The theory of SVM was developed by Vapnik (1995). The SVM algorithm determines a hyperplane that separates the dataset into a discrete number of classes. The advantage of the SVM is that it is a non-parametric classifier and does not require an assumption of normal distribution of the dataset. The SVM has been also shown to obtain a higher classification accuracy than other traditional parametric classifiers in a complex landscape (Dalponte et al., 2009; Pham et al., 2016c).

The object feature variables considered for mangrove classification included the spectral and texture values listed in Table 5.3, as well as topography (elevation and slope), and distance from the river. A SVM with Gaussian Radial Basis Function (RBF) was used for this study. Two parameters are required for the RBF kernel

SVM training: a cost parameter C and gamma (γ). The cost parameter controls the trade-off between the misclassification rates for the training data and the model's complexity (Cortes and Vapnik, 1995). A smaller value for C leads to a larger error on the training data with a simple prediction function, while a higher value C creates a lower classifying error on training data with a complex prediction function (Joachims, 2002). The γ controls the width of the Gaussian function. A smaller γ value gives a lower bias and higher variance, while a large γ leads to a higher bias and lower variance (Ben-Hur et al., 2008).

5.3.3 *Estimating biomass*

5.3.3.1 *Features for predicting biomass*

Table 5.3 lists the wide range of feature variables that were considered for predicting biomass. They include spectral, texture, vegetation indices, and vegetation association type (obtained from Section 5.3.2.2). The object texture features were based on Haralick et al. (1973) and vegetation indices were calculated in eCognition software. The 2000 ground truthed biomass values were compared with the variables derived from the 2000 SPOT image, and the 2016 ground truthed biomass values were compared with the variables derived from the 2011 SPOT image because the 2011 biomass data were not available. Both sets of comparisons were used to develop the biomass models.

Table 5.3. Variables for calculating biomass (spectral and texture variables were also used for classification)

Categories	Object's feature variables	Algorithm	References
Spectral	<ul style="list-style-type: none"> • Mean Green • Mean Red • Mean NIR • Mean MIR 		
Texture	Haralick texture variables: <ul style="list-style-type: none"> - GLCM mean - GLCM homogeneity - GLCM standard deviation - GLCM entropy - GLCM contrast - GLCM correlation - GLCM angular second moment 	Haralick texture variables derived from individual SPOT bands and calculated in four directions (0^0 , 45^0 , 90^0 , and 135^0)	Haralick et al. (1973)
Vegetation Indices	<ul style="list-style-type: none"> • NDVI • NDII • OSAVI • EVI2 • MSAVI • SAVI 	$NDVI = \frac{NIR - red}{NIR + red}$ $NDII = \frac{NIR - MIR}{NIR + MIR}$ $OSAVI = \frac{NIR - red}{NIR + red + 0.16}$ $EVI2 = 2.5 \left(\frac{NIR - red}{NIR + 2.4red + 1} \right)$ $MSAVI = \frac{2NIR + 1 - \sqrt{(2NIR + 1)^2 - 8(NIR - red)}}{2}$	Tucker (1979) Hardisky et al. (1983) Rondeaux et al. (1996) Jiang et al. (2008) Qi et al. (1994)

		$SAVI = 1.75 \left(\frac{NIR - red}{NIR + red + 0.75} \right)$	Huete (1988)
Vegetation association type	Objects classified in section 5.3.2.2		

Note: NDVI: Normalized difference vegetation index; NDII: Normalized difference infrared index; OSAVI: Optimized soil-adjusted vegetation index; EVI2: Enhanced vegetation index; MSAVI: Modified soil-adjusted vegetation index; SAVI: Soil-adjusted vegetation index

5.3.3.2 *Random Forest*

Random forest (RF) is an ensemble method that combines multiple decision trees and obtains results by averaging the predictions from all individual regression trees. Random forest was developed by Breiman (2001a). The advantages of RF compared to other tree ensemble methods are: (1) high accuracy for prediction outcomes, (2) robustness to outliers and noise, (3) fast computation speed, and (4) ability to estimate the importance of predictor variables (Cutler et al., 2007; Rodriguez-Galiano et al., 2012). In addition, RF can use a large number of predictor variables (Breiman, 2001a; Chaudhary et al., 2015). These characteristics led to the use of RF for this research.

RF is built using bagging (bootstrap aggregating) with random predictor selection (Breiman, 2001a). The process involves the following steps:

- (1) Given the training dataset of size k , bagging generates n new training datasets D_i ($i = 1, 2, \dots, n$) - the same size as the original dataset - by picking data randomly with replacement from the original dataset. This is called a bootstrap sample. Some data points in the original dataset can be used more than once to generate a bootstrap sample while others may never be used.
- (2) The bootstrap samples are then used to build decision trees (*ntree*). To construct a decision tree, a random subset of the predictors (*mtry*) is used to determine the best split at each node of the tree (Breiman, 2001a). Such a random predictive variable selection reduces correlation among trees, which decreases bias (Breiman, 2001a). The trees are grown to maximum size and not pruned, hence the computation is light (Rodriguez-Galiano et al., 2012).
- (3) The prediction at a target point x results from averaging the predictions of all trees.

It is usual for $2/3$ of data points from the original dataset to be included in a bootstrap sample ('in bag' data) while the $1/3$ remaining data set is excluded from the bootstrap sample – known as 'out-of-bag' (OOB) data (Rodriguez-Galiano et al., 2012). The OOB data are used to calculate a prediction error, known as the OOB error estimate, by contrasting the predictions from the in-bag data and the OOB data (Poulos and Camp, 2010). The OOB samples are also used to measure the variable importance (the prediction strength of each variable) by changing randomly the

values of a given variable in the OOB samples. The increase of OOB error from these changes are averaged over all trees and is a measure of the importance of the variable (Hastie et al., 2009).

In this research, the randomForest package in the R statistical software (R Core Team, 2015) was used for fitting Random Forest regression models. Two parameters – *mtry* and *ntree* – were specified. Choosing good values for *mtry* and *ntree* was necessary to build a RF model with low OOB root mean square residuals (RMSE_{OOB}). The mean of square residuals was computed as: $MSE_{OOB} = n^{-1} \sum_1^n \{y_i - \hat{y}_i^{OOB}\}^2$ (Liaw and Wiener, 2002), where \hat{y}_i^{OOB} was the average of the OOB predictions for the *i*th observation.

The *ntree* values were tested from 50 – 2000 trees with intervals of 50. The *ntree* was selected based on the stability of RMSE_{OOB} (Adelabu and Dube, 2015) (see Figure 5.3). With *mtry*, the values provided by the tuneRF function in the randomForest package varied due to the randomness associated with RF. Running the tuneRF function many times and then assigning the value of *mtry* with the most frequent occurrence is an accepted method for addressing this variation of *mtry* (Li et al., 2014).

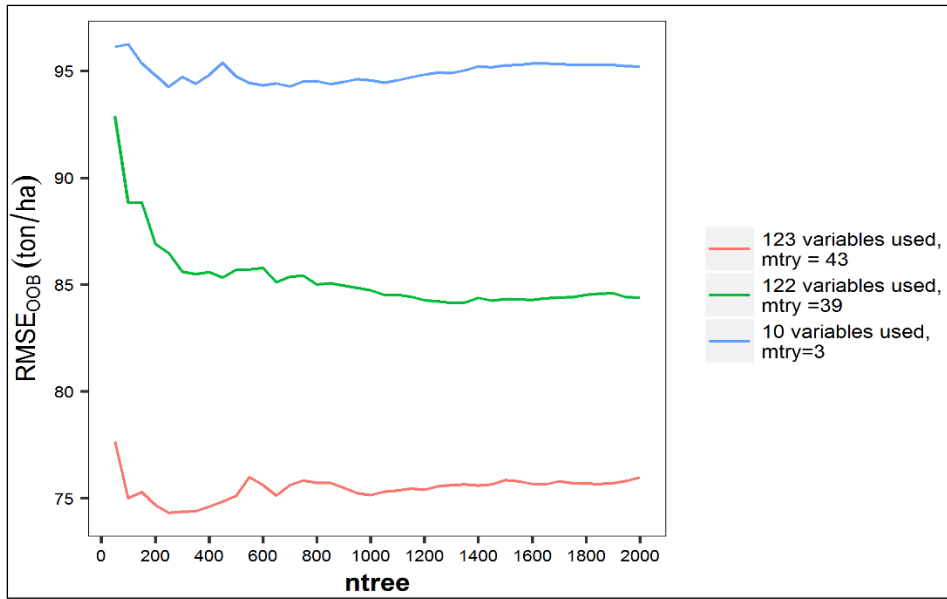


Figure 5.3. The $RMSE_{OOB}$ is stable after $ntree = 1000$ for all three cases: spectral + texture + vegetation association type + vegetation indices (123 variables); spectral + texture + vegetation indices (122 variables); and spectral + vegetation indices (10 variables) used respectively.

RF provided importance values of each variable. While the importance rankings of the most important variables were relatively stable among different iterations, the order of least important variables was unstable among iterations.

It was important to optimise the number of variables to improve model accuracy. Removing irrelevant variables results in higher predictive power and easier interpretation (Gregorutti et al., 2016). To choose the optimal number of variables for predicting biomass, the `rfcv` function in the `randomForest` package was used. This function compares the cross-validated prediction performance of models as the number of predictors is reduced (R Core Team, 2015). Using recommendations by Li et al. (2014), this research replicated the `rfcv` 100 times, with 10-fold cross-validation, to obtain the optimal number of variables.

To test the accuracy of different combinations of variables, three RF models were investigated. These models were:

- Model 1 - spectral, texture, vegetation indices (VI), and vegetation association type variables (123 variables).
- Model 2 - spectral, texture, and VI (122 variables).
- Model 3 - spectral and VI (10 variables).

5.3.4 Accuracy assessment

5.3.4.1 Classification accuracy assessment

The classification accuracy metrics were reported using producer accuracy (PA), user accuracy (UA), overall accuracy (OA), and the overall Kappa coefficient of agreement (K). Furthermore, three additional indices developed by Pontius Jr and Millones (2011) were used to evaluate the performance of the classifications. These included quantity disagreement (QD), allocation disagreement (AD), and total disagreement (TD).

5.3.4.2 Validation biomass result

The accuracy of the biomass predictions from the RF models was calculated using a withheld validation data set. These included the adjusted coefficient of determination (R_{adj}^2), and root mean square error (RMSE) between observed and predicted values. The formulas to calculate these indices were:

$$R_{adj}^2 = 1 - \frac{(n-1) \sum_{i=1}^n (y_i - \hat{y}_i)^2}{(n-2) \sum_{i=1}^n (y_i - \bar{y})^2}$$

$$RMSE = \sqrt{\frac{\sum_{i=1}^n (\hat{y}_i - y_i)^2}{n-2}}$$

Where \hat{y}_i and y_i were the predicted and observed biomass for the i^{th} plot respectively, n was the number of validation plots, and \bar{y} was observed mean of biomass.

5.4 Results and Discussion

5.4.1 Classification results

The resulting mangrove association maps of the Cangio mangrove forest in 2000 and 2011 are shown in Figure 5.4, while the classification accuracy is shown in Tables 5.4a and 5.4b.

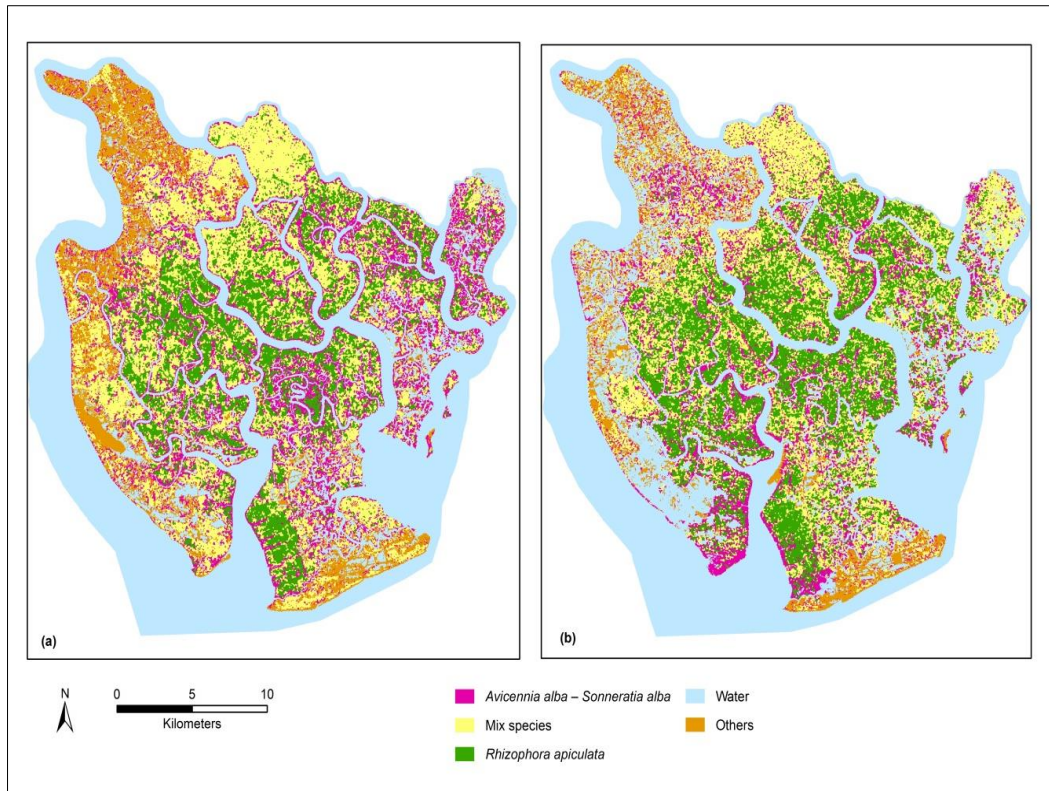


Figure 5.4. Mangrove classification map of the Cangio in: (a) 26th March 2000 and (b) 24th February 2011

The overall accuracy of mangrove classifications in this research were 77.1% and 82.9% for the year 2000 and 2011 respectively. These accuracy ranges are similar to other studies that used object-based analysis and machine learning algorithms for mapping mangrove stand types (cf. Wang et al. (2004b) and Xin et al. (2009)).

Overall, the accuracy of the 2011 classified map is greater than that of the 2000 map. This is reflected in most of the accuracy assessment indices (the Kappa index, OA, AD, TD, UA and PA) across all vegetation associations (See Tables 5.4a and 5.4b). The lower classification accuracy for the year 2000 can be explained by the 2000 SPOT4 image having more cloud cover than the 2011 SPOT5 image. Regarding the mangrove associations, *Rhizophora apiculata* had the highest classification accuracy. This is because approximately 90% of the *Rhizophora apiculata* association in Cangio is planted and tends to be more homogeneous. The two remaining associations are natural regions, which have more heterogeneity.

Table 5.4. Confusion matrix of classification accuracies obtained through SVM classifier in 2000 and 2011

(a) Confusion matrix of classification accuracies obtained through SVM classifier in 2000

Class	Reference data			
	A1	A2	A3	UA(%)
A1	54	3	13	77.1
A2	3	60	7	85.7
A3	15	7	48	68.6
PA(%)	75	85.7	70.6	
OA(%)	77.1			
K (%)	65.7			
QD(%)	1			
AD(%)	21.9			
TD(%)	22.9			

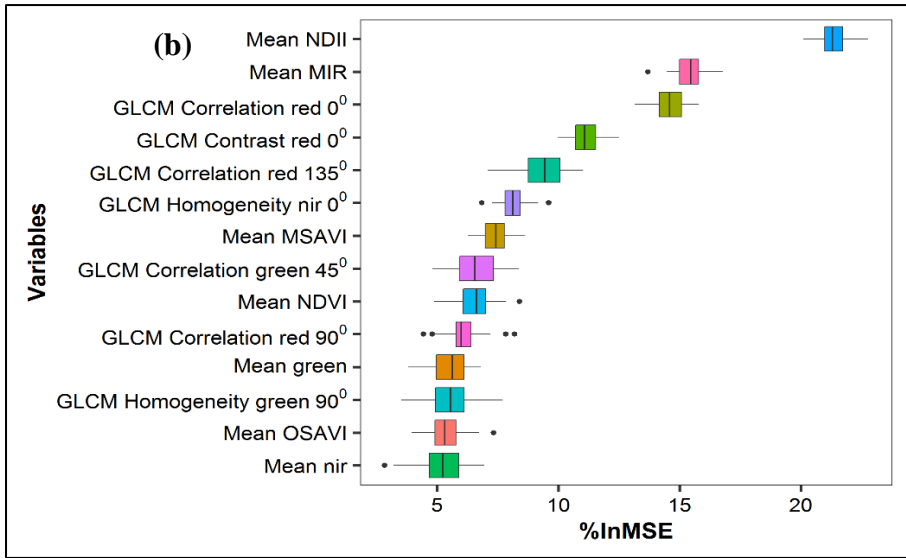
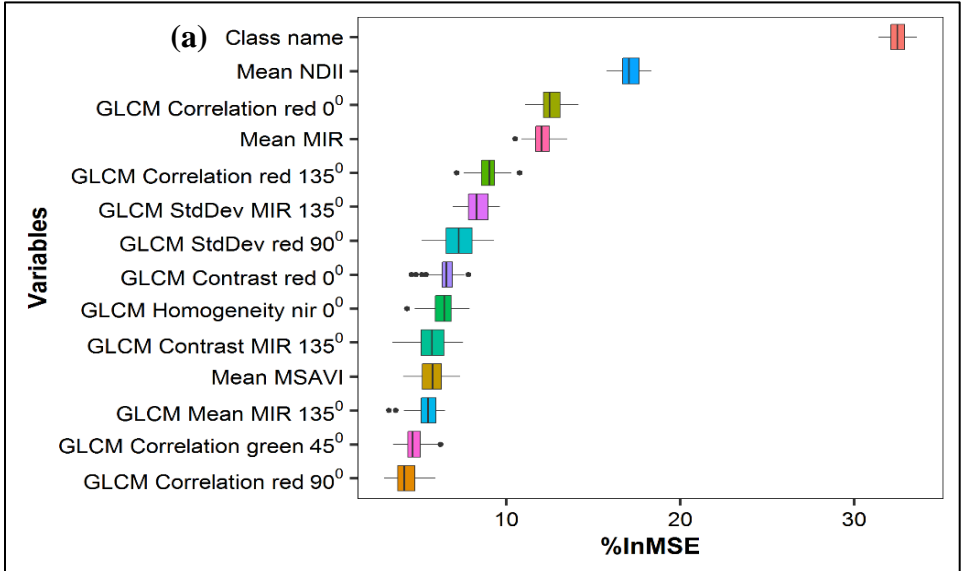
(b) Confusion matrix of classification accuracies obtained through SVM classifier in 2011

Class	Reference data			
	A1	A2	A3	UA(%)
A1	61	1	8	87.1
A2	3	63	4	90
A3	15	5	50	71.4
PA(%)	77.2	91.3	80.6	
OA(%)	82.9			
K (%)	74.3			
QD(%)	4.3			
AD(%)	12.9			
TD(%)	17.2			

Class key: A1: *Avicennia alba* – *Sonneratia alba* association; A2: *Rhizophora apiculata* association; A3: mixed species

5.4.2 Variable importance

The importance of each predictive variable for the three RF models investigated are shown in Figure 5.5.



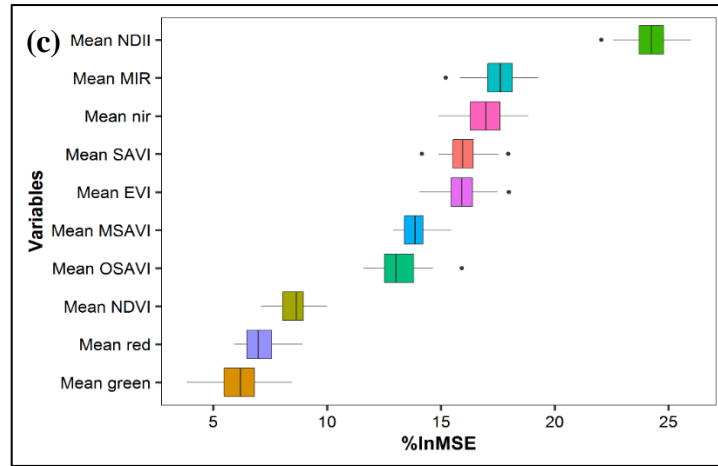


Figure 5.5. The importance of different features measured by %IncMSE (the percentage increase in the mean squared error) determined from 100 runs of the RF for: (a) all 123 variables used (spectral + texture + VI + vegetation association type); (b) 122 variables used (spectral + texture + VI); (c) 10 variables (spectral + VI).

5.4.3 Variable selection for the final three RF models

For Model 1, the optimal number of variables was nine based on the rfcv results (see Figure 5.6a). Therefore, the top nine variables in the variable importance ranking were used in the final predictive model. For Model 2, there were two local optimal number of variables – 12 and 28 (see Figure 5.6b). Consequently, the top 12 variables and the top 28 variables were further tested with RF using 100 iterations to determine the final model. The result showed that using the top 12 variables provided the best result. For Model 3, the optimal number of variables was 7 (see Figure 5.6c). Table 5.5 summarises for each of the three models - the number of variables, *ntree*, and *mtry*.

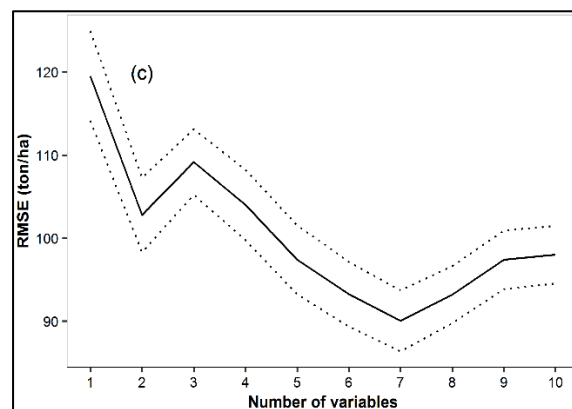
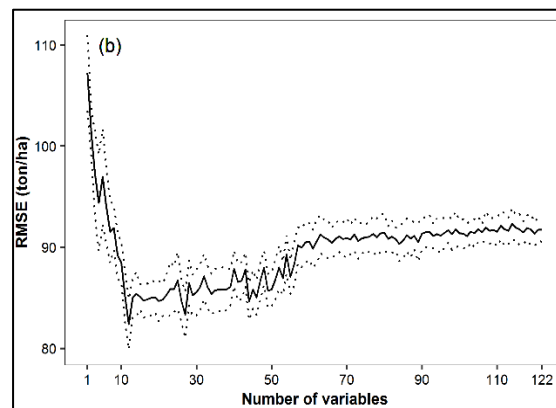
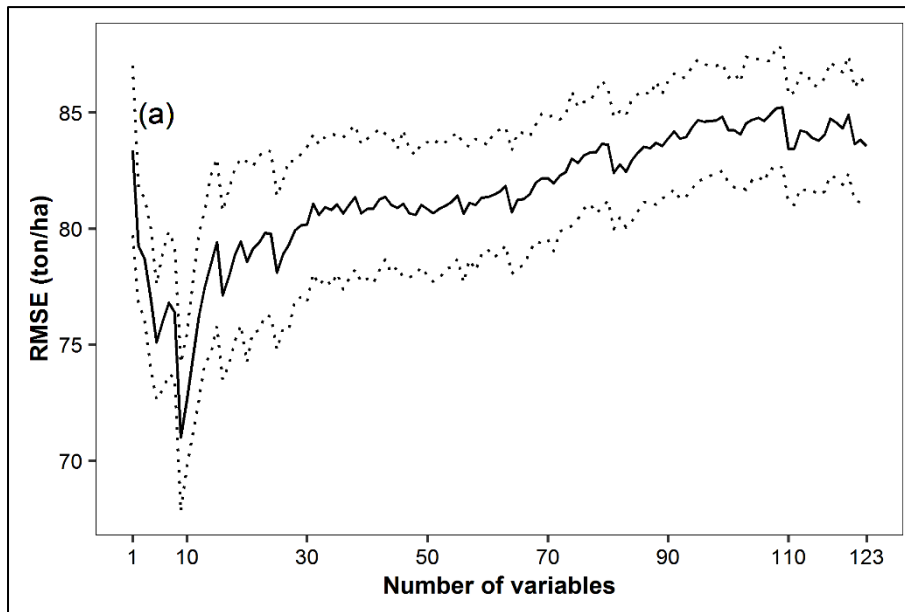


Figure 5.6. The number of variables used and the average RMSE of models based on 100 times of 10-fold cross validation: (a) all 123 variables; (b) 122 variables; (c) 10 variables.

Table 5.5. Summary of settings for Random Forest Models

Models	Number of variables	Ntree	mtry
Spectral + Vegetation indices + Texture + vegetation association type (1)	9	1000	3
Spectral + Vegetation indices + Texture (2)	12	1000	4
Spectral + Vegetation indices (3)	7	1000	2

Table 5.6 shows the results of the calibration and testing for each of the three models. Figure 5.7 shows the accuracy assessment of the final three RF biomass models. Model 1 had the highest accuracy, and was therefore used for the final estimate and map of biomass.

Table 5.6. Calibration and validation results

Models	% Variance explained		Root mean squared residuals	
	Calibration sample	Validation sample	Calibration sample	Validation sample
Spectral + Vegetation indices + texture + vegetation association type (1)	74.4	73.9	69.8	71.4
Spectral + Vegetation indices + Texture (2)	63.1	62.2	81.3	82.5
Spectral + Vegetation indices (3)	52.3	51.9	90.3	92.1

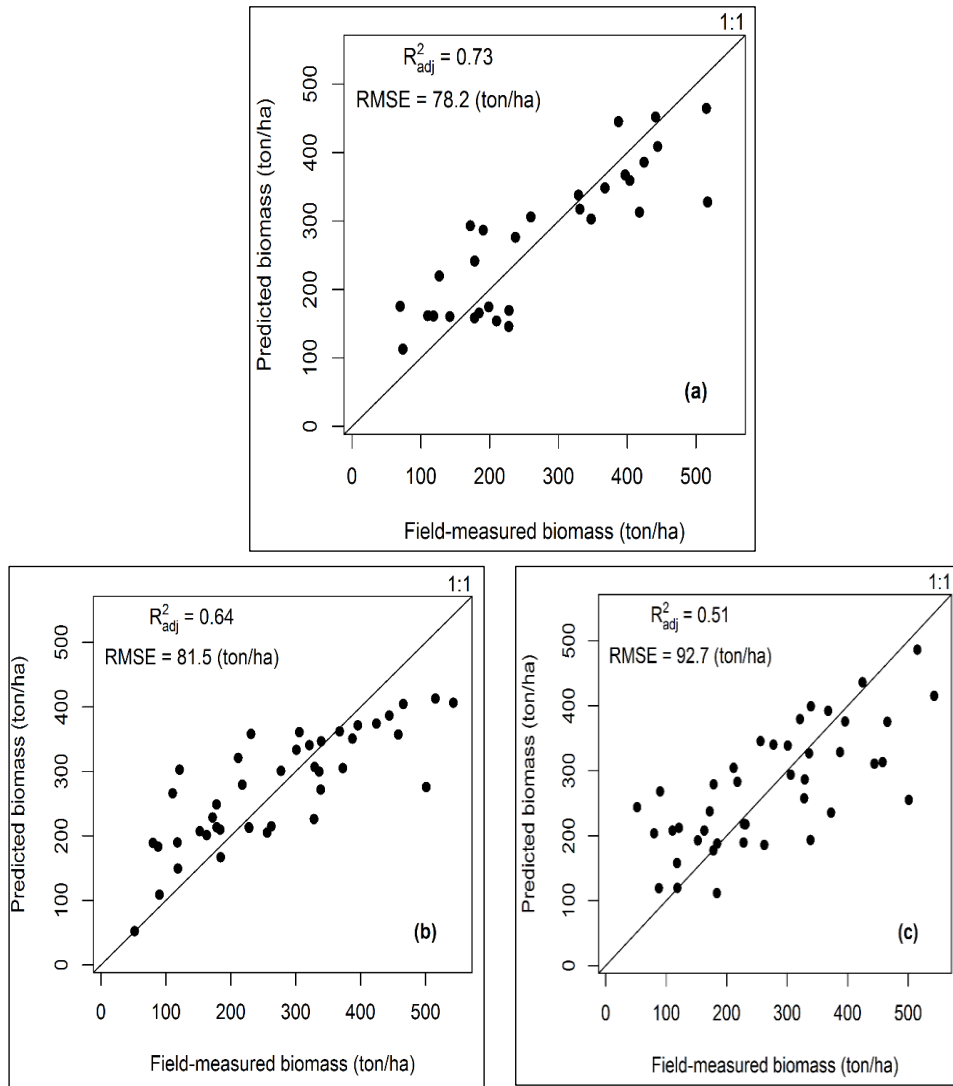


Figure 5.7. Plots of the observed and predicted biomass values using RF with a) Model 1; b) Model 2; c) Model 3

5.4.4 Biomass distribution and change between 2000 -2011

The biomass maps shown in Figure 5.8 were generated using the final RF model (Model 1). Summary statistics of the AGB for each year are shown in Table 5.7. There was an overall increase in AGB of 9.6%. However, only the AGB of the *Rhizophora apiculata* association increased, while the other two associations showed an overall decrease. Regarding the *Avicennia alba* – *Sonneratia alba* association, the change was not spatially consistent. The North-East part of the Cango diminished in 2011, but increased in the Southern part (see the circled regions in Figure 5.8). Such inconsistent change can be explained by soil accretion in this Southern region, which helped the *Avicennia alba* – *Sonneratia alba* develop.

In the Northern region, mixed species replaced the pioneering *Avicennia alba* – *Sonneratia alba* association.

Table 5.7. General descriptive statistics of AGB in the Cangio mangrove forest in the years 2000 and 2011

	Year 2000	Year 2011	Change	
Vegetation association type	Total (ton)	Total (ton)	Total change (ton)	% Change
Association I	2,124,818	1,847,434	-277,384	-13.1
Association II	3,525,279	4,896,419	1,371,140	+38.9
Association III	2,921,280	2,647,661	-273,619	-9.4
All associations	8,571,379	9,391,515	820,136	+9.6

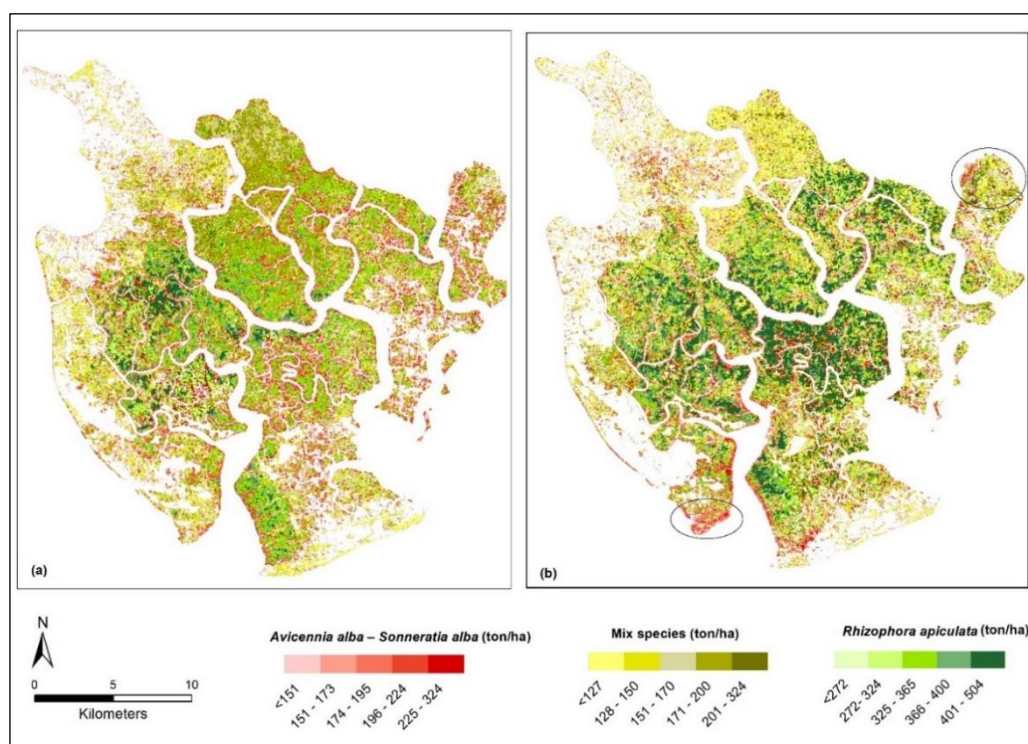


Figure 5.8. Biomass map of the Cangio mangrove forest: (a) 2000 derived from SPOT4 and (b) 2011 derived from SPOT5

5.4.5 *The role of different feature variables for predicting biomass*

Figure 5.5a shows that vegetation association type was the most important variable for predicting biomass. A similar finding was made by Zhu et al. (2015), whose research used a Back Propagation Artificial Neural Network with WorldView-2 to estimate biomass for mangrove areas in Guangdong Province, China. The next two most important variables were vegetation index - derived from MIR and NIR bands, and texture - derived from the red band.

It is noticeable that among the spectral bands, the middle infrared spectrum has the strongest relationship with AGB (see Figures 5.5a, 5.5b, and 5.5c). This result was also observed by Lu et al. (2014). An explanation for this is that MIR reflectance is more sensitive to change in forest characteristics, such as wood volume, than visible and near-infrared reflectance (Lu et al., 2004).

Texture features played a less important role in biomass estimation than features derived from spectral information. This is similar to Lu's (2005) observation that when the forest stand structure is relatively simple, texture is less important than spectral information. In general, most forested areas in the Cangio are planted, therefore its forest structure is quite homogeneous and simple. However, this research also showed that using texture features and spectral information improves biomass estimation compared to using spectral information alone (see Table 5.6 and Figure 5.7). This is because texture parameters are sensitive to the shape, height, and size of the canopy, and can therefore identify different characteristics of forest stand structure, including age, top height, and stand density (Dube and Mutanga, 2015; Kayitakire et al., 2006; Sarker and Nichol, 2011).

This research also found that the MSAVI variable is more useful for predicting biomass than NDVI. The reason is that MSAVI reduces the background soil reflectance which is added to vegetation reflectance. In the Cangio reserve, tree fall caused by strong winds or lightning strikes creates small gaps in the canopy (Vogt et al., 2013). This can cause a mixed spectral signature between the soil and vegetation.

5.5 Conclusion

The accuracy of AGB estimation in the Cangio mangrove forest was affected by many factors. Identifying these factors is important for improving the AGB estimation. As discussed in Section 5.4.5, vegetation association type is one of the most important variables affecting the AGB model. It also means that the accuracy of mangrove classification contributes to the AGB accuracy prediction. Therefore, increasing the classification accuracy through using supplementary ancillary data, such as soil conditions, could improve the AGB estimation performance. Plot location error is also an important factor that needs to be considered for biomass prediction. This type of error was reduced in this study by choosing the plots in the middle of large homogeneous objects. In addition, the use of generic allometric equations increased the biomass estimation errors. This limitation could be reduced through improved allometric equations. Besides reducing errors, integrating other data sets such as climate and soil could improve AGB estimation accuracy as suggested by Lu (2005). This is because these additional variables affect AGB accumulation rates and the development of forest stand structures. Time for collecting ground truthed biomass is also a factor that needs to be considered for monitoring biomass change. It is best if ground truthed data were collected at the same time as the images are captured. In this research, the ground truthed biomass data collected in 2016 were used for the 2011 image because there was no available ground truthed biomass data for the year 2011.

This research shows that using vegetation association type and texture information can significantly improve biomass estimation in mangrove forests. It also demonstrates that the RF algorithm is suitable for estimating biomass in the context of mangrove forests where the sample sizes are often small due to difficulty in collecting field data. The study area chosen to demonstrate the method was a large and complex area. Therefore, although this research was based on only one study area, its method can be applied to other mangrove regions. This research has also developed a technique that works with relatively low-resolution satellite imagery, which is affordable for developing countries.

Acknowledgments

We would like to thank Cangio Mangrove Protection Forest Management Board for their help in the field. We are also grateful to Dr. Vo Quoc Tuan and Phan Van Trung for their assistance field work and data acquisition. We also thank the reviewers for making useful suggestions which have been incorporated into this paper.

REFERENCES

- Addink, E.A., de Jong, S.M., Pebesma, E.J., 2007. The importance of scale in object-based mapping of vegetation parameters with hyperspectral imagery. *Photogrammetric Engineering & Remote Sensing* 73(8), 905-912. <https://doi.org/10.14358/PERS.73.8.905>
- Adelabu, S., Dube, T., 2015. Employing ground and satellite-based QuickBird data and random forest to discriminate five tree species in a Southern African Woodland. *Geocarto International* 30(6), 457-471. <https://doi.org/10.1080/10106049.2014.885589>
- Ben-Hur, A., Ong, C.S., Sonnenburg, S., Schölkopf, B., Rätsch, G., 2008. Support vector machines and kernels for computational biology. *PLoS Computational Biology* 4(10), e1000173. <https://doi.org/10.1371/journal.pcbi.1000173>
- Bergen, K.M., Dobson, M.C., 1999. Integration of remotely sensed radar imagery in modeling and mapping of forest biomass and net primary production. *Ecological Modelling* 122(3), 257-274. [https://doi.org/http://dx.doi.org/10.1016/S0304-3800\(99\)00141-6](https://doi.org/http://dx.doi.org/10.1016/S0304-3800(99)00141-6)
- Binh, C.H., Nam, V.N., 2014. Carbon sequestration of *Ceriops zippeliana* in Cangio mangroves Mangrove ecosystems technical reports, Vol. 6, Sendai, Japan.
- Blaschke, T., 2010. Object based image analysis for remote sensing. *ISPRS Journal of Photogrammetry and Remote Sensing* 65(1), 2-16. <https://doi.org/10.1016/j.isprsjprs.2009.06.004>
- Breiman, L., 2001a. Random forests. *Machine Learning* 45(1), 5-32. <https://doi.org/10.1023/A:1010933404324>
- Charoenjit, K., Zuddas, P., Allemand, P., Pattanakit, S., Pachana, K., 2015. Estimation of biomass and carbon stock in Para rubber plantations using object-based classification from Thaichote satellite data in Eastern Thailand. *J Appl Remote Sens* 9(1). <https://doi.org/10.1117/1.JRS.9.096072>
- Chaudhary, N., Sharma, A.K., Agarwal, P., Gupta, A., Sharma, V.K., 2015. 16S classifier: a tool for fast and accurate taxonomic classification of 16S rRNA hypervariable regions in metagenomic datasets. *PloS One* 10(2), e0116106. <https://doi.org/10.1371/journal.pone.0116106>
- Chemura, A., van Duren, I., van Leeuwen, L.M., 2015. Determination of the age of oil palm from crown projection area detected from WorldView-2 multispectral remote sensing data: The case of Ejisu-Juaben district, Ghana. *ISPRS Journal of Photogrammetry and Remote Sensing* 100, 118-127. <https://doi.org/10.1016/j.isprsjprs.2014.07.013>
- Chen, Q., 2013. Lidar remote sensing of vegetation biomass, in: Wang, G., Weng, Q. (Eds.), *Remote Sensing of Natural Resources*. CRC Press, Boca Raton, pp. 399-420.
- Chen, Q., Laurin, G.V., Battles, J.J., Saah, D., 2012. Integration of airborne lidar and vegetation types derived from aerial photography for mapping aboveground live biomass. *Remote Sensing of Environment* 121, 108-117. <https://doi.org/10.1016/j.rse.2012.01.021>
- Cortes, C., Vapnik, V., 1995. Support-vector networks. *Machine Learning* 20(3), 273-297. <https://doi.org/10.1007/bf00994018>

- Cutler, D.R., Edwards, T.C., Beard, K.H., Cutler, A., Hess, K.T., Gibson, J., Lawler, J.J., 2007. Random forests for classification in ecology. *Ecology* 88(11), 2783-2792. <https://doi.org/10.1890/07-0539.1>
- Dalponte, M., Bruzzone, L., Vescovo, L., Gianelle, D., 2009. The role of spectral resolution and classifier complexity in the analysis of hyperspectral images of forest areas. *Remote Sensing of Environment* 113(11), 2345-2355. <https://doi.org/10.1016/j.rse.2009.06.013>
- Donato, D.C., Kauffman, J.B., Murdiyarso, D., Kurnianto, S., Stidham, M., Kanninen, M., 2011. Mangroves among the most carbon-rich forests in the tropics. *Nature Geoscience* 4(5), 293-297. <https://doi.org/10.1038/ngeo1123>
- Drake, J.B., Dubayah, R.O., Clark, D.B., Knox, R.G., Blair, J.B., Hofton, M.A., Chazdon, R.L., Weishampel, J.F., Prince, S., 2002. Estimation of tropical forest structural characteristics using large-footprint lidar. *Remote Sensing of Environment* 79(2-3), 305-319. [https://doi.org/10.1016/S0034-4257\(01\)00281-4](https://doi.org/10.1016/S0034-4257(01)00281-4)
- Dube, T., Mutanga, O., 2015. Investigating the robustness of the new Landsat-8 Operational Land Imager derived texture metrics in estimating plantation forest aboveground biomass in resource constrained areas. *ISPRS Journal of Photogrammetry and Remote sensing* 108, 12-32. <https://doi.org/10.1016/j.isprsjprs.2015.06.002>
- Feliciano, E.A., Wdowinski, S., Potts, M.D., 2014. Assessing mangrove above-ground biomass and structure using terrestrial laser scanning: A case study in the Everglades National Park. *Wetlands* 34(5), 955-968. <https://doi.org/10.1007/s13157-014-0558-6>
- Giri, C., Long, J., Abbas, S., Murali, R.M., Qamer, F.M., Pengra, B., Thau, D., 2015. Distribution and dynamics of mangrove forests of South Asia. *Journal of Environmental Management* 148, 101-111. <https://doi.org/10.1016/j.jenvman.2014.01.020>
- Gregorutti, B., Michel, B., Saint-Pierre, P., 2016. Correlation and variable importance in random forests. *Statistics and Computing*. <https://doi.org/10.1007/s11222-016-9646-1>
- Hamdan, O., Khairunnisa, M.R., Ammar, A.A., Hasmadi, I.M., Aziz, H.K., 2013. Mangrove carbon stock assessment by optical satellite imagery. *Journal of Tropical Forest Science* 25(4), 554-565.
- Hamdan, O., Khali Aziz, H., Mohd Hasmadi, I., 2014. L-band ALOS PALSAR for biomass estimation of Matang Mangroves, Malaysia. *Remote Sensing of Environment* 155, 69-78. <https://doi.org/10.1016/j.rse.2014.04.029>
- Haralick, R.M., Shanmugam, K., Dinstein, I.H., 1973. Textural features for image classification. *IEEE Transactions on Systems, Man and Cybernetics* 3(6), 610-621. <https://doi.org/10.1109/tsmc.1973.4309314>
- Hardisky, M.A., Klemas, V., Smart, R.M., 1983. The influence of soil-salinity, growth form, and leaf moisture on the spectral radiance of spartina-alterniflora canopies. *Photogrammetric Engineering and Remote Sensing* 49(1), 77-83.
- Hastie, T.J., Tibshirani, R.J., Friedman, J.H., 2009. *The Elements of Statistical Learning: Data Mining, Inference, and Prediction*. Springer, New York, NY.
- Huete, A.R., 1988. A soil-adjusted vegetation index (SAVI). *Remote Sensing of Environment* 25(3), 295-309. [https://doi.org/10.1016/0034-4257\(88\)90106-X](https://doi.org/10.1016/0034-4257(88)90106-X)

- Jachowski, N.R.A., Quak, M.S.Y., Friess, D.A., Duangnamon, D., Webb, E.L., Ziegler, A.D., 2013. Mangrove biomass estimation in Southwest Thailand using machine learning. *Applied Geography* 45, 311-321. <https://doi.org/10.1016/j.apgeog.2013.09.024>
- Ji, L., Zhang, L., Wylie, B., 2009. Analysis of dynamic thresholds for the normalized difference water index. *Photogrammetric Engineering & Remote Sensing* 75(11), 1307-1317. <https://doi.org/10.14358/PERS.75.11.1307>
- Jiang, Z., Huete, A.R., Didan, K., Miura, T., 2008. Development of a two-band enhanced vegetation index without a blue band. *Remote Sensing of Environment* 112(10), 3833-3845. <https://doi.org/10.1016/j.rse.2008.06.006>
- Joachims, T., 2002. *Learning to Classify Text Using Support Vector Machines: Methods, Theory and Algorithms*. Kluwer Academic Publishers, Boston, MA.
- Kajisa, T., Murakami, T., Mizoue, N., Top, N., Yoshida, S., 2009. Object-based forest biomass estimation using Landsat ETM+ in Kampong Thom Province, Cambodia. *Journal of Forest Research* 14(4), 203-211. <https://doi.org/http://dx.doi.org/10.1007/s10310-009-0125-9>
- Kayitakire, F., Hamel, C., Defourny, P., 2006. Retrieving forest structure variables based on image texture analysis and IKONOS-2 imagery. *Remote Sensing of Environment* 102(3-4), 390-401. <https://doi.org/10.1016/j.rse.2006.02.022>
- Ke, Y., Quackenbush, L.J., Im, J., 2010. Synergistic use of QuickBird multispectral imagery and LIDAR data for object-based forest species classification. *Remote Sensing of Environment* 114(6), 1141-1154. <https://doi.org/10.1016/j.rse.2010.01.002>
- Komiyama, A., Sasitorn, P., Shogo, K., 2005. Common allometric equations for estimating the tree weight of mangroves. *Journal of Tropical Ecology* 21(4), 471-477. <https://doi.org/10.1017/S0266467405002476>
- Kuenzer, C., Tuan, V.Q., 2013. Assessing the ecosystem services value of Cangio Mangrove Biosphere Reserve: Combining earth-observation- and household-survey-based analyses. *Applied Geography* 45, 167-184. <https://doi.org/10.1016/j.apgeog.2013.08.012>
- Le Toan, T., Beaudoin, A., Riom, J., Guyon, D., 1992. Relating forest biomass to SAR data. *IEEE Transactions on Geoscience and Remote Sensing* 30(2), 403-411. <https://doi.org/10.1109/36.134089>
- Lefsky, M.A., Cohen, W.B., Harding, D.J., Parker, G.G., Acker, S.A., Gower, S.T., 2002. Lidar remote sensing of above-ground biomass in three biomes. *Global Ecology and Biogeography* 11(5), 393-399.
- Li, J., Justy, P., Siwabessy, W., Tran, M., Huang, Z., Heap, A.D., 2014. Predicting seabed hardness using random forest in R, in: Zhao, Y., Cen, Y. (Eds.), *Data Mining Applications with R*. Academic Press, Boston, MA, pp. 299-329.
- Liaw, A., Wiener, M., 2002. Classification and regression by randomForest. *R News* 2(3), 18-22.
- Lu, D., 2005. Aboveground biomass estimation using Landsat TM data in the Brazilian Amazon. *International Journal of Remote Sensing* 26(12), 2509-2525. <https://doi.org/10.1080/01431160500142145>
- Lu, D., 2006. The potential and challenge of remote sensing-based biomass estimation. *International Journal of Remote Sensing* 27(7), 1297-1328.

- Lu, D., Chen, Q., Wang, G., Liu, L., Li, G., Moran, E., 2014. A survey of remote sensing-based aboveground biomass estimation methods in forest ecosystems. *International Journal of Digital Earth* 9(1), 63-105. <https://doi.org/10.1080/17538947.2014.990526>
- Lu, D., Mausel, P., Brondízio, E., Moran, E., 2004. Relationships between forest stand parameters and Landsat TM spectral responses in the Brazilian Amazon Basin. *Forest Ecology and Management* 198(1-3), 149-167. <https://doi.org/10.1016/j.foreco.2004.03.048>
- Luong, N.V., Tateishi, R., Hoan, N.T., 2015. Analysis of an impact of succession in mangrove forest association using remote sensing and GIS technology. *Journal of Geography and Geology* 7(1), 106-116. <https://doi.org/10.5539/jgg.v7n1p106>
- Mutanga, O., Adam, E., Cho, M.A., 2012. High density biomass estimation for wetland vegetation using WorldView-2 imagery and random forest regression algorithm. *International Journal of Applied Earth Observation and Geoinformation* 18, 399-406. <https://doi.org/10.1016/j.jag.2012.03.012>
- Myint, S.W., Giri, C.P., Wang, L., Zhu, Z., Gillette, S.C., 2008. Identifying mangrove species and their surrounding land use and land cover classes using an object-oriented approach with a lacunarity spatial measure. *GIScience & Remote Sensing* 45(2), 188-208. <https://doi.org/10.2747/1548-1603.45.2.188>
- Nam, V.N., 2003. Nghiên cứu sinh khối và năng suất sơ cấp của rừng tràm (*Avicennia alba* BL.) tự nhiên tại Càngio, Thành phố Hồ Chí Minh, Vietnamese Academy of Forest Sciences, Hà Nội, Vietnam. PhD thesis.
- Nam, V.N., 2011a. Nghiên cứu khả năng hấp thụ CO₂ của rừng cóc tràm (*Lumnitzera racemosa* Willd) trong ô khu dự trữ sinh quyển rừng ngập mặn Cần Giờ, Thành phố Hồ Chí Minh. *Tạp Chí Nông Nghiệp & Phát Triển Nông Thôn = Agriculture & Rural Development Review* 2, 162-166.
- Nam, V.N., 2011b. Nghiên cứu tích trữ carbon của rừng đước (*Rhizophora apiculata* Blume) trong ô khu dự trữ sinh quyển rừng ngập mặn Cần Giờ, thành phố Hồ Chí Minh. *Tạp Chí Nông Nghiệp & Phát Triển Nông Thôn = Agriculture & Rural Development Review* 2, 78-83.
- Nguyen, H.N., 2006. The environment in Ho Chi Minh City harbours, in: Wolanski, E. (Ed.), *The Environment in Asia Pacific Harbours*. Springer, Dordrecht, The Netherlands, pp. 261-291.
- Pham, L.T.H., Brabyn, L., Ashraf, S., 2016b. Combining QuickBird, LiDAR, and GIS topography indices to identify a single native tree species in a complex landscape using an object-based classification approach. *International Journal of Applied Earth Observation and Geoinformation* 50, 187-197. <https://doi.org/10.1016/j.jag.2016.03.015>
- Pontius Jr, R.G., Millones, M., 2011. Death to Kappa: Birth of quantity disagreement and allocation disagreement for accuracy assessment. *International Journal of Remote Sensing* 32(15), 4407-4429. <https://doi.org/10.1080/01431161.2011.552923>
- Popescu, S.C., Zhao, K., Neuenschwander, A., Lin, C., 2011. Satellite lidar vs. small footprint airborne lidar: Comparing the accuracy of aboveground biomass estimates and forest structure metrics at footprint level. *Remote Sensing of Environment* 115(11), 2786-2797. <https://doi.org/10.1016/j.rse.2011.01.026>

- Poulos, H.M., Camp, A.E., 2010. Decision support for mitigating the risk of tree induced transmission line failure in utility rights-of-way. *Environmental Management* 45(2), 217-226. <https://doi.org/10.1007/s00267-009-9422-5>
- Proisy, C., Coutron, P., Fromard, F., 2007. Predicting and mapping mangrove biomass from canopy grain analysis using Fourier-based textural ordination of IKONOS images. *Remote Sensing of Environment* 109(3), 379-392. <https://doi.org/10.1016/j.rse.2007.01.009>
- Proisy, C., Mougin, E., Fromard, F., Karam, M.A., 2000. Interpretation of polarimetric radar signatures of mangrove forests. *Remote Sensing of Environment* 71(1), 56-66. [https://doi.org/10.1016/S0034-4257\(99\)00064-4](https://doi.org/10.1016/S0034-4257(99)00064-4)
- Qi, J., Chehbouni, A., Huete, A.R., Kerr, Y.H., Sorooshian, S., 1994. A modified soil adjusted vegetation index. *Remote Sensing of Environment* 48(2), 119-126. [https://doi.org/10.1016/0034-4257\(94\)90134-1](https://doi.org/10.1016/0034-4257(94)90134-1)
- R Core Team, 2015. R: A language and environment for statistical computing.
- Rodriguez-Galiano, V.F., Ghimire, B., Rogan, J., Chica-Olmo, M., Rigol-Sanchez, J.P., 2012. An assessment of the effectiveness of a random forest classifier for land-cover classification. *ISPRS Journal of Photogrammetry and Remote Sensing* 67, 93-104. <https://doi.org/10.1016/j.isprsjprs.2011.11.002>
- Rondeaux, G., Steven, M., Baret, F., 1996. Optimization of soil-adjusted vegetation indices. *Remote Sensing of Environment* 55(2), 95-107. [https://doi.org/10.1016/0034-4257\(95\)00186-7](https://doi.org/10.1016/0034-4257(95)00186-7)
- Sang, K.V., 2011. Nghien cuu kha nang tich tu carbon cua cha la bien (Phoenix paludosa Roxb.) tai khu du tru sinh quyen rung ngap man CanGio, Nong Lam University, Ho Chi Minh City. Master's thesis.
- Sarker, L.R., Nichol, J.E., 2011. Improved forest biomass estimates using ALOS AVNIR-2 texture indices. *Remote Sensing of Environment* 115(4), 968-977. <https://doi.org/10.1016/j.rse.2010.11.010>
- Simard, M., Zhang, K., Rivera-Monroy, V.H., Ross, M.S., Ruiz, P.L., Castañeda-Moya, E., Twilley, R.R., Rodriguez, E., 2006. Mapping height and biomass of mangrove forests in Everglades National Park with SRTM elevation data. *Photogrammetric Engineering and Remote Sensing* 72(3), 299-311.
- Tian, X., Li, Z., Su, Z., Chen, E., van der Tol, C., Li, X., Guo, Y., Li, L., Ling, F., 2014. Estimating montane forest above-ground biomass in the upper reaches of the Heihe River Basin using Landsat-TM data. *International Journal of Remote Sensing* 35(21), 7339-7362. <https://doi.org/10.1080/01431161.2014.967888>
- Trimble Germany GmbH, 2015b. Trimble Documentation: eCognition Developer 9.1 User Guide. Trimble Germany GmbH, Munich, Germany.
- Tucker, C.J., 1979. Red and photographic infrared linear combinations for monitoring vegetation. *Remote Sensing of Environment* 8(2), 127-150. [https://doi.org/10.1016/0034-4257\(79\)90013-0](https://doi.org/10.1016/0034-4257(79)90013-0)
- Vapnik, V.N., 1995. *The Nature of Statistical Learning Theory*. Springer-Verlag, New York, NY.
- Viet Nam Environment Protection Agency, 2005. Overview of Wetlands Status in Viet Nam Following 15 Years of Ramsar Convention Implementation, Hanoi, Viet Nam.
- Vogt, J., Kautz, M., Herazo, M.L.F., Triet, T., Walther, D., Saint-Paul, U., Diele, K., Berger, U., 2013. Do canopy disturbances drive forest plantations into more natural conditions?—A case study from Cangio Biosphere Reserve,

- Viet Nam. *Global and Planetary Change* 110, 249-258.
<https://doi.org/10.1016/j.gloplacha.2011.09.002>
- Wang, L., Sousa, W.P., Gong, P., 2004a. Integration of object-based and pixel-based classification for mapping mangroves with IKONOS imagery. *International Journal of Remote Sensing* 25(24), 5655-5668.
<https://doi.org/10.1080/014311602331291215>
- Wang, L., Sousa, W.P., Gong, P., Biging, G.S., 2004b. Comparison of IKONOS and QuickBird images for mapping mangrove species on the Caribbean coast of Panama. *Remote Sensing of Environment* 91(3), 432-440.
<https://doi.org/10.1016/j.rse.2004.04.005>
- Wicaksono, P., Danoedoro, P., Hartono, Nehren, U., 2016. Mangrove biomass carbon stock mapping of the Karimunjawa Islands using multispectral remote sensing. *International Journal of Remote Sensing* 37(1), 26-52.
<https://doi.org/10.1080/01431161.2015.1117679>
- Xin, H., Liangpei, Z., Le, W., 2009. Evaluation of morphological texture features for mangrove forest mapping and species discrimination using multispectral IKONOS imagery. *IEEE Geoscience and Remote Sensing Letters* 6(3), 393-397. <https://doi.org/10.1109/lgrs.2009.2014398>
- Zhu, Y., Liu, K., Liu, L., Wang, S., Liu, H., 2015. Retrieval of mangrove aboveground biomass at the individual species level with WorldView-2 images. *Remote Sensing* 7(9), 12192-12214.
<https://doi.org/10.3390/rs70912192>

CHAPTER 6

DISCUSSION AND CONCLUSION

6.1 Key questions addressed by this research

As stated in the introduction, the main objective of this research was to evaluate the accuracy of a range of remote sensing techniques for mapping coastal vegetation, including the best combination of techniques. Four key questions resulting from this objective were provided in Chapter 1. This section describes how each of these questions have been answered.

Q.1. What levels of segmentation are required to separate individual tree crowns/mangrove associations from other land-cover types such as grasslands, buildings, and water?

This research has shown the flexibility of OBIA application for identifying coastal vegetation at different levels of detail ranging from a broad-scale such as vegetation associations to a single tree species. Choosing how many levels of segmentation and classification depends on the classification targets and the surrounding environment of these targets. The more detailed the classification targets are, the more levels of segmentation that are required. Chapter 3 has illustrated that classifying individual trees in a mixed landscape required the use of multiple levels of segmentation with complex criteria and a variety of classification algorithms. These levels of segmentation range from separating objects at a large scale (e.g. distinguishing vegetation from other objects) and to detailed scales (e.g. distinguishing individual crowns from clump trees).

Q2. Which dimensionality reduction methods improve the accuracy of vegetation classification or biomass prediction?

This research has demonstrated that the improvements in classification accuracy obtained from dimensionality reduction depend on not only the properties of the input data but also the classifiers used. As mentioned in Chapter 4, dimensionality reduction includes feature selection and extraction. In Chapter 3, the SVM classifier with the Random Forest as a feature selection method achieved higher classification accuracy (OA= 85.4, Kappa= 80.6) than that without the feature selection (OA=

80.4, Kappa=73.9), however, the increase in accuracy was not large (5%). The study of dimensionality reduction methods and classifiers investigated in Chapter 5 showed that only Naïve Bayes improved with feature selection, while Logistic Regression, RF, and SVM did not. The difference in the impact of the feature selection on the classification accuracy in Chapter 3 and Chapter 5 may be explained by the fact that the training dataset used in Chapter 5 was less noisy than that used in Chapter 3. The position of trees in Chapter 5 was recorded with higher accuracy GPS than was the case in Chapter 3. Consequently, the position errors were reduced in Chapter 5, which resulted in less noise in the training samples. This research concluded that the feature selection should be applied prior to classification to make classification faster and/or better for identifying tree species as demonstrated in Chapters 3 and 5 regardless of the quality of training samples.

Q3. Which classifier algorithms should be used for identifying coastal vegetation?

In order to answer this question, this research investigated and compared tree species classification performance for a variety of classification schemes (Naïve Bayes, Logistic Regression, Random Forest, and Support Vector Machine). This research concluded that SVM and RF had the best classification accuracy. The overall accuracy (OA) of SVM and RF were 88.2% and 87.2% (Kappa 0.84 and 0.83) respectively, followed closely by LR (OA: 84.8%, Kappa: 0.79) and more distantly by NB (OA: 79%, Kappa: 0.72).

Q.4. Does the combination of spectral and GIS derived data improve the accuracy of vegetation classification and biomass prediction?

The research findings demonstrated that combining LiDAR and spectral data improved classification of Pohutukawa trees. Using a combination of spectral and LiDAR data it was shown that Pohutukawa trees can be identified with an overall accuracy of 85.4% (Kappa 80.6%). Classification using just the spectral data alone produced an overall accuracy of 75.8% (Kappa 67.8%). Terrain context (based on slope, elevation, and wetness), tree height, canopy shape and branch density (based on LiDAR return intensity) have been shown to be useful variables that can be combined with spectral data to improve the classification of vegetation.

This research also showed that using vegetation association type and texture information can significantly improve biomass estimation in mangrove forests. The model that integrated spectral, vegetation association type, texture, and vegetation indices obtained the higher accuracy ($R^2_{adj} = 0.73$) compared to just using spectral, texture, and vegetation index ($R^2_{adj} = 0.64$) or just spectral and vegetation index ($R^2_{adj} = 0.51$). This research demonstrated that using texture features and spectral information improves biomass estimation compared to using just spectral information alone. This is because texture parameters are sensitive to the shape, height, and size of the canopy, and can therefore identify different characteristics of forest stand structure, including age, top height, and stand density (Dube and Mutanga, 2015; Kayitakire et al., 2006; Sarker and Nichol, 2011).

6.2 Limitations

LiDAR data is an important input for separating individual tree crowns from tree clusters. The vegetation classification in Vietnam case study would have improved with LiDAR data.

Regarding the identification of individual trees in the New Zealand case, the research focused on the upper vegetation layer which was higher than 2m. This height limitation was set because the LiDAR data set used had a density of 1.5 points per m^2 , which was not detailed enough for the lower vegetation layers, which is smaller in size. This limitation could be resolved by using LiDAR datasets with higher resolution.

The separation of individual trees from tree clusters and other structures was performed by identifying treetops. Treetop detection can lead to under-segmentation (omission errors) or over-segmentation (commission error). In the future, combining LiDAR and spectral data could be used to improve treetop identification and object segmentation. Individual tree segmentation was performed by the sequential growth algorithm, which depended on the order of growth specified. To avoid reliance on this growth specification, a simultaneous growth algorithm developed by Zhen et al. (2014) could be used.

The use of a generic allometric equation rather than a species specific equation limited biomass estimation, which increased the biomass estimation errors. This

limitation could be reduced through improved species specific allometric equations. Another improvement for biomass estimation could be to integrate other data sets such as climate and soil. This is because these additional variables affect above ground biomass accumulation rates and the development of forest stand structures. Time for collecting ground truthed biomass is also a factor that needs to be considered for monitoring biomass change. It is best if ground truthed data were collected at the same time as the images are captured. In this research, ground truthed biomass data collected in 2016 were used for the 2011 image because there was no available ground truthed biomass data for the year 2011 and there were no recent SPOT5 images available.

The methodology for predicting mangrove biomass in Vietnam case study can be applied to other mangrove regions. However, different mangrove regions may have different types of mangroves. Therefore, the parameters and input variables should be modified to be suitable with the research location.

6.3 Implications for mapping vegetation and future research

Accurate spatiotemporal distribution of tree species plays an important role for a wide variety of vegetation management tasks such as monitoring disease and biodiversity assessment. For example, in the New Zealand context, a number of tree species in the myrtle family have recently been attacked by a fungal disease, known as myrtle rust. The myrtle family includes iconic natives such as pohutukawa, kanuka, manuka and rata, and commercially-grown species such as eucalyptus and feijoa. The myrtle rust can cause a deformation of the leaves and shoots, and twig dieback, and the plant can die if the infection is severe. (<http://www.doc.govt.nz/myrtlerust>). Using remotely sensed data with the advanced techniques tested in this thesis (object-based analysis and machine learning algorithms) can spatially map the impact of this fungal disease cost-effectively. Such mapping is important to monitor the spread of the disease or its retreat.

Integrating LiDAR data and optical data can be used to map individual trees as demonstrated in this research. Another advantage of using LiDAR data is that it can measure the height of trees. Combining maps of individual trees and tree height

derived from time series of optical and LiDAR data would provide an opportunity for monitoring tree growth in future research.

As mentioned in Chapter 5, radar data can estimate biomass with higher accuracy than optical data. In this thesis, only optical datasets were used for predicting biomass of mangrove forests. Future research could use both optical datasets and radar datasets to improve biomass mapping. These datasets are now freely available, e.g. Sentinel-1 and ALOS-PALSAR.

The methodology for predicting biomass include two main sections: 1) identifying different mangrove types and then 2) using allometric algorithm combined with random forest for predicting biomass.

For identifying different mangrove types, the surrounding environment of mangroves in NZ is different from Vietnam. The research location in Vietnam is protected mangrove forests which include mangrove associations as a dominant land cover type and other land cover types such as shrimp ponds, bare lands, and muddy flats. On the other hand, mangrove in NZ is closed to urban residential areas and pasture.

6.4 Overall conclusion

The overall motivation for this research was to investigate whether the inclusion of a wide range of context and shape variables can improve the accuracy of vegetation classification, as well as investigate which machine learning techniques work best. The overall conclusion of this research is that these additional variables can be obtained using OBIA and that they do improve vegetation classification accuracy. The research has also shown that machine learning techniques when used in combination with OBIA also improve vegetation classification accuracy.

Humans can accurately identify individual tree objects, such as Pohutukawa trees in the field and also from detailed images, because the human brain is capable of integrating a diverse range of information such as the surrounding context, density of branches, canopy shape, and height. Human do not limit their perceptual information to just spectral colours. This research has shown that computers can now also utilise a wide range of information, which is available in digital form due to the addition of LiDAR and GIS derived variables that describe context and shape.

Remote sensing can now integrate the same complex information that humans use, but have the added advantage of being cost effective and consistent.

REFERENCES

- Dube, T., Mutanga, O., 2015. Investigating the robustness of the new Landsat-8 Operational Land Imager derived texture metrics in estimating plantation forest aboveground biomass in resource constrained areas. *ISPRS Journal of Photogrammetry and Remote sensing* 108, 12-32.
<https://doi.org/10.1016/j.isprsjprs.2015.06.002>
- Kayitakire, F., Hamel, C., Defourny, P., 2006. Retrieving forest structure variables based on image texture analysis and IKONOS-2 imagery. *Remote Sensing of Environment* 102(3-4), 390-401.
<https://doi.org/10.1016/j.rse.2006.02.022>
- Sarker, L.R., Nichol, J.E., 2011. Improved forest biomass estimates using ALOS AVNIR-2 texture indices. *Remote Sensing of Environment* 115(4), 968-977.
<https://doi.org/10.1016/j.rse.2010.11.010>
- Zhen, Z., Quackenbush, L.J., Zhang, L., 2014. Impact of tree-oriented growth order in marker-controlled region growing for individual tree crown delineation using Airborne Laser Scanner (ALS) data. *Remote Sensing* 6(1), 555-579.
<https://doi.org/10.3390/rs6010555>

REFERENCES

- Abdi, H., Williams, L.J., 2010. Principal component analysis. *Wiley Interdisciplinary Reviews: Computational Statistics* 2(4), 433-459. <https://doi.org/10.1002/wics.101>
- Addink, E.A., de Jong, S.M., Pebesma, E.J., 2007. The importance of scale in object-based mapping of vegetation parameters with hyperspectral imagery. *Photogrammetric Engineering & Remote Sensing* 73(8), 905-912. <https://doi.org/10.14358/PERS.73.8.905>
- Adelabu, S., Dube, T., 2015. Employing ground and satellite-based QuickBird data and random forest to discriminate five tree species in a Southern African Woodland. *Geocarto International* 30(6), 457-471. <https://doi.org/10.1080/10106049.2014.885589>
- Aguirre-Gutiérrez, J., Seijmonsbergen, A.C., Duivenvoorden, J.F., 2012. Optimizing land cover classification accuracy for change detection, a combined pixel-based and object-based approach in a mountainous area in Mexico. *Applied Geography* 34, 29-37. <https://doi.org/10.1016/j.apgeog.2011.10.010>
- Alonzo, M., Bookhagen, B., Roberts, D.A., 2014. Urban tree species mapping using hyperspectral and lidar data fusion. *Remote Sensing of Environment* 148, 70-83. <https://doi.org/10.1016/j.rse.2014.03.018>
- Álvarez-Molina, L.L., Martínez, M.L., Pérez-Maqueo, O., Gallego-Fernández, J.B., Flores, P., 2012. Richness, diversity, and rate of primary succession over 20 year in tropical coastal dunes. *Plant Ecology* 213(10), 1597-1608. <https://doi.org/10.1007/s11258-012-0114-5>
- Archer, K.J., Kimes, R.V., 2008. Empirical characterization of random forest variable importance measures. *Computational Statistics & Data Analysis* 52(4), 2249-2260. <https://doi.org/10.1016/j.csda.2007.08.015>
- Arenas-Castro, S., Julien, Y., Jiménez-Muñoz, J.C., Sobrino, J.A., Fernández-Haeger, J., Jordano-Barbudo, D., 2012. Mapping wild pear trees (*Pyrus bourgaeana*) in Mediterranean forest using high-resolution QuickBird satellite imagery. *International Journal of Remote Sensing* 34(9-10), 3376-3396. <https://doi.org/10.1080/01431161.2012.716909>
- Belgiu, M., Drăguț, L., 2016. Random forest in remote sensing: A review of applications and future directions. *ISPRS Journal of Photogrammetry and Remote Sensing* 114, 24-31. <https://doi.org/10.1016/j.isprsjprs.2016.01.011>
- Ben-Hur, A., Ong, C.S., Sonnenburg, S., Schölkopf, B., Rätsch, G., 2008. Support vector machines and kernels for computational biology. *PLoS Computational Biology* 4(10), e1000173. <https://doi.org/10.1371/journal.pcbi.1000173>
- Bergen, K.M., Dobson, M.C., 1999. Integration of remotely sensed radar imagery in modeling and mapping of forest biomass and net primary production. *Ecological Modelling* 122(3), 257-274. [https://doi.org/http://dx.doi.org/10.1016/S0304-3800\(99\)00141-6](https://doi.org/http://dx.doi.org/10.1016/S0304-3800(99)00141-6)
- Bergin, D., Hosking, G., 2006. Pohutukawa-ecology, establishment, growth and management. *New Zealand Indigenous Tree Series No. 4*. New Zealand Forest Research Institute, Rotorua.
- Beven, K.J., Kirkby, M.J., 1979. A physically based, variable contributing area model of basin hydrology / Un modèle à base physique de zone d'appel

- variable de l'hydrologie du bassin versant. *Hydrological Sciences Bulletin* 24(1), 43-69. <https://doi.org/10.1080/02626667909491834>
- Binh, C.H., Nam, V.N., 2014. Carbon sequestration of *Ceriops zippeliana* in Can Gio mangroves Mangrove ecosystems technical reports, Vol. 6, Sendai, Japan.
- Bishop, C.M., 2007. *Pattern Recognition and Machine Learning*. Springer, New York, NY.
- Blaschke, T., 2010. Object based image analysis for remote sensing. *ISPRS Journal of Photogrammetry and Remote Sensing* 65(1), 2-16. <https://doi.org/10.1016/j.isprsjprs.2009.06.004>
- Blaschke, T., Burnett, C., Pekkarinen, A., 2004. Image segmentation methods for object-based analysis and classification, in: de Jong, S.M., van der Meer, F.D. (Eds.), *Remote Sensing Image Analysis: Including the Spatial Domain*. Springer, Dordrecht, pp. 211-236.
- Blaschke, T., Feizizadeh, B., Hölbling, D., 2014. Object-based image analysis and digital terrain analysis for locating landslides in the Urmia Lake basin, Iran. *IEEE Journal of Selected Topics in Applied Earth Observations and Remote Sensing* 7(12), 4806-4817. <https://doi.org/10.1109/JSTARS.2014.2350036>
- Blaschke, T., Hay, G.J., Kelly, M., Lang, S., Hofmann, P., Addink, E., Queiroz Feitosa, R., van der Meer, F., van der Werff, H., van Coillie, F., Tiede, D., 2014. Geographic object-based image analysis – towards a new paradigm. *ISPRS Journal of Photogrammetry and Remote Sensing* 87, 180-191. <https://doi.org/10.1016/j.isprsjprs.2013.09.014>
- Bolón-Canedo, V., Sánchez-Marono, N., Alonso-Betanzos, A., 2013. A review of feature selection methods on synthetic data. *Knowledge and Information Systems* 34(3), 483-519. <https://doi.org/10.1007/s10115-012-0487-8>
- Breiman, L., 2001a. Random forests. *Machine Learning* 45(1), 5-32. <https://doi.org/10.1023/A:1010933404324>
- Breiman, L., 2001b. Statistical modeling: The two cultures (with comments and a rejoinder by the author). *Statistical Science* 16(3), 199-231.
- Bunting, P., Lucas, R., 2006. The delineation of tree crowns in Australian mixed species forests using hyperspectral Compact Airborne Spectrographic Imager (CASI) data. *Remote Sensing of Environment* 101(2), 230-248. <https://doi.org/10.1016/j.rse.2005.12.015>
- Burnett, C., Blaschke, T., 2003. A multi-scale segmentation/object relationship modelling methodology for landscape analysis. *Ecological Modelling* 168(3), 233-249. [https://doi.org/10.1016/S0304-3800\(03\)00139-X](https://doi.org/10.1016/S0304-3800(03)00139-X)
- Bylsma, R.J., 2012. Structure, composition and dynamics of *Metrosideros excelsa* (pōhutukawa) forest, Bay of Plenty, New Zealand University of Waikato.
- Bylsma, R.J., Clarkson, B.D., Efford, J.T., 2014. Biological flora of New Zealand 14: *Metrosideros excelsa*, pōhutukawa, New Zealand Christmas tree. *New Zealand Journal of Botany* 52(3), 365-385. <https://doi.org/10.1080/0028825x.2014.926278>
- Castillejo-González, I.L., López-Granados, F., García-Ferrer, A., Peña-Barragán, J.M., Jurado-Expósito, M., de la Orden, M.S., González-Audicana, M., 2009. Object- and pixel-based analysis for mapping crops and their agro-environmental associated measures using QuickBird imagery. *Computers and Electronics in Agriculture* 68(2), 207-215. <https://doi.org/10.1016/j.compag.2009.06.004>

- Chandrashekar, G., Sahin, F., 2014. A survey on feature selection methods. *Computers & Electrical Engineering* 40(1), 16-28. <https://doi.org/10.1016/j.compeleceng.2013.11.024>
- Chang, C.-C., Lin, C.-J., 2011. LIBSVM: A library for support vector machines. *ACM Transactions on Intelligent Systems and Technology (TIST)* 2(3), 1-27. <https://doi.org/10.1145/1961189.1961199>
- Charoenjit, K., Zuddas, P., Allemand, P., Pattanakiat, S., Pachana, K., 2015. Estimation of biomass and carbon stock in Para rubber plantations using object-based classification from Thaichote satellite data in Eastern Thailand. *J Appl Remote Sens* 9(1). <https://doi.org/10.1117/1.JRS.9.096072>
- Chaudhary, N., Sharma, A.K., Agarwal, P., Gupta, A., Sharma, V.K., 2015. 16S classifier: a tool for fast and accurate taxonomic classification of 16S rRNA hypervariable regions in metagenomic datasets. *PloS One* 10(2), e0116106. <https://doi.org/10.1371/journal.pone.0116106>
- Chemura, A., van Duren, I., van Leeuwen, L.M., 2015. Determination of the age of oil palm from crown projection area detected from WorldView-2 multispectral remote sensing data: The case of Ejisu-Juaben district, Ghana. *ISPRS Journal of Photogrammetry and Remote Sensing* 100, 118-127. <https://doi.org/10.1016/j.isprsjprs.2014.07.013>
- Chen, Q., 2013. Lidar remote sensing of vegetation biomass, in: Wang, G., Weng, Q. (Eds.), *Remote Sensing of Natural Resources*. CRC Press, Boca Raton, pp. 399-420.
- Chen, Q., Baldocchi, D., Gong, P., Kelly, M., 2006. Isolating individual trees in a savanna woodland using small footprint lidar data. *Photogrammetric Engineering & Remote Sensing* 72(8), 923-932. <https://doi.org/10.14358/PERS.72.8.923>
- Chen, Q., Laurin, G.V., Battles, J.J., Saah, D., 2012. Integration of airborne lidar and vegetation types derived from aerial photography for mapping aboveground live biomass. *Remote Sensing of Environment* 121, 108-117. <https://doi.org/10.1016/j.rse.2012.01.021>
- Chen, Z., Gao, B., 2014. An object-based method for urban land cover classification using airborne lidar data. *IEEE Journal of Selected Topics in Applied Earth Observations and Remote Sensing* 7(10), 4243-4254. <https://doi.org/10.1109/Jstars.2014.2332337>
- Cho, M.A., Mathieu, R., Asner, G.P., Naidoo, L., van Aardt, J., Ramoelo, A., Debba, P., Wessels, K., Main, R., Smit, I.P.J., Erasmus, B., 2012. Mapping tree species composition in South African savannas using an integrated airborne spectral and LiDAR system. *Remote Sensing of Environment* 125(0), 214-226. <https://doi.org/10.1016/j.rse.2012.07.010>
- Chuvieco, E., 2016. *Fundamentals of Satellite Remote Sensing: An Environmental Approach*, 2nd ed. CRC press, Boca Raton, FL.
- Clark, M.L., Roberts, D.A., Clark, D.B., 2005. Hyperspectral discrimination of tropical rain forest tree species at leaf to crown scales. *Remote Sensing of Environment* 96(3-4), 375-398. <https://doi.org/10.1016/j.rse.2005.03.009>
- Clinton, N., Holt, A., Scarborough, J., Yan, L., Gong, P., 2010. Accuracy assessment measures for object-based image segmentation goodness. *Photogrammetric Engineering & Remote Sensing* 76(3), 289-299.
- Comber, A., Fisher, P., Brunsdon, C., Khmag, A., 2012. Spatial analysis of remote sensing image classification accuracy. *Remote Sensing of Environment*

- 127(Supplement C), 237-246.
<https://doi.org/https://doi.org/10.1016/j.rse.2012.09.005>
- Congalton, R.G., 1991. A review of assessing the accuracy of classifications of remotely sensed data. *Remote Sensing of Environment* 37(1), 35-46.
[https://doi.org/10.1016/0034-4257\(91\)90048-B](https://doi.org/10.1016/0034-4257(91)90048-B)
- Congalton, R.G., Green, K., 2008. *Assessing the Accuracy of Remotely Sensed Data: Principles and Practices*. CRC Press, Boca Raton, FL.
- Cortes, C., Vapnik, V., 1995. Support-vector networks. *Machine Learning* 20(3), 273-297. <https://doi.org/10.1007/bf00994018>
- Cox, D.R., 1958. The regression analysis of binary sequences. *Journal of the Royal Statistical Society. Series B (Methodological)* 20(2), 215-242.
- Cracknell, M.J., Reading, A.M., 2014. Geological mapping using remote sensing data: A comparison of five machine learning algorithms, their response to variations in the spatial distribution of training data and the use of explicit spatial information. *Computers & Geosciences* 63, 22-33.
<https://doi.org/10.1016/j.cageo.2013.10.008>
- Cutler, D.R., Edwards, T.C., Beard, K.H., Cutler, A., Hess, K.T., Gibson, J., Lawler, J.J., 2007. Random forests for classification in ecology. *Ecology* 88(11), 2783-2792. <https://doi.org/10.1890/07-0539.1>
- Dalponte, M., Bruzzone, L., Gianelle, D., 2012. Tree species classification in the Southern Alps based on the fusion of very high geometrical resolution multispectral/hyperspectral images and LiDAR data. *Remote Sensing of Environment* 123, 258-270. <https://doi.org/10.1016/j.rse.2012.03.013>
- Dalponte, M., Bruzzone, L., Vescovo, L., Gianelle, D., 2009. The role of spectral resolution and classifier complexity in the analysis of hyperspectral images of forest areas. *Remote Sensing of Environment* 113(11), 2345-2355.
<https://doi.org/10.1016/j.rse.2009.06.013>
- Dalponte, M., Ørka, H.O., Gobakken, T., Gianelle, D., Næsset, E., 2013. Tree species classification in boreal forests with hyperspectral data. *IEEE Transactions on Geoscience and Remote Sensing* 51(5), 2632-2645.
<https://doi.org/10.1109/TGRS.2012.2216272>
- Donato, D.C., Kauffman, J.B., Murdiyarso, D., Kurnianto, S., Stidham, M., Kanninen, M., 2011. Mangroves among the most carbon-rich forests in the tropics. *Nature Geoscience* 4(5), 293-297.
<https://doi.org/10.1038/ngeo1123>
- Drake, J.B., Dubayah, R.O., Clark, D.B., Knox, R.G., Blair, J.B., Hofton, M.A., Chazdon, R.L., Weishampel, J.F., Prince, S., 2002. Estimation of tropical forest structural characteristics using large-footprint lidar. *Remote Sensing of Environment* 79(2-3), 305-319. [https://doi.org/10.1016/S0034-4257\(01\)00281-4](https://doi.org/10.1016/S0034-4257(01)00281-4)
- Dube, T., Mutanga, O., 2015. Investigating the robustness of the new Landsat-8 Operational Land Imager derived texture metrics in estimating plantation forest aboveground biomass in resource constrained areas. *ISPRS Journal of Photogrammetry and Remote sensing* 108, 12-32.
<https://doi.org/10.1016/j.isprsjprs.2015.06.002>
- Duda, R.O., Hart, P.E., 1973. *Pattern Classification and Scene Analysis*. John Wiley, New York, NY.
- Duro, D.C., Franklin, S.E., Dubé, M.G., 2012. A comparison of pixel-based and object-based image analysis with selected machine learning algorithms for the classification of agricultural landscapes using SPOT-5 HRG imagery.

- Remote Sensing of Environment 118, 259-272.
<https://doi.org/10.1016/j.rse.2011.11.020>
- Fassnacht, F.E., Hartig, F., Latifi, H., Berger, C., Hernández, J., Corvalán, P., Koch, B., 2014. Importance of sample size, data type and prediction method for remote sensing-based estimations of aboveground forest biomass. *Remote Sensing of Environment* 154, 102-114.
<https://doi.org/10.1016/j.rse.2014.07.028>
- Fassnacht, F.E., Neumann, C., Förster, M., Buddenbaum, H., Ghosh, A., Clasen, A., Joshi, P.K., Koch, B., 2014. Comparison of feature reduction algorithms for classifying tree species with hyperspectral data on three central European test sites. *IEEE Journal of Selected Topics in Applied Earth Observations and Remote Sensing* 7(6), 2547-2561.
<https://doi.org/10.1109/Jstars.2014.2329390>
- Feliciano, E.A., Wdowinski, S., Potts, M.D., 2014. Assessing mangrove above-ground biomass and structure using terrestrial laser scanning: A case study in the Everglades National Park. *Wetlands* 34(5), 955-968.
<https://doi.org/10.1007/s13157-014-0558-6>
- Flanders, D., Hall-Beyer, M., Pereverzoff, J., 2003. Preliminary evaluation of eCognition object-based software for cut block delineation and feature extraction. *Canadian Journal of Remote Sensing* 29(4), 441-452.
- Fong, S., Zhuang, Y., Liu, K., Zhou, S., 2015. Classifying forum questions using PCA and machine learning for improving online CQA, *International Conference on Soft Computing in Data Science*, Putrajaya, Malaysia, pp. 13-22.
- Foody, G.M., 2002. Status of land cover classification accuracy assessment. *Remote Sensing of Environment* 80(1), 185-201.
[https://doi.org/10.1016/S0034-4257\(01\)00295-4](https://doi.org/10.1016/S0034-4257(01)00295-4)
- Foody, G.M., 2004. Thematic map comparison: Evaluating the statistical significance of differences in classification accuracy. *Photogrammetric Engineering & Remote Sensing* 70(5), 627-634.
- Frank, E., Hall, M.A., Witten, I.H., 2016. The WEKA Workbench. Online Appendix for "Data Mining: Practical Machine Learning Tools and Techniques", 4th ed. Morgan Kaufmann, Cambridge, MA.
- Fu, B., Wang, Y., Campbell, A., Li, Y., Zhang, B., Yin, S., Xing, Z., Jin, X., 2017. Comparison of object-based and pixel-based Random Forest algorithm for wetland vegetation mapping using high spatial resolution GF-1 and SAR data. *Ecological Indicators* 73, 105-117.
<https://doi.org/10.1016/j.ecolind.2016.09.029>
- Galelli, S., Humphrey, G.B., Maier, H.R., Castelletti, A., Dandy, G.C., Gibbs, M.S., 2014. An evaluation framework for input variable selection algorithms for environmental data-driven models. *Environmental Modelling & Software* 62, 33-51. <https://doi.org/10.1016/j.envsoft.2014.08.015>
- Gao, Y., Mas, J., Niemeyer, I., Marpu, P., Palacio, J., 2007. Object-based image analysis for mapping land-cover in a forest area, 5th International Symposium: Spatial Data Quality, Enschede, The Netherlands, pp. 13-15.
- Gebreslasie, M.T., Ahmed, F.B., Van Aardt, J.A.N., Blakeway, F., 2011. Individual tree detection based on variable and fixed window size local maxima filtering applied to IKONOS imagery for even-aged Eucalyptus plantation forests. *International Journal of Remote Sensing* 32(15), 4141-4154.

- Ghosh, A., Joshi, P., 2014. A comparison of selected classification algorithms for mapping bamboo patches in lower Gangetic plains using very high resolution WorldView 2 imagery. *International Journal of Applied Earth Observation and Geoinformation* 26, 298-311. <https://doi.org/10.1016/j.jag.2013.08.011>
- Giri, C., Long, J., Abbas, S., Murali, R.M., Qamer, F.M., Pengra, B., Thau, D., 2015. Distribution and dynamics of mangrove forests of South Asia. *Journal of Environmental Management* 148, 101-111. <https://doi.org/10.1016/j.jenvman.2014.01.020>
- Gregorutti, B., Michel, B., Saint-Pierre, P., 2016. Correlation and variable importance in random forests. *Statistics and Computing*. <https://doi.org/10.1007/s11222-016-9646-1>
- Hall, M.A., 1999. Correlation-Based Feature Selection for Machine Learning (Unpublished PhD thesis). University of Waikato, Hamilton, New Zealand.
- Hamdan, O., Khairunnisa, M.R., Ammar, A.A., Hasmadi, I.M., Aziz, H.K., 2013. Mangrove carbon stock assessment by optical satellite imagery. *Journal of Tropical Forest Science* 25(4), 554-565.
- Hamdan, O., Khali Aziz, H., Mohd Hasmadi, I., 2014. L-band ALOS PALSAR for biomass estimation of Matang Mangroves, Malaysia. *Remote Sensing of Environment* 155, 69-78. <https://doi.org/10.1016/j.rse.2014.04.029>
- Han, J., Kamber, M., Pei, J., 2012. *Data Mining: Concepts and Techniques*, 3rd ed. Morgan Kaufmann, Boston, MA.
- Han, N., Du, H., Zhou, G., Sun, X., Ge, H., Xu, X., 2014. Object-based classification using SPOT-5 imagery for Moso bamboo forest mapping. *International Journal of Remote Sensing* 35(3), 1126-1142. <https://doi.org/10.1080/01431161.2013.875634>
- Haralick, R.M., Shanmugam, K., Dinstein, I.H., 1973. Textural features for image classification. *IEEE Transactions on Systems, Man and Cybernetics* 3(6), 610-621. <https://doi.org/10.1109/tsmc.1973.4309314>
- Hardisky, M.A., Klemas, V., Smart, R.M., 1983. The influence of soil-salinity, growth form, and leaf moisture on the spectral radiance of spartina-alterniflora canopies. *Photogrammetric Engineering and Remote Sensing* 49(1), 77-83.
- Hastie, T.J., Tibshirani, R.J., Friedman, J.H., 2009. *The Elements of Statistical Learning: Data Mining, Inference, and Prediction*. Springer, New York, NY.
- Holmgren, J., Persson, A., 2004. Identifying species of individual trees using airborne laser scanner. *Remote Sensing Of Environment* 90(4), 415-423. [https://doi.org/10.1016/S0034-4257\(03\)00140-8](https://doi.org/10.1016/S0034-4257(03)00140-8)
- Houborg, R., Fisher, J.B., Skidmore, A.K., 2015. Advances in remote sensing of vegetation function and traits. *International Journal of Applied Earth Observation and Geoinformation* 43, 1-6. <https://doi.org/10.1016/j.jag.2015.06.001>
- Huang, C.-L., Wang, C.-J., 2006. A GA-based feature selection and parameters optimization for support vector machines. *Expert Systems with Applications* 31(2), 231-240. <https://doi.org/10.1016/j.eswa.2005.09.024>
- Huete, A.R., 1988. A soil-adjusted vegetation index (SAVI). *Remote Sensing of Environment* 25(3), 295-309. [https://doi.org/10.1016/0034-4257\(88\)90106-X](https://doi.org/10.1016/0034-4257(88)90106-X)

- Humphreys, E.A., Tyler, A.M., 1990. Coromandel Ecological Region: survey report for the Protected Natural Areas Programme. Department of Conservation, Waikato Conservancy.
- Hussin, Y., Gilani, H., Leeuwen, L., Murthy, M.S.R., Shah, R., Baral, S., Tsendbazar, N.-E., Shrestha, S., Shah, S., Qamer, F., 2014. Evaluation of object-based image analysis techniques on very high-resolution satellite image for biomass estimation in a watershed of hilly forest of Nepal. *Appl Geomat* 6(1), 59-68. <https://doi.org/10.1007/s12518-014-0126-z>
- Izenman, A.J., 2008. *Modern Multivariate Statistical Techniques*. Springer, New York, NY.
- Jachowski, N.R.A., Quak, M.S.Y., Friess, D.A., Duangnamon, D., Webb, E.L., Ziegler, A.D., 2013. Mangrove biomass estimation in Southwest Thailand using machine learning. *Applied Geography* 45, 311-321. <https://doi.org/10.1016/j.apgeog.2013.09.024>
- Jakubowski, M.K., Li, W., Guo, Q., Kelly, M., 2013. Delineating individual trees from Lidar data: A comparison of vector-and raster-based segmentation approaches. *Remote Sensing* 5(9), 4163-4186. <https://doi.org/10.3390/rs5094163>
- Ji, L., Zhang, L., Wylie, B., 2009. Analysis of dynamic thresholds for the normalized difference water index. *Photogrammetric Engineering & Remote Sensing* 75(11), 1307-1317. <https://doi.org/10.14358/PERS.75.11.1307>
- Jiang, Z., Huete, A.R., Didan, K., Miura, T., 2008. Development of a two-band enhanced vegetation index without a blue band. *Remote Sensing of Environment* 112(10), 3833-3845. <https://doi.org/10.1016/j.rse.2008.06.006>
- Joachims, T., 2002. *Learning to Classify Text Using Support Vector Machines: Methods, Theory and Algorithms*. Kluwer Academic Publishers, Boston, MA.
- Kajisa, T., Murakami, T., Mizoue, N., Top, N., Yoshida, S., 2009. Object-based forest biomass estimation using Landsat ETM+ in Kampong Thom Province, Cambodia. *Journal of Forest Research* 14(4), 203-211. <https://doi.org/http://dx.doi.org/10.1007/s10310-009-0125-9>
- Kayitakire, F., Hamel, C., Defourny, P., 2006. Retrieving forest structure variables based on image texture analysis and IKONOS-2 imagery. *Remote Sensing of Environment* 102(3-4), 390-401. <https://doi.org/10.1016/j.rse.2006.02.022>
- Ke, Y., Quackenbush, L.J., 2011. A review of methods for automatic individual tree-crown detection and delineation from passive remote sensing. *International Journal of Remote Sensing* 32(17), 4725-4747. <https://doi.org/10.1080/01431161.2010.494184>
- Ke, Y., Quackenbush, L.J., Im, J., 2010. Synergistic use of QuickBird multispectral imagery and LIDAR data for object-based forest species classification. *Remote Sensing of Environment* 114(6), 1141-1154. <https://doi.org/10.1016/j.rse.2010.01.002>
- Khosravipour, A., Skidmore, A.K., Isenburg, M., Wang, T., Hussin, Y.A., 2014. Generating pit-free canopy height models from airborne Lidar. *Photogrammetric Engineering & Remote Sensing* 80(9), 863-872. <https://doi.org/10.14358/PERS.80.9.863>

- Kim, M., Madden, M., Warner, T.A., 2009a. Forest type mapping using object-specific texture measures from multispectral IKONOS imagery: Segmentation quality and image classification issues. *Photogrammetric Engineering and Remote Sensing* 75(7), 819-829.
- Kim, M., Warner, T.A., Madden, M., Atkinson, D.S., 2011. Multi-scale GEOBIA with very high spatial resolution digital aerial imagery: Scale, texture and image objects. *International Journal of Remote Sensing* 32(10), 2825-2850. <https://doi.org/10.1080/01431161003745608>
- Kim, S., McGaughey, R.J., Andersen, H.-E., Schreuder, G., 2009b. Tree species differentiation using intensity data derived from leaf-on and leaf-off airborne laser scanner data. *Remote Sensing of Environment* 113(8), 1575-1586. <https://doi.org/10.1016/j.rse.2009.03.017>
- Komiyama, A., Sasitorn, P., Shogo, K., 2005. Common allometric equations for estimating the tree weight of mangroves. *Journal of Tropical Ecology* 21(4), 471-477. <https://doi.org/10.1017/S0266467405002476>
- Korpela, I., Dahlin, B., Schäfer, H., Bruun, E., Haapaniemi, F., Honkasalo, J., Ilvesniemi, S., Kuutti, V., Linkosalmi, M., Mustonen, J., 2007. Single-tree forest inventory using lidar and aerial images for 3D treetop positioning, species recognition, height and crown width estimation, *Proceedings of ISPRS Workshop on Laser Scanning*, pp. 227-233.
- Kuenzer, C., Tuan, V.Q., 2013. Assessing the ecosystem services value of Can Gio Mangrove Biosphere Reserve: Combining earth-observation- and household-survey-based analyses. *Applied Geography* 45, 167-184. <https://doi.org/10.1016/j.apgeog.2013.08.012>
- Lang, S., 2008. Object-based image analysis for remote sensing applications: Modeling reality—dealing with complexity, in: Blaschke, T., Lang, S., Hay, G.J. (Eds.), *Object-Based Image Analysis*. Springer-Verlag, Berlin, pp. 3-27.
- Lang, S., Langanke, T., 2006. Object-based mapping and object-relationship modeling for land use classes and habitats. *Photogrammetrie Fernerkundung Geoinformation* 2006(1), 5.
- Larsen, M., Eriksson, M., Descombes, X., Perrin, G., Brandtberg, T., Gougeon, F.A., 2011. Comparison of six individual tree crown detection algorithms evaluated under varying forest conditions. *International Journal of Remote Sensing* 32(20), 5827-5852. <https://doi.org/10.1080/01431161.2010.507790>
- Le Toan, T., Beaudoin, A., Riou, J., Guyon, D., 1992. Relating forest biomass to SAR data. *IEEE Transactions on Geoscience and Remote Sensing* 30(2), 403-411. <https://doi.org/10.1109/36.134089>
- Leckie, D., Gougeon, F., Hill, D., Quinn, R., Armstrong, L., Shreenan, R., 2003. Combined high-density lidar and multispectral imagery for individual tree crown analysis. *Canadian Journal of Remote Sensing* 29(5), 633-649. <https://doi.org/10.5589/m03-024>
- Lefsky, M.A., Cohen, W.B., Harding, D.J., Parker, G.G., Acker, S.A., Gower, S.T., 2002. Lidar remote sensing of above-ground biomass in three biomes. *Global Ecology and Biogeography* 11(5), 393-399.
- Li, J., Justy, P., Siwabessy, W., Tran, M., Huang, Z., Heap, A.D., 2014. Predicting seabed hardness using random forest in R, in: Zhao, Y., Cen, Y. (Eds.), *Data Mining Applications with R*. Academic Press, Boston, MA, pp. 299-329.

- Li, W., Guo, Q., Jakubowski, M.K., Kelly, M., 2012. A new method for segmenting individual trees from the lidar point cloud. *Photogrammetric Engineering & Remote Sensing* 78(1), 75-84.
- Li, X., Meng, Q., Gu, X., Jancso, T., Yu, T., Wang, K., Mavromatis, S., 2013. A hybrid method combining pixel-based and object-oriented methods and its application in Hungary using Chinese HJ-1 satellite images. *International journal of remote sensing* 34(13), 4655-4668. <https://doi.org/10.1080/01431161.2013.780669>
- Liaw, A., Wiener, M., 2002. Classification and regression by randomForest. *R News* 2(3), 18-22.
- Lillesand, T., Kiefer, R.W., Chipman, J., 2014. Remote sensing and image interpretation. John Wiley & Sons, Hoboken, NJ.
- Liu, D., Xia, F., 2010. Assessing object-based classification: advantages and limitations. *Remote Sensing Letters* 1(4), 187-194. <https://doi.org/10.1080/01431161003743173>
- Löw, F., Conrad, C., Michel, U., 2015. Decision fusion and non-parametric classifiers for land use mapping using multi-temporal RapidEye data. *ISPRS Journal of Photogrammetry and Remote Sensing* 108, 191-204. <https://doi.org/10.1016/j.isprsjprs.2015.07.001>
- Lu, D., 2005. Aboveground biomass estimation using Landsat TM data in the Brazilian Amazon. *International Journal of Remote Sensing* 26(12), 2509-2525. <https://doi.org/10.1080/01431160500142145>
- Lu, D., 2006. The potential and challenge of remote sensing - based biomass estimation. *International Journal of Remote Sensing* 27(7), 1297-1328.
- Lu, D., Chen, Q., Wang, G., Liu, L., Li, G., Moran, E., 2014. A survey of remote sensing-based aboveground biomass estimation methods in forest ecosystems. *International Journal of Digital Earth* 9(1), 63-105. <https://doi.org/10.1080/17538947.2014.990526>
- Lu, D., Mausel, P., Brondizio, E., Moran, E., 2004. Relationships between forest stand parameters and Landsat TM spectral responses in the Brazilian Amazon Basin. *Forest Ecology and Management* 198(1-3), 149-167. <https://doi.org/10.1016/j.foreco.2004.03.048>
- Lu, D., Weng, Q., 2007. A survey of image classification methods and techniques for improving classification performance. *International Journal of Remote Sensing* 28(5), 823-870. <https://doi.org/10.1080/01431160600746456>
- Luong, N.V., Tateishi, R., Hoan, N.T., 2015. Analysis of an impact of succession in mangrove forest association using remote sensing and GIS technology. *Journal of Geography and Geology* 7(1), 106-116. <https://doi.org/10.5539/jgg.v7n1p106>
- Ma, L., Fu, T., Blaschke, T., Li, M., Tiede, D., Zhou, Z., Ma, X., Chen, D., 2017. Evaluation of feature selection methods for object-based land cover mapping of unmanned aerial vehicle imagery using random forest and support vector machine classifiers. *ISPRS International Journal of Geo-Information* 6(2), ARTN 51. <https://doi.org/10.3390/ijgi6020051>
- MacFaden, S.W., O'Neil-Dunne, J.P.M., Royar, A.R., Lu, J.W.T., Rundle, A.G., 2012. High-resolution tree canopy mapping for New York City using LIDAR and object-based image analysis. *J Appl Remote Sens* 6(1), 063567-063561-063567-063523. <https://doi.org/10.1117/1.JRS.6.063567>
- Mishra, N.B., Crews, K.A., 2014. Mapping vegetation morphology types in a dry savanna ecosystem: integrating hierarchical object-based image analysis

- with Random Forest. *International Journal of Remote Sensing* 35(3), 1175-1198. <https://doi.org/10.1080/01431161.2013.876120>
- Mountrakis, G., Im, J., Ogole, C., 2011. Support vector machines in remote sensing: A review. *ISPRS Journal of Photogrammetry and Remote Sensing* 66(3), 247-259. <https://doi.org/10.1016/j.isprsjprs.2010.11.001>
- Mutanga, O., Adam, E., Cho, M.A., 2012. High density biomass estimation for wetland vegetation using WorldView-2 imagery and random forest regression algorithm. *International Journal of Applied Earth Observation and Geoinformation* 18, 399-406. <https://doi.org/10.1016/j.jag.2012.03.012>
- Myint, S.W., Giri, C.P., Wang, L., Zhu, Z., Gillette, S.C., 2008. Identifying mangrove species and their surrounding land use and land cover classes using an object-oriented approach with a lacunarity spatial measure. *GIScience & Remote Sensing* 45(2), 188-208. <https://doi.org/10.2747/1548-1603.45.2.188>
- Nadeau, C., Bengio, Y., 2003. Inference for the generalization error. *Machine Learning* 52(3), 239-281. <https://doi.org/10.1023/A:1024068626366>
- Nam, V.N., 2003. Nghiên cứu sinh khối và năng suất sơ cấp quần thể Mắm trắng (*Avicennia alba* BL.) tự nhiên tại Cần Giuộc, Thành phố Hồ Chí Minh (PhD thesis). Vietnamese Academy of Forest Sciences, Hà Nội, Vietnam.
- Nam, V.N., 2011. Nghiên cứu khả năng hấp thụ CO₂ của rừng cóc trắng (*Lumnitzera racemosa* Willd) trong ô khu dự trữ sinh quyển rừng ngập mặn Cần Giuộc, Thành phố Hồ Chí Minh. *Tạp Chí Nông Nghiệp & Phát Triển Nông Thôn = Agriculture & Rural Development Review* 2, 162-166.
- Nam, V.N., 2011. Nghiên cứu tích tụ carbon của rừng đước doi (*Rhizophora apiculata* Blume) trong ô khu dự trữ sinh quyển rừng ngập mặn Cần Giuộc, thành phố Hồ Chí Minh. *Tạp Chí Nông Nghiệp & Phát Triển Nông Thôn = Agriculture & Rural Development Review* 2, 78-83.
- Ng, A.Y., Jordan, M.I., 2002. On discriminative vs. generative classifiers: A comparison of logistic regression and naive bayes. *Adv Neur In* 2, 841-848.
- Nguyen, H.N., 2006. The environment in Ho Chi Minh City harbours, in: Wolanski, E. (Ed.), *The Environment in Asia Pacific Harbours*. Springer, Dordrecht, The Netherlands, pp. 261-291.
- Olofsson, K., Wallerman, J., Holmgren, J., Olsson, H., 2006. Tree species discrimination using Z/I DMC imagery and template matching of single trees. *Scandinavian Journal of Forest Research* 21(S7), 106-110. <https://doi.org/10.1080/14004080500486955>
- Ørka, H.O., Næsset, E., Bollandsås, O.M., 2009. Classifying species of individual trees by intensity and structure features derived from airborne laser scanner data. *Remote Sensing of Environment* 113(6), 1163-1174. <https://doi.org/10.1016/j.rse.2009.02.002>
- Otukei, J., Blaschke, T., 2010. Land cover change assessment using decision trees, support vector machines and maximum likelihood classification algorithms. *International Journal of Applied Earth Observation and Geoinformation* 12, S27-S31. <https://doi.org/10.1016/j.jag.2009.11.002>
- Ouyang, Z.-T., Zhang, M.-Q., Xie, X., Shen, Q., Guo, H.-Q., Zhao, B., 2011. A comparison of pixel-based and object-oriented approaches to VHR imagery for mapping saltmarsh plants. *Ecological Informatics* 6(2), 136-146. <https://doi.org/10.1016/j.ecoinf.2011.01.002>

- Pal, M., 2005. Random forest classifier for remote sensing classification. *International Journal of Remote Sensing* 26(1), 217-222. <https://doi.org/10.1080/01431160412331269698>
- Pal, M., Foody, G.M., 2010. Feature selection for classification of hyperspectral data by SVM. *IEEE Transactions on Geoscience and Remote Sensing* 48(5), 2297-2307. <https://doi.org/10.1109/TGRS.2009.2039484>
- Pal, N.R., Pal, S.K., 1993. A review on image segmentation techniques. *Pattern recognition* 26(9), 1277-1294. [https://doi.org/10.1016/0031-3203\(93\)90135-J](https://doi.org/10.1016/0031-3203(93)90135-J)
- Pettorelli, N., Laurance, W.F., O'Brien, T.G., Wegmann, M., Nagendra, H., Turner, W., 2014. Satellite remote sensing for applied ecologists: opportunities and challenges. *Journal of Applied Ecology* 51(4), 839-848. <https://doi.org/10.1111/1365-2664.12261>
- Pham, B.T., Pradhan, B., Tien Bui, D., Prakash, I., Dholakia, M.B., 2016a. A comparative study of different machine learning methods for landslide susceptibility assessment: A case study of Uttarakhand area (India). *Environmental Modelling & Software* 84, 240-250. <https://doi.org/10.1016/j.envsoft.2016.07.005>
- Pham, L.T.H., Brabyn, L., Ashraf, S., 2016b. Combining QuickBird, LiDAR, and GIS topography indices to identify a single native tree species in a complex landscape using an object-based classification approach. *International Journal of Applied Earth Observation and Geoinformation* 50, 187-197. <https://doi.org/10.1016/j.jag.2016.03.015>
- Pontius Jr, R.G., Millones, M., 2011. Death to Kappa: Birth of quantity disagreement and allocation disagreement for accuracy assessment. *International Journal of Remote Sensing* 32(15), 4407-4429. <https://doi.org/10.1080/01431161.2011.552923>
- Popescu, S.C., Zhao, K., Neuenschwander, A., Lin, C., 2011. Satellite lidar vs. small footprint airborne lidar: Comparing the accuracy of aboveground biomass estimates and forest structure metrics at footprint level. *Remote Sensing of Environment* 115(11), 2786-2797. <https://doi.org/10.1016/j.rse.2011.01.026>
- Poulos, H.M., Camp, A.E., 2010. Decision support for mitigating the risk of tree induced transmission line failure in utility rights-of-way. *Environmental Management* 45(2), 217-226. <https://doi.org/10.1007/s00267-009-9422-5>
- Prasad, A.M., Iverson, L.R., Liaw, A., 2006. Newer classification and regression tree techniques: bagging and random forests for ecological prediction. *Ecosystems* 9(2), 181-199.
- Proisy, C., Couteron, P., Fromard, F., 2007. Predicting and mapping mangrove biomass from canopy grain analysis using Fourier-based textural ordination of IKONOS images. *Remote Sensing of Environment* 109(3), 379-392. <https://doi.org/10.1016/j.rse.2007.01.009>
- Proisy, C., Mougin, E., Fromard, F., Karam, M.A., 2000. Interpretation of polarimetric radar signatures of mangrove forests. *Remote Sensing of Environment* 71(1), 56-66. [https://doi.org/10.1016/S0034-4257\(99\)00064-4](https://doi.org/10.1016/S0034-4257(99)00064-4)
- Qi, J., Chehbouni, A., Huete, A.R., Kerr, Y.H., Sorooshian, S., 1994. A modified soil adjusted vegetation index. *Remote Sensing of Environment* 48(2), 119-126. [https://doi.org/10.1016/0034-4257\(94\)90134-1](https://doi.org/10.1016/0034-4257(94)90134-1)
- R Core Team, 2015. R: A language and environment for statistical computing.

- Richter, R., Schlöpfer, D., 2014. ATCOR-2/3 user guide, version 8.3. 1. Zurich, Switzerland.
- Rodrigues, M., de la Riva, J., 2014. An insight into machine-learning algorithms to model human-caused wildfire occurrence. *Environmental Modelling & Software* 57, 192-201. <https://doi.org/10.1016/j.envsoft.2014.03.003>
- Rodriguez-Galiano, V.F., Ghimire, B., Rogan, J., Chica-Olmo, M., Rigol-Sanchez, J.P., 2012. An assessment of the effectiveness of a random forest classifier for land-cover classification. *ISPRS Journal of Photogrammetry and Remote Sensing* 67, 93-104. <https://doi.org/10.1016/j.isprsjprs.2011.11.002>
- Rogers, B., Qiao, Y., Gung, J., Mathur, T., Burge, J.E., 2015. Using text mining techniques to extract rationale from existing documentation, in: Gero, J.S., Hanna, S. (Eds.), *Design Computing and Cognition '14*. Springer International Publishing, Cham, pp. 457-474.
- Rondeaux, G., Steven, M., Baret, F., 1996. Optimization of soil-adjusted vegetation indices. *Remote Sensing of Environment* 55(2), 95-107. [https://doi.org/10.1016/0034-4257\(95\)00186-7](https://doi.org/10.1016/0034-4257(95)00186-7)
- Saeys, Y., Inza, I., Larrañaga, P., 2007. A review of feature selection techniques in bioinformatics. *Bioinformatics*. <https://doi.org/10.1093/bioinformatics/btm344>
- Sang, K.V., 2011. Nghien cuu kha nang tich tu carbon cua cha la bien (Phoenix paludosa Roxb.) tai khu du tru sinh quyen rung ngap man CanGio (Master's thesis). Nong Lam University, Ho Chi Minh City.
- Sarker, L.R., Nichol, J.E., 2011. Improved forest biomass estimates using ALOS AVNIR-2 texture indices. *Remote Sensing of Environment* 115(4), 968-977. <https://doi.org/10.1016/j.rse.2010.11.010>
- Shannon, C.E., Weaver, W., 1949. *The Mathematical Theory of Communication*. University of Illinois Press, Urbana, IL.
- Simard, M., Zhang, K., Rivera-Monroy, V.H., Ross, M.S., Ruiz, P.L., Castañeda-Moya, E., Twilley, R.R., Rodriguez, E., 2006. Mapping height and biomass of mangrove forests in Everglades National Park with SRTM elevation data. *Photogrammetric Engineering and Remote Sensing* 72(3), 299-311.
- Simpson, P., 2005. *Pohutukawa and Rata: New Zealand's Iron-Hearted Trees*. Te Papa Press, Wellington, New Zealand.
- Soria, D., Garibaldi, J.M., Ambrogi, F., Biganzoli, E.M., Ellis, I.O., 2011. A 'non-parametric' version of the naive Bayes classifier. *Knowledge-Based Systems* 24(6), 775-784. <https://doi.org/10.1016/j.knosys.2011.02.014>
- Strobl, C., Malley, J., Tutz, G., 2009. An introduction to recursive partitioning: Rationale, application and characteristics of classification and regression trees, bagging and random forests. *Psychological Methods* 14(4), 323-348. <https://doi.org/10.1037/a0016973>
- Tanaka, N., Sasaki, Y., Mowjood, M.I.M., Jinadasa, K.B.S.N., Homchuen, S., 2007. Coastal vegetation structures and their functions in tsunami protection: experience of the recent Indian Ocean tsunami. *Landscape Ecol Eng* 3(1), 33-45. <https://doi.org/10.1007/s11355-006-0013-9>
- Tian, X., Li, Z., Su, Z., Chen, E., van der Tol, C., Li, X., Guo, Y., Li, L., Ling, F., 2014. Estimating montane forest above-ground biomass in the upper reaches of the Heihe River Basin using Landsat-TM data. *International Journal of Remote Sensing* 35(21), 7339-7362. <https://doi.org/10.1080/01431161.2014.967888>


- Tien Bui, D., Pradhan, B., Lofman, O., Revhaug, I., 2012. Landslide susceptibility assessment in Vietnam using support vector machines, decision tree, and Naive Bayes Models. *Mathematical Problems in Engineering* 2012, 1-26. <https://doi.org/10.1155/2012/974638>
- Trimble Germany GmbH, 2015a. Trimble Documentation: eCognition Developer 9.1 Reference Book. Trimble Germany GmbH, Munich, Germany.
- Trimble Germany GmbH, 2015b. Trimble Documentation: eCognition Developer 9.1 User Guide. Trimble Germany GmbH, Munich, Germany.
- Tucker, C.J., 1979. Red and photographic infrared linear combinations for monitoring vegetation. *Remote Sensing of Environment* 8(2), 127-150. [https://doi.org/10.1016/0034-4257\(79\)90013-0](https://doi.org/10.1016/0034-4257(79)90013-0)
- Uğuz, H., 2011. A two-stage feature selection method for text categorization by using information gain, principal component analysis and genetic algorithm. *Knowledge-Based Systems* 24(7), 1024-1032. <https://doi.org/10.1016/j.knosys.2011.04.014>
- Ustin, S., Jacquemoud, S., Palacios-Orueta, A., Li, L., Whiting, M., 2009. Remote sensing based assessment of biophysical indicators for land degradation and desertification, in: Röder, A., Hill, J. (Eds.), *Recent Advances in Remote Sensing and Geoinformation, Processing for Land Degradation Assessment*. CRC Press, Boca Raton, FL, pp. 15-44.
- Van Coillie, F.M.B., Verbeke, L.P.C., De Wulf, R.R., 2007. Feature selection by genetic algorithms in object-based classification of IKONOS imagery for forest mapping in Flanders, Belgium. *Remote Sensing of Environment* 110(4), 476-487. <https://doi.org/10.1016/j.rse.2007.03.020>
- Vapnik, V.N., 1995. *The Nature of Statistical Learning Theory*. Springer-Verlag, New York, NY.
- Viet Nam Environment Protection Agency, 2005. *Overview of Wetlands Status in Viet Nam Following 15 Years of Ramsar Convention Implementation*, Hanoi, Viet Nam.
- Vin, A., Gitelson, A.A., 2011. Sensitivity to Foliar Anthocyanin Content of Vegetation Indices Using Green Reflectance. *Geoscience and Remote Sensing Letters, IEEE* 8(3), 464-468. <https://doi.org/10.1109/LGRS.2010.2086430>
- Vogt, J., Kautz, M., Herazo, M.L.F., Triet, T., Walther, D., Saint-Paul, U., Diele, K., Berger, U., 2013. Do canopy disturbances drive forest plantations into more natural conditions?—A case study from Can Gio Biosphere Reserve, Viet Nam. *Global and Planetary Change* 110, 249-258. <https://doi.org/10.1016/j.gloplacha.2011.09.002>
- Wang, L., Sousa, W.P., Gong, P., 2004a. Integration of object-based and pixel-based classification for mapping mangroves with IKONOS imagery. *International Journal of Remote Sensing* 25(24), 5655-5668. <https://doi.org/10.1080/014311602331291215>
- Wang, L., Sousa, W.P., Gong, P., Biging, G.S., 2004b. Comparison of IKONOS and QuickBird images for mapping mangrove species on the Caribbean coast of Panama. *Remote Sensing of Environment* 91(3), 432-440. <https://doi.org/10.1016/j.rse.2004.04.005>
- Wang, Y., 2009. *Remote Sensing of Coastal Environments*. CRC Press, Boca Raton, FL.

- Wang, Y., Wang, J., 2010. Remote sensing of coastal environments: An overview, in: Wang, Y. (Ed.), *Remote Sensing of Coastal Environments*. CRC Press, Boca Raton, FL, pp. 1-24.
- Weeks, E., Newsome, P., Shepherd, J., 2009. National SPOT-5 Image Orthorectification and Reflectance Standardisation: Final Project Report Landcare Research Contract Report: LC0809/102, Palmerston North, New Zealand.
- Whiteside, T.G., Boggs, G.S., Maier, S.W., 2011. Comparing object-based and pixel-based classifications for mapping savannas. *International Journal of Applied Earth Observation and Geoinformation* 13(6), 884-893. <https://doi.org/10.1016/j.jag.2011.06.008>
- Wicaksono, P., Danoedoro, P., Hartono, Nehren, U., 2016. Mangrove biomass carbon stock mapping of the Karimunjawa Islands using multispectral remote sensing. *International Journal of Remote Sensing* 37(1), 26-52. <https://doi.org/10.1080/01431161.2015.1117679>
- Widodo, A., Yang, B.-S., Han, T., 2007. Combination of independent component analysis and support vector machines for intelligent faults diagnosis of induction motors. *Expert Systems with Applications* 32(2), 299-312. <https://doi.org/10.1016/j.eswa.2005.11.031>
- Witten, I.H., Frank, E., 2005. *Data Mining: Practical machine learning tools and techniques*. Morgan Kaufmann, Cambridge, MA.
- Xie, Y., Sha, Z., Yu, M., 2008. Remote sensing imagery in vegetation mapping: a review. *Journal of Plant Ecology* 1(1), 9-23. <https://doi.org/10.1093/jpe/rtm005>
- Xin, H., Liangpei, Z., Le, W., 2009. Evaluation of morphological texture features for mangrove forest mapping and species discrimination using multispectral IKONOS imagery. *IEEE Geoscience and Remote Sensing Letters* 6(3), 393-397. <https://doi.org/10.1109/lgrs.2009.2014398>
- Xue, B., Zhang, M., Browne, W.N., 2014. Particle swarm optimisation for feature selection in classification: Novel initialisation and updating mechanisms. *Applied Soft Computing* 18, 261-276. <https://doi.org/10.1016/j.asoc.2013.09.018>
- Yu, Q., Gong, P., Clinton, N., Biging, G., Kelly, M., Schirokauer, D., 2006. Object-based detailed vegetation classification with airborne high spatial resolution remote sensing imagery. *Photogrammetric Engineering and Remote Sensing* 72(7), 799-811.
- Zhen, Z., Quackenbush, L.J., Zhang, L., 2014. Impact of tree-oriented growth order in marker-controlled region growing for individual tree crown delineation using Airborne Laser Scanner (ALS) data. *Remote Sensing* 6(1), 555-579. <https://doi.org/10.3390/rs6010555>
- Zhu, Y., Liu, K., Liu, L., Wang, S., Liu, H., 2015. Retrieval of mangrove aboveground biomass at the individual species level with WorldView-2 images. *Remote Sensing* 7(9), 12192-12214. <https://doi.org/10.3390/rs70912192>

APPENDICES

APPENDIX 1

Co-authorship form



**THE UNIVERSITY OF
WAIKATO**
Te Whare Wānanga o Waikato

Co-Authorship Form

Postgraduate Studies Office
Student and Academic Services Division
Whareanga Rangatahi Mātauranga Akeanga
The University of Waikato
Private Bag 3105
Hamilton 3240, New Zealand
Phone +64 7 838 4439
Website: <http://www.waikato.ac.nz/ead/postgraduate/>

This form is to accompany the submission of any PhD that contains research reported in published or unpublished co-authored work. **Please include one copy of this form for each co-authored work.** Completed forms should be included in your appendices for all the copies of your thesis submitted for examination and library deposit (including digital deposit).

Please indicate the chapter/section/pages of this thesis that are extracted from a co-authored work and give the title and publication details or details of submission of the co-authored work.

Chapter 3 of this thesis that are extracted from a co-authored work. The title and publication details are: "Pham, L.T., Brabyn, L., Ashraf, S., 2016. Combining QuickBird, LIDAR, and GIS topography indices to identify a single native tree species in a complex landscape using an object-based classification approach. International Journal of Applied Earth Observation and Geoinformation 50, 187-197". <http://dx.doi.org/10.1016/j.jag.2016.03.015>

Nature of contribution by PhD candidate

Extent of contribution by PhD candidate (%)

The lead author

90

CO-AUTHORS

Name	Nature of Contribution
Lars Brabyn	Second author
Salman Asraf	Third author

Certification by Co-Authors

The undersigned hereby certify that:

- the above statement correctly reflects the nature and extent of the PhD candidate's contribution to this work, and the nature of the contribution of each of the co-authors; and

Name
Lars Brabyn
Salman Ashraf

Signature
<i>Lars Brabyn</i>
<i>Salman Ashraf</i>

Date
10/10/2017
16/10/2017

July 2017

APPENDIX 2

Co-authorship form



Co-Authorship Form

Postgraduate Studies Office
Student and Academic Services Division
Wahanga Ratonga Matauranga Ake
The University of Waikato
Private Bag 3105
Hamilton 3240, New Zealand
Phone +64 7 838 4439
Website: <http://www.waikato.ac.nz/sasdi/postgraduate/>

This form is to accompany the submission of any PhD that contains research reported in published or unpublished co-authored work. **Please include one copy of this form for each co-authored work.** Completed forms should be included in your appendices for all the copies of your thesis submitted for examination and library deposit (including digital deposit).

Please indicate the chapter/section/pages of this thesis that are extracted from a co-authored work and give the title and publication details or details of submission of the co-authored work.

Chapter 5 of this thesis that are extracted from a co-authored work. The title and publication details are: "Pham, L.T.H., Brabyn, L., 2017. Monitoring mangrove biomass change in Vietnam using SPOT images and an object-based approach combined with machine learning algorithms". ISPRS Journal of Photogrammetry and Remote Sensing 128, 86 -97". <http://dx.doi.org/10.1016/j.isprsjprs.2017.03.013>

Nature of contribution
by PhD candidate

The lead author

Extent of contribution
by PhD candidate (%)

90

CO-AUTHORS

Name	Nature of Contribution
Lars Brabyn	Second author

Certification by Co-Authors

The undersigned hereby certify that:

- ❖ the above statement correctly reflects the nature and extent of the PhD candidate's contribution to this work, and the nature of the contribution of each of the co-authors; and

Name	Signature	Date
Lars Brabyn	<i>Lars Brabyn</i>	10/10/2017

July 2017

APPENDIX 3

Co-authorship form



THE UNIVERSITY OF
WAIKATO
Te Whare Wānanga o Waikato

Co-Authorship Form

Postgraduate Studies Office
Student and Academic Services Division
Wahanga Raukanga Matauranga Ake
The University of Waikato
Private Bag 3105
Hamilton 3240, New Zealand
Phone +64 7 838 4439
Website: <http://www.waikato.ac.nz/sasdp/postgraduate/>

This form is to accompany the submission of any PhD that contains research reported in published or unpublished co-authored work. **Please include one copy of this form for each co-authored work.** Completed forms should be included in your appendices for all the copies of your thesis submitted for examination and library deposit (including digital deposit).

Please indicate the chapter/section/pages of this thesis that are extracted from a co-authored work and give the title and publication details or details of submission of the co-authored work.

Chapter 4 of this thesis that are extracted from a co-authored work. The title and publication details are: "Pham, L.T.H., Brabyn, L., Gouk, H. An evaluation of dimensionality reduction and classification techniques for identifying tree species using integrated QuickBird imagery and Lidar data". Chapter 4 is a paper submitted to the "IEEE Transactions on Geoscience and Remote Sensing" Journal on 16 July 2017.

Nature of contribution
by PhD candidate

The lead author

Extent of contribution
by PhD candidate (%)

90

CO-AUTHORS

Name	Nature of Contribution
Lars Brabyn	Second author
Henry Gouk	Third author

Certification by Co-Authors

The undersigned hereby certify that:

- ❖ the above statement correctly reflects the nature and extent of the PhD candidate's contribution to this work, and the nature of the contribution of each of the co-authors; and

Name	Signature	Date
Lars Brabyn	<i>Lars Brabyn</i>	10/10/2017
Henry Gouk	<i>HG</i>	10/10/2017

July 2017